UNIVERSIDADE D
COIMBRA

Carlos André Almeida Paiva

EPILEPTIC SEIZURE DETECTION AND PREDICTION BASED ON SPATIOTEMPORAL EEG DATA AND DEEP MACHINE LEARNING (EPI-DEEP)

Dissertation Epileptic seizure detection and prediction based on EEG data and deep machine learning (EPI-DEEP) in the context of the Master's in Informatics Engineering, Specialization in Intelligent Systems, advised by Professors César Alexandre Domingues Teixeira and Adriana Costa Leal and presented to Faculty of Sciences and Technology / Department of Informatics Engineering.

September 2019

Resumo

Conhecida como uma das doenças neurológicas mais comuns, a epilepsia afeta 1% da população mundial. Para 30% dos pacientes diagnosticados com epilepsia, não há tratamento ou medicação viável para evitar a ocorrência de crises. Esse tipo de epilepsia é chamado de epilepsia resistente a medicamentos. Isso significa que integridade física desses pacients pode estar comprometida a qualquer momento, o que pode colocar suas vidas em risco. Para essas pessoas, todo esforço bem-sucedido em prever ou detectar crises epilépticas tem o potencial de melhorar significativamente suas vidas.

Esse assunto tem sido explorado na literatura bastante extensivamente, principalmente quando se trata de analisar características temporais e dados extraídos de vários electrodos. No entanto, existem muito poucos estudos que se concentram também em explorar as relações espaciais entre electrodos. A nossa ideia é explorar o potencial das relações espaciais entre os electrodos, através de mapas de electrodos, a fim de criar um modelo que possa prever ou detectar crises, possivelmente com melhor desempenho do que as já existentes. Nesse sentido, este projecto de tese aplicará técnicas de aprendizagem computacional profunda ao problema de detecção ou previsão de crises epilépticas, usando mapas de eletrodos derivados de dados do eletroencefalograma (EEG).

Nosso modelo final é um detector de crises realista, que deve produzir alertas para crises em tempo real, usando redes neurais convolucionais em dados brutos de EEG. Esta tese explora os vários desafios da construção de um modelo capaz de alta sensibilidade e detecção precoce de um sistema como esse.

Esta tese foi conduzida usando dados de EEG incluídos na European Epilepsy Database (banco de dados EPILEPSIA).

Palavras chave

Epilepsia, Eletroencefalografia, EEG, Aprendizagem Computacional Profunda

Abstract

Known as one of the most common neurological disorders, epilepsy affects 1% of the world's population. For 30% of epilepsy diagnosed patients, there is no viable treatment or medication to prevent the occurrence of seizures. This type of epilepsy is called drug-resistant epilepsy. This means that their physical integrity is compromised, which eventually may put their lives at risk. For these people, every successful effort in predicting or detecting seizure events has the potential to significantly improve their lives.

This subject has been explored in literature quite extensively, particularly when it comes to analyzing temporal features and data retrieved from various electrodes. However, there aver very few studies that focus also on exploring the spatial relations between electrodes. Our idea is to explore the potential of spatial relations between electrodes, through electrode maps, in order to create a model that can predict or detect seizures, possibly with better performance than already existing ones. Towards that end, this thesis project will be applying deep learning techniques to the problem of detecting or predicting epileptic seizures, using electrode maps derived from electroencephalogram (EEG) data.

Our final model is a realistic seizure detector that is expected to produce alerts for seizures in real-time using convolutional neural networks on raw EEG data. This thesis explores the various challenges of building a model capable of high sensitivity and early detection for a system like this.

This thesis was conducted using scalp EEG data comprised in the European Epilepsy Database (EPILEPSIA database).

Keywords

Epilepsy, Electroencephalography, EEG, Deep Learning

Acknowledgments

Queria agradecer, antes de mais, aos meus pais pelo amor que me deram, pela paciência que tiveram e pelo dinheiro que gastaram nestes anos todos em que estive na universidade. Sem eles, obviamente que nada disto teria sido possível.

Queria também agradecer ao meu orientador César Teixeira por se ter sempre preocupado em me acompanhar e dar sugestões para que este projecto de tese ficasse o melhor possível.

Não podia deixar de agradecer ao pessoal do laboratório em que trabalhei, mais especificamente ao Diogo Nunes, Diogo Pessoa, Fábio Lopes, Fellipe Allevato, Francisco Valente (que não era de lá mas estava sempre presente), Júlio Medeiros e Patrick Kojanec. Dois especiais agradecimentos vão para a Adriana Leal e o Mauro Pinto, que sempre se disponibilizaram para me ajudar em tudo o que precisasse, muitas vezes chegando ao ponto de mostrarem mais preocupação com a minha tese do que eu próprio!

Não podem também faltar aqui os meus amigos Dorivaldo da Silva, Joel Pires e Jomar Domingos que me acompanharam durante todo este processo, estando sempre disponíveis para me ajudar e motivar. Mais uma vez, dois especiais agradecimentos vão para o Hélio Pires, que neste momento até está aqui comigo na recta final e o João Batanete que não só me ajudou a estruturar como até mechegou a rever a tese!

I would also like to thank all the countless people that have contributed to the development of science and technology. Without them, the world would just be dull.

Index

Acronyms

EEG – electroencephalogram/electroencephalography

ILAE – International League Against Epilepsy

ANN – Artificial neural network

MLP – Multilayer Perceptron

DBN – Deep belief network

RNN – Recurrent neural network

LSTM – Long short-term memory

CNN – Convolutional neural network

TCN – Temporal convolutional neural network

FPR – False positive rate

FNR – False negative rate

FRAR – False red alert rate

NSAR – Near seizure false red alert

FSFRAR – Far seizure false red alert rate

FRA/B – False red alerts per batch

ALFRA – Average length of false red alerts

STDFRAL – Standard deviation of false red alert's length

FS – Failed seizures

ATFTRA – Average time for the first true red alert

ORAS – Occurrence of red alerts in a seizure

List of Figures

List of Tables

Chapter 1

Introduction

In this chapter, we are going to describe the reasons why the theme of this thesis project is important and interesting and what we intend to achieve throughout and in the end of this thesis project.

1.1 Motivation

About 1% of the world's population suffers from epilepsy [1]. About one third of these patients suffer from drug resistant (refractory or intractable) epilepsy [101] meaning that the administration of antiepileptic drugs is not effective. People who belong to this group have their lives impaired by the unpredictability of seizures. The ability to somehow know when they are going to experience a seizure so they can prepare accordingly would provide them some security and comfort.

Scalp EEG is a non-invasive tool to retrieve information about the state of the subject's brain. Due to this, a device can be built in order to provide the aforementioned seizure detection and prediction capabilities that so many people can benefit from [2].

Several studies [25, 36, 37] have shown that there are significant changes in the EEG signal produced before a seizure that can potentially be exploited to predict it. However, the results of such attempts to create prediction models have not been as successful as it is desired yet.

Seizure detection consists in detecting, as early as possible preferably, when a patient is starting to have a seizure event. It is distinguished from prediction, as detection attempts to identify when seizure is happening rather than when it is about to happen. This is also a very important problem to solve, as monitoring patients that suffer from epilepsy in an automatic fashion [79], can be essential to keep them healthy and safe, as not detecting a seizure in time to provide proper assistance to the patient may lead to otherwise avoidable injuries or other complications.

Much has already been done when it comes to exploring the temporal variations on EEG electrodes but not so much has been done when it comes to exploring spatial variations. This is a more recent perspective that has not been extensively studied yet. This innovative way of approaching this problem may open up the way for new possibly important features and, together with temporal features, may improve the prediction and detection rates for epileptic seizures. The proposal of this thesis project is to approach this problem by using topographic maps as a way of retrieving spatial features of EEG.

Another method that is proposed to be used in this thesis project is the use of artificial neural networks (ANNs). ANNs, if adapted carefully to this problem, can successfully use features, both in the

temporal and spatial domains, to create very complex classifiers that can weight in a number of features that would perhaps be impossible for a human being to think of. To add to this, they provide enough flexibility to create different models for different patients or types of epilepsy. In this thesis, we are free to work with Deep ANNs of various types, such as the ones that have been proposed for this thesis, specifically: Convolutional Neural Networks (CNN), Deep Belief Networks (DBNs) and Long Short-term Memory networks (LSTM). Each of these networks and more will be described further in this document, with their potential advantages and disadvantages properly explored. The chosen model ended up using typical CNN and other propose Deep ANNs were not used.

As for the much-needed data, Centro de Informática e Sistemas da Universidade de Coimbra (CISUC) has access to the European Epilepsy Database (EPILEPSIAE) which contains long-term EEG recordings of 275 patients [3]. This database is expected to provide the required data to fulfill this thesis.

1.2 Objectives

The main objective of this master's dissertation is to apply deep learning to explore spatiotemporal relations between EEG electrodes.

The first step for its completion would be **to contextualize the problem**. This step requires studying and understanding the various concepts and applications associated to epilepsy, EEG, topographic maps, analysis of temporal and spatial data, feature selection and extraction and the functionality and reasoning behind the different types of deep neural networks. The state of the art methods that were used to try to solve this problem will also be referred to.

Afterwards, the following steps were undertaken:

- **Creation of topographic brain maps**: create a framework that is able to organize the various electrodes used to measure EEG into a map, assign their respective values relating to the feature that we are mapping and interpolate the values within them (ended up not being used).
- **Finding an efficient and accurate representation for the maps:** The goal of this step is to mitigate the enormous amount of time that deep learning methods take to be optimized by finding a compressed yet accurate representation for our maps.
- **Creating a framework for extraction and classification of data**: The goal of this step is to create a framework that allows extraction of data from the EPILEPSIAE database and use it to train a neural network of our choice;
- **Finding the appropriate architecture and optimal parameters for classification**: This step requires extensive testing to compare various possible neural network architectures and different parameters to try to find those that produce the best results on average, using data from the EPILEPSIA database
- **Test the final algorithm on real data**: this final step requires using the EPILEPSIAE database to validate the methods and features obtained in the previous steps,

analyzing the obtained results and show if they represent improvements over the state of the art methods.

1.3 Outline

The structure of this thesis is detailed bellow.

Chapter 2 explains the most important background concepts required to tackle this problem.

Chapter 3 presents the state of the art of epileptic seizure detection and prediction methodologies.

Chapter 4 presents the methods, results and performance evaluation

Chapter 5 presents the results and discussion

Chapter 6 presents the final conclusions of our project

Chapter 2

Background concepts

In this chapter, the necessary concepts to understand epilepsy disorder and seizure prediction are presented.

2.1 Electroencephalography and its origins in the brain

EEG (Figure 1) is an electrophysiological method used to monitor electrical activity generated by the brain. In order to achieve this, electrodes are placed either over the scalp (non-invasive EEG) or directly over the surface or inside of the brain (invasive EEG). These electrodes measure potential differences (voltages) where they are placed, in the brain, generally to a reference electrode, allowing the fluctuations in those voltages to be plotted and analyzed.

Figure 1 – Typical human EEG recording of a seizure (Source: [12])

In order to understand how EEG is generated in the brain, we must first take a look at how electrical current and activity is produced and transmitted throughout the brain. This requires explaining different types of neurons synapses and other concepts of neurophysiology.

2.2 Neurons

Neurons (Figure 2) or nerve cells are the primary components of the nervous systems and consist of electrically excitable cells that are able to transmit signals and information through electrochemical processes [8]. This signal transmission processes occur through a structure called **synapse**. A typical neuron is constituted by:

- **Soma**: this is the cell body which contains the nucleus organelles and much of the neuron's mass. The soma is able to store ions and, thus, electric potential.
- **Dendrites (dendrons)**: which are small protoplasmic ramifications of the nerve cell that are able to propagate electrochemical signals received by other nerve cells. These signals are usually received from the axon (or, more specifically the axon terminal) of another neuron via synapses located at various points throughout the dendritic tree;
- **Axon**: the axon is a slender projection of the neuron that serves to conduct electrical charges away from the soma and into dendrites of other neurons. The interface with other neurons happens through synapses located at the axon terminal, which is located in the extremities of the axon.

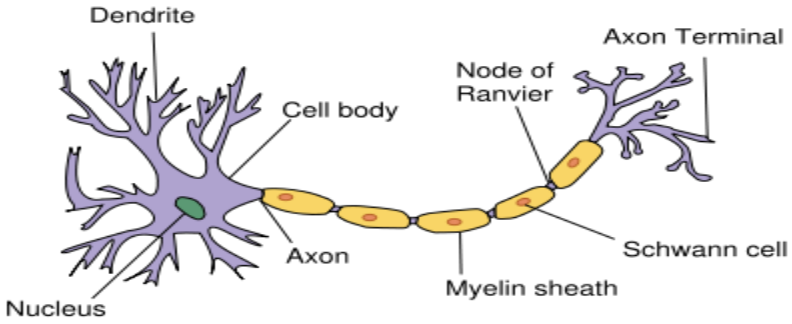

Figure 2 – Multipolar neuron (Taken from [8])

For EEG a specific type of neurons called **pyramidal neurons** are of special interest, as they are considered to be the primary source of EEG signal. These are multipolar neurons (one long-projecting axon, two or more dendrites) characterized by the fact that they have a triangular soma and a long projecting axon (Golgi I). These are considered to be the primary excitatory sources in a mammal's prefrontal cortex [9]. Synchronous activity of these neurons will produce EEG signal.

2.3 EEG signal generation

At rest, each neuron stands typically at -60mV to -70mV compared to the extracellular environment [10]. This is due to the fact that the cellular body of the neuron contains an unequal distribution of positive and negative ions (Na^+, K^+ and Cl^-, for example). A typical synapse is chemical and is characterized by exchange of neurotransmitters between the post-synaptic and pre-synaptic neurons. These neurotransmitters make the cellular membrane at the synapse more permeable. Depending on which neurotransmitters are in play, this chemical reaction will allow either a flow of positively charged ions from the pre-synaptic neuron to the post-synaptic neuron, making the post-synaptic cell more positively charged, which causes an excitatory postsynaptic potential (EPSP), or a flow of negative ions in the same direction, or of positive ions in the opposite direction, making the post-synaptic cell more negatively charged, both of which cause an inhibitory postsynaptic potentials (IPSP) [95].

Successive EPSPs, without IPSPs rebalancing the neuron's potential, will cause the neuron to accumulate more and more positive charges and when a certain threshold is reached, the axon of the neuron lets the positive ions diffuse through itself and let's some negative ions in, becoming negatively charged again (Figure 3). This process, by its nature, will cause an action potential to be triggered. This is commonly referred to as the neuron firing and causes the neuron to transmit the signal to one or more neurons.

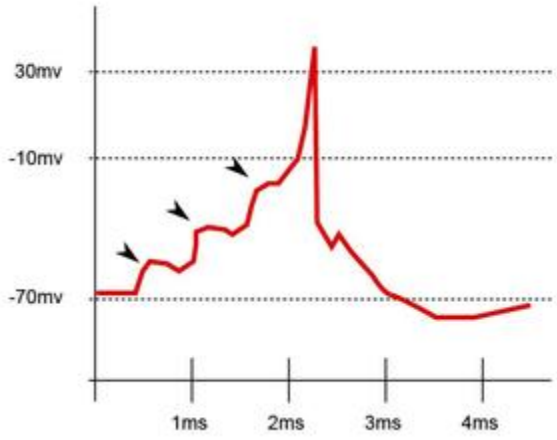

Figure 3 – Repeated EPSPs generating an action potential (Taken from [11])

EEG signal is generated when various neurons fire in a synchronous way or in quick succession (101), as the movement of the positive and negative charges through the dendrites and the axon of the neurons causes a voltage to occur. When EEG is recorded non-invasively, the problem is that the electrodes are placed over the scalp and thus will only be able to measure voltages that are at least close and generated by neurons that are perpendicular to the scalp. The only neurons considered to be able to generate measurable scalp EEG signal are thus the **pyramidal neurons that are perpendicular to the scalp**. When these pyramidal neurons are firing synchronously, they generate synchronous and periodic activity that is commonly known **as neural oscillations** or **brain waves**.

Much of the electrical signal being generated in the brain is not measured by EEG electrodes and this can definitely be a problem when using EEG signal to make predictions about the behavior of certain areas of the brain, especially if they are further away from the scalp and have a lower prevalence of pyramidal neuron.

There is some evidence that non-synaptic currents, fast action potentials, calcium spikes, voltage-dependent intrinsic oscillations, intrinsic spike afterhyperpolarization, ephaptic effects, and glia-generated slow potential shifts also play a role in EEG generation [98].

2.4 Brain waves

Brain waves or neural oscillations are rhythmic or repetitive patterns of neural activity in the central nervous system [13]. They are typically categorized by their frequency in five groups (note that that there is no absolute consensus on the literature for the frequency bands):

- **Delta waves** (0.5 Hz to 4 Hz): These waves are typically associated with deep sleep. If high delta activity is registered during an awoken state it can be associated with brain damage, dissociative states of mind or sleep deprivation. High relative delta wave power is correlated to inhibitory neural activity that is required to filter actions, thoughts or sensorial information and inhibit movements [14]. This can be interesting as loss of sensorial information, interruption of the thinking process and motor inhibition occur during seizures. Delta wave generation is regulated by the thalamus and the suprachiasmatic nuclei [15] and its sources are generally located in the frontal and cingulate cortex [16]. These oscillations have high amplitude and span throughout a wide portion of the brain. A subset of low frequency (0.5 Hz to 1 Hz) delta waves is sometimes differentiated and labeled as sub-delta waves.
- **Theta waves** (4 Hz to 7.5 Hz): There are two types of theta waves: *hippocampal theta waves* and *cortical theta waves*, classified according to their origin in the brain. Due to being generated from deep inside the head, scalp electrodes have considerable difficulties detecting hippocampal theta waves, however, theta activity in the cortex generally signifies communication between the hippocampus and the cortex [17]. High theta wave power is associated with lighter sleep stages, but also appears during REM (rapid eye movement) sleep, mental imagery and sensations and memory related information processing, as well as other activities and functions. As with delta waves, theta waves are also correlated to motor and response inhibition [18].
- **Alpha waves** (7.5 Hz to 12.5 Hz): Alpha waves are associated with a relaxed mental state. They are known to appear when a person closes his/her eyes during an awaken state [20]. They are correlated with primary sensory processing [19] and with attention and memory processes [16]. This waves also inhibit the cognitive process and are thus hypothesized to be a necessary element of suppression of information in the cognitive process, working in conjunction with higher frequency waves to create the selection

mechanism necessary for cognition [16]. They are often measured in the occipital region, as they are related to the processing of visual information.

- **Beta waves** (12.5 Hz to 30 Hz): Beta waves are more commonly measured in higher powers in the frontal and central regions of the cortex [21]. They are modeled during cognitive processes that require sensorimotor activity [16]. Beta waves are sometimes divided into three different frequency ranges:
    - **Low beta waves** (12.5 Hz to 15 Hz): known as beta 1 waves or **SMR** (Sensorimotor Rhythm) **waves**, they are correlated with relaxed attention and idle the motor strip, quieting down the body but not the mind [22]. These waves have been used to as a basis for neurofeedback training for epilepsy [23];
    - **Mid-range beta waves** (15 Hz to 20 Hz): This beta waves are known also as beta 2 waves and are correlated to increase in energy, anxiety and optimal concentration and performance on a task. This category of brainwaves is often considered to go as far as 23 Hz;
    - **High Beta waves** (20 Hz to 30 Hz): known as beta 3 waves, these waves are associated with stressful situations, hyper-vigilance, arousal and rage [24]. This category of brainwaves is often considered to go as far as 40Hz;
- **Gamma waves** (>30 Hz): Similar to high beta waves, these waves are correlated to arousal, intensive focus and hypervigilance. Contrary to the lower frequency waves, gamma waves are associated with cortical activation and action. There is evidence that these waves can be modulated by lower frequency waves to create a cognitive process or carry out tasks [25].

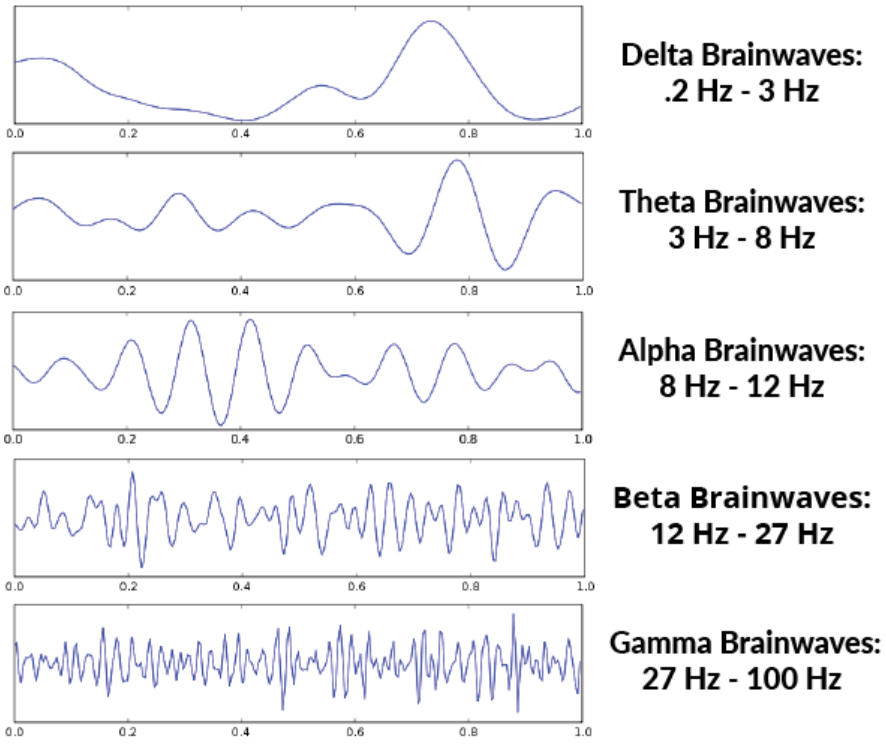

Figure 4 – How brain waves look like (Taken from [49])

2.5 Electrode positioning systems

There is a wide variety of ways that electrodes can be distributed throughout the scalp. There are some internationally recognized systems that were created to standardize testing methods and allow scientists and medical personnel to be able to compare each other's results accurately.

In each system, each electrode on the scalp is given a standardized name and position. The name reflects above which lobe the electrode is placed. Electrodes can be placed on pre-frontal (Fp), frontal (F), temporal (T), parietal (P), occipital (O), and central (C) lobes. The "z" stands for zero and indicates that the electrode should be placed on the midline sagittal plane of the skull. The "A" electrodes, sometimes called "M" for mastoid process, are to be placed behind the ear and are used for contralateral referencing other electrodes. In high-resolution systems, "AF" (anterior-frontal) electrodes are to be placed between "Fp" and "F" electrodes [99] and the I and N electrodes stand for inion and nasion, respectively, and should be placed on those locations.

2.5.1 The 10-20 system

The 10–20 (Figure 5) system is a standardized electrode system where the distances between adjacent electrodes are either 10% or 20% of the total diameter of the skull.

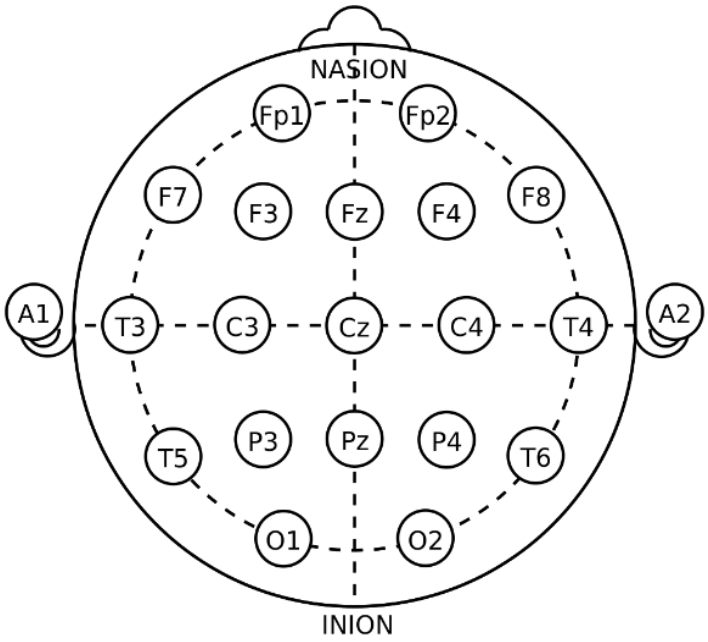

Figure 5 – The 10–20 system (Source: [33]). Note that the T5 and T6 electrodes are also named P5 and P6, respectively.

2.5.2 The 10-10 system

In an analogous way to the 10-20 system, the 10-10 system (Figure 6) is a standardized electrode system where the various electrodes are always at a distance equal to 10% of the front to back diameter of the skull. It is basically a higher resolution version of the 10-20 system.

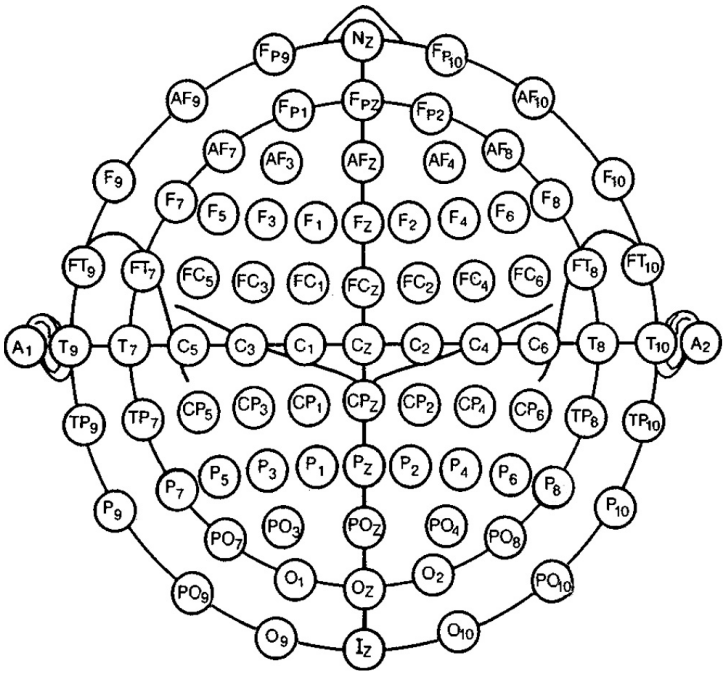

Figure 6 – A representation of a 10-10 electrode system extended with anterior and posterior electrodes in the inferior chain. (Source: [34]).

2.6 Epilepsy and epileptic seizures

According to the World Health Organization (WHO) [4], epilepsy is a chronic disorder of the brain that is characterized by recurrent seizures (Figure 7) that can produce involuntary movements in a given part of the body (partial seizures) or throughout it (generalized seizures).

Seizures events are characterized by symptoms that range from simple lapses of attention or muscle jerks to convulsions and/or loss of control of certain bodily functions. They happen when a certain region in the brain enters on a hyperexcitable state, which can result from increased excitatory synaptic neurotransmission, decreased inhibitory neurotransmission, an alteration in voltage-gated ion channels, or alteration of intra or extra-cellular ion concentrations in favor of membrane depolarization [5]. It can also result from synchronous excitatory external signals (for example flickering lights) with a frequency above a certain threshold (more on this 2.5).In broad terms, seizures occur when, in a certain region of the brain, there is a sufficiently high discrepancy between the brain's ability to inhibit neuronal action potentials and its ability to generate and propagate them. A common cause for this is improper functioning of the inhibitory neurons in this region [5].

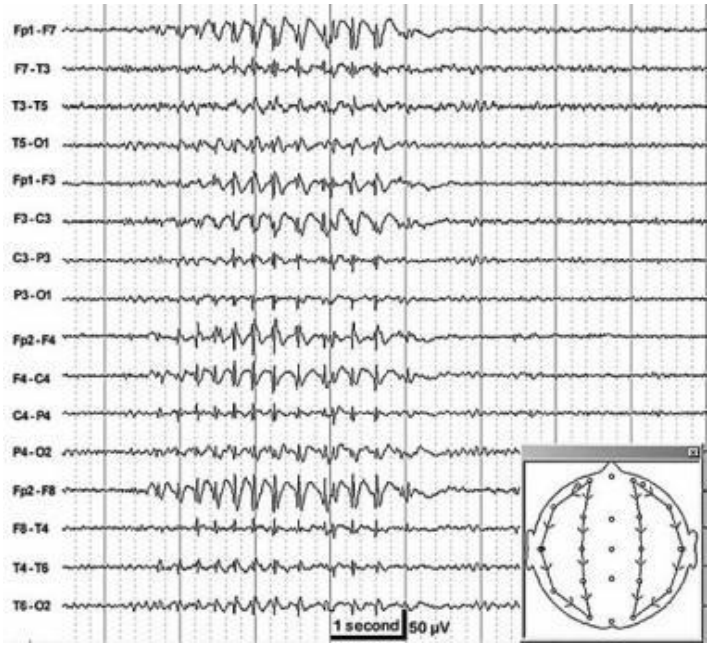

Figure 7 – EEG showing 3 Hz spike discharges: a typical pattern of an absence seizure. (Taken from [97])

The occurrence of seizures can endanger the person's health in many ways, from possible brain damage to injury due to loss of physical control. People with drug resistant epilepsy cannot rely on medication to stop seizure discharges and therefore being unable to live without constraints.

The nature of an epileptic seizure depends on many factors such as the person's age, the sleep-wake cycle, prior injuries to the brain, genetic tendencies, medications, which circuits in the brain are involved, among others [26].

Additionally, according to the 2017 classification of seizures (Figure 8) by the International League (ILAE) [27], seizures may be classified by their onset location, how they affect the person's awareness and their psychosomatic effects.

According to their onset location in the central nervous system, seizures can be classified as follows [28]:

- **Focal seizures**: Previously known as partial seizures, these start in a specific area of the brain. Given the onset area, they can be classified as temporal, frontal, hippocampal, parietal, etc.
- **Generalized seizures**: These seizures' onset involves neural networks in both sides of the brain.
- **Unknown onset**: The onset of the seizure is undefined.
- **Focal to bilateral seizures**: Previously known as secondary generalized seizures, these seizures start on one side of the brain and extend to the other one.

Awareness is the ability to perceive the world around us. On generalized seizures, the awareness of the patient is always considered to be impaired, so there is no need for classification. **Focal seizures** classification has been described as follows [28]:

- **Focal aware seizures**: Previously known as simple partial seizures, these are focal seizures in which the person's awareness remains intact, despite a possible loss of mental or bodily control. These seizures are commonly found in people who have brain injuries [29].
- **Focal impaired awareness seizures**: Seizures are classified as such if awareness is lost at some point during the seizure discharge. These seizures were previously known as complex partial seizures.
- **Awareness unknown**: this classification is assigned to the cases in which the person's awareness cannot be determined. For seizures reported to occur when the person is sleeping, this classification may be adequate.

Regarding psychosomatic symptoms, seizures are classified in two different ways [28]:

- **Motor seizures**: During these seizures, some type of involuntary movement occurs, such as jerking, stiffening or even automatic rather complex movements such as walking, rubbing hands, etc. Terms such as "generalized tonic-clonic seizure", describing a seizure in which body stiffening (tonic) and jerking (clonic) occur are also used.
- **Non-motor seizures**: When it comes to focal seizures, this term refers to seizures in which non-motor symptoms, such as changes in mood, thinking and sensations, occur in the first place. Regarding generalized seizures, this term most often refers to absence seizures, which are seizures that involve primarily brief changes in awareness, sometimes paired with minor movements such as lip-smacking.

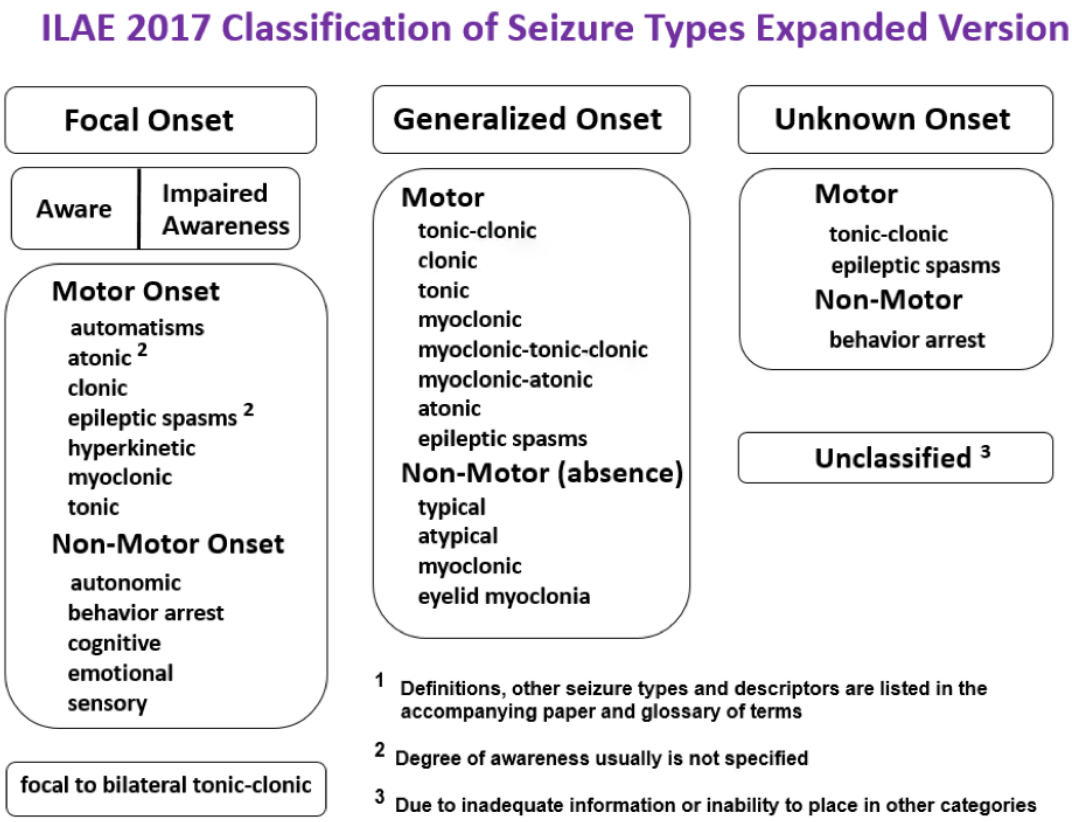

Figure 8 – Seizure classification chart, by ILAE (Taken from [28]).

Many of these types of seizures can be classified directly in EEG recordings, as they will produce different patterns on the recording. Figure 7 shows a typical epileptic pattern.

2.7 Epileptic brain states

When looking for predictors and identifiers of seizures in EEG data, we consider four different states:

- **Ictal state**: this state corresponds to the EEG segment capturing the moment when the seizure is taking place.
  - **Postictal state**: this state corresponds to the period of time, after the ictal state, when the EEG recordings show transitional patterns from the ictal state to normal brain functioning (interictal), and the patient experiences symptoms such as headaches, confusion and nausea derived from the exhaustion of the brain caused by the seizure [35]. It can last from a few minutes to more than a day, depending on the severity of the seizure [54].
- **Preictal state**: This state corresponds to an altered state of consciousness that leads or evolves into a seizure. Numerous studies have concluded that this state indeed exists and is distinct from the normal brain state with statistical significance [25, 36, 37]. The

time period before the seizure considered to be preictal has not been yet clinically defined and varies considerably in the literature [82]. Direito et al. [37], through statistical analysis of topographic maps, concluded that there are statistically significant changes in EGG, on average, 52 minutes before a seizure. However, Mormann et al. [36] found a period of 5 to 30 minutes using univariate measures and of 240 minutes using bivariate measures, while, in absence seizures, periods of less than 1 minute were found for the pre-ictal state [47]. This indicates that more studies need to be done to find where the preictal state really begins. However, the earlier the prediction the better.

- **Interictal state**: Every EEG segment that is considered to not be related to ictal state is considered interictal.

A classifier must be able to, as accurately as possible, distinguish between these periods. The main goal of this thesis is to build a classifier that can do exactly this.

2.8 Ictal patterns

Epileptic seizures generally follow an activity pattern that can be observed on the EEG recording during the time of the seizure or at its onset, that marks the transition from the preictal state to the ictal [104]. These patterns allow us to pinpoint where a seizure begins, as well as separating seizures in different groups. Here are the patterns recorded and utilized in the EPILEPSIA database (maybe explain them):

1. Amplitude depression (figure 9): There is a consistent observable difference in amplitude between some electrodes and others, usually observable between electrodes on opposite sides of the brain [105]. Labeled as 'm' in the EPILEPSIA database.

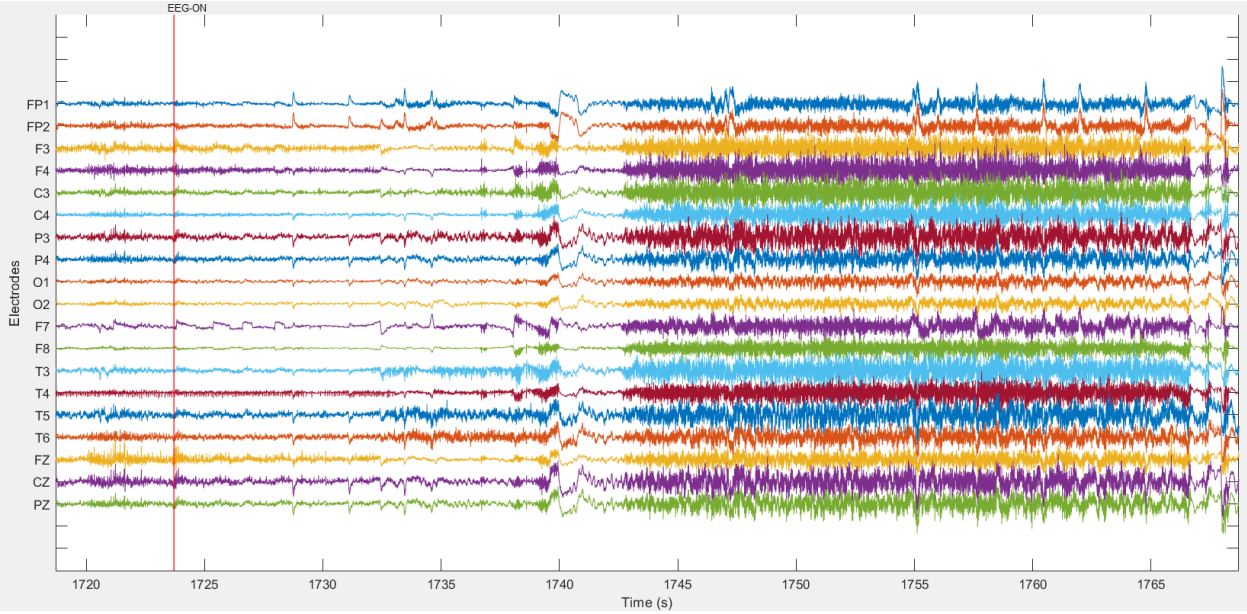

Figure 9: Seizure from patient #85202 showing an amplitude depression pattern. It can be observed more clearly on T4 around the onset, where an initial flattening happens while keeping the high frequencies. This pattern disappears latter on the seizure.

2. Low amplitude fast activity (LAFTA): This pattern corresponds to a flattening of the EEG signal caused by a sudden lowering in voltage and a decrease in low-frequency activity in the brain [104]. Labeled as 'l' in the EPILEPSIA database.
3. Repetitive spiking (figure 10): This pattern is characterized by repetitive voltage bursts causing a pattern of high amplitude and low frequency that resembles a spike [106]. Labeled as 'r' in the EPILEPSIA database.

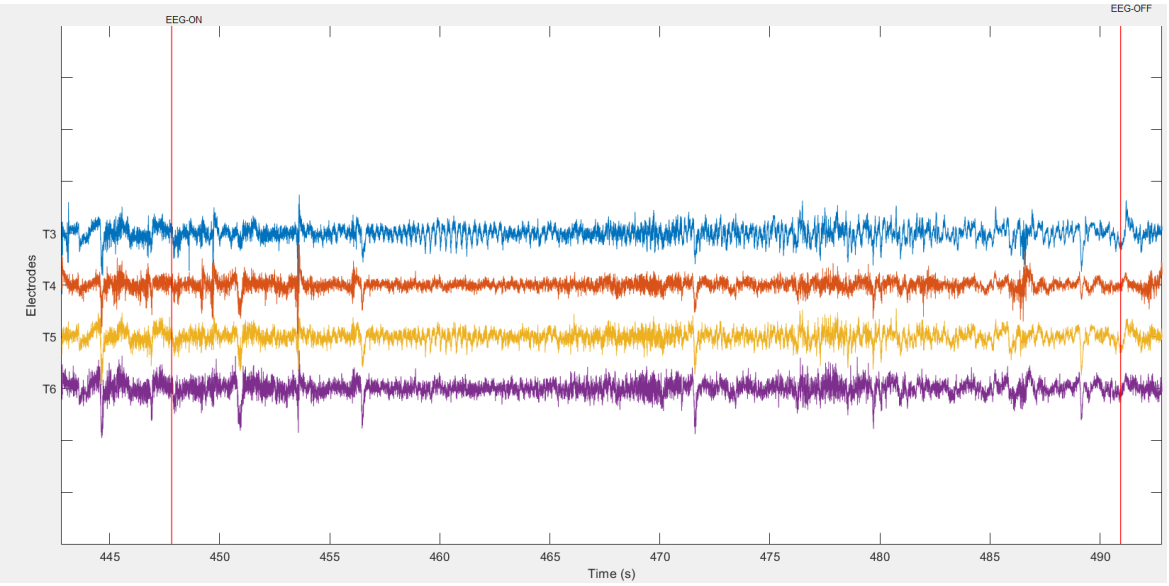

Figure 10: Repetitive spiking pattern on a seizure from patient #58602. Screenshot taken from Epilab.

4. Rhythmic alpha waves: The ictal onset is characterized by an increase in alpha wave activity. Labeled as ‘a’ in the EPILEPSIA database.
5. Rhythmic beta waves: The ictal onset is characterized by an increase in beta wave activity. Labeled as ‘b’ in the EPILEPSIA database.
6. Rhythmic delta waves: The ictal onset is characterized by an increase in delta wave activity. Labeled as ‘d’ in the EPILEPSIA database.
7. Rhythmic sub-delta waves: The ictal onset is characterized by an increase in sub-delta wave activity. Labeled as ‘e’ in the EPILEPSIA database.
8. Rhythmic theta waves (figure 11): The ictal onset is characterized by an increase in theta wave activity. Labeled as ‘t’ in the EPILEPSIA database.

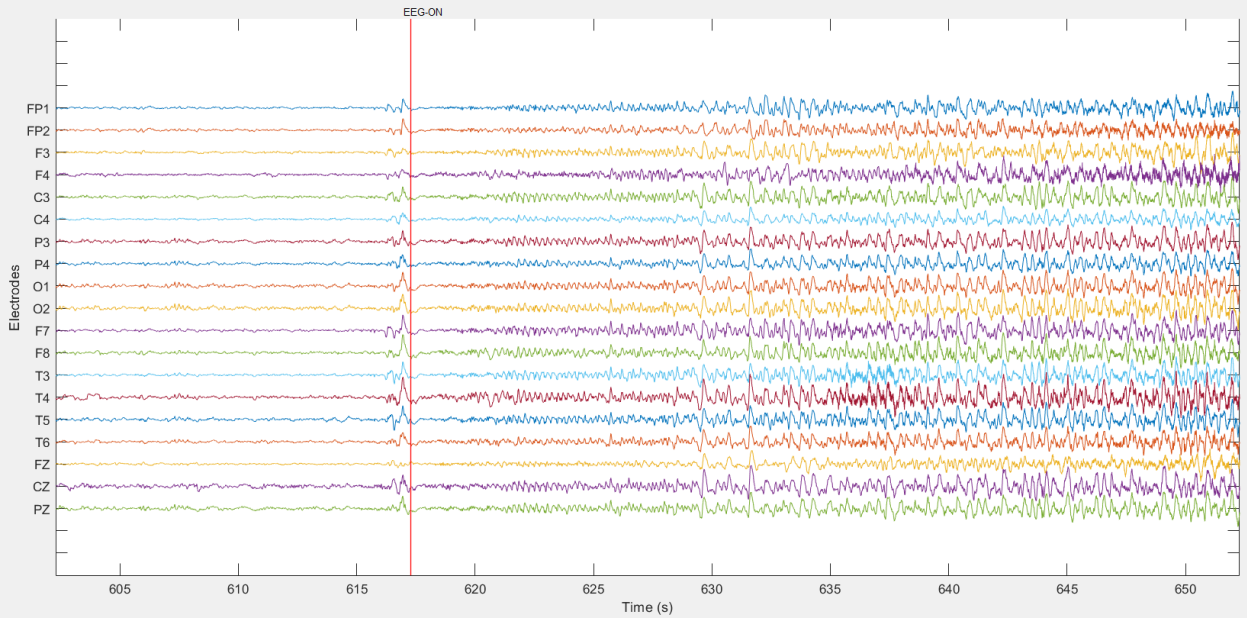

Figure 11: Seizure showing a rhythmic theta wave pattern. Screenshot taken from Epilab.

9. Rhythmic sharp waves (figure 13): Sharp waves (figure 12) are oscillatory patterns that have origin in the hippocampus. They can also appear during the onset of a seizure. Labeled as ‘s’ in the EPILEPSIA database.

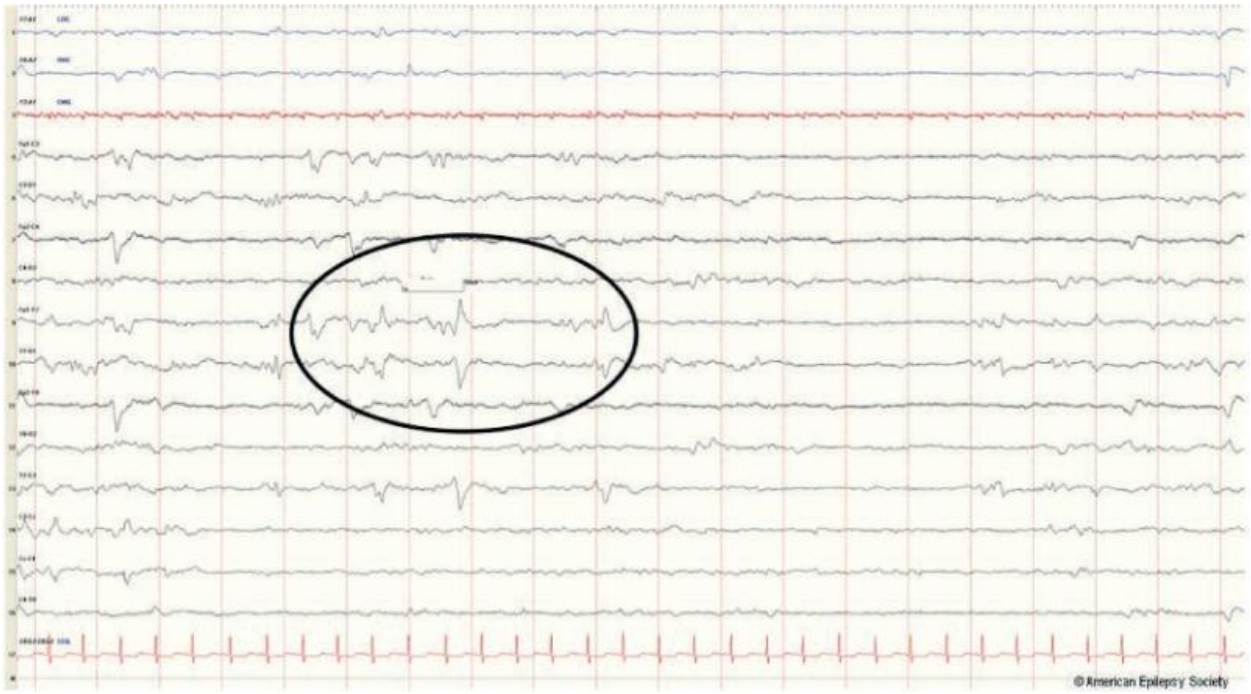

Figure 12: Sharp wave pattern in EEG. Taken from [107].

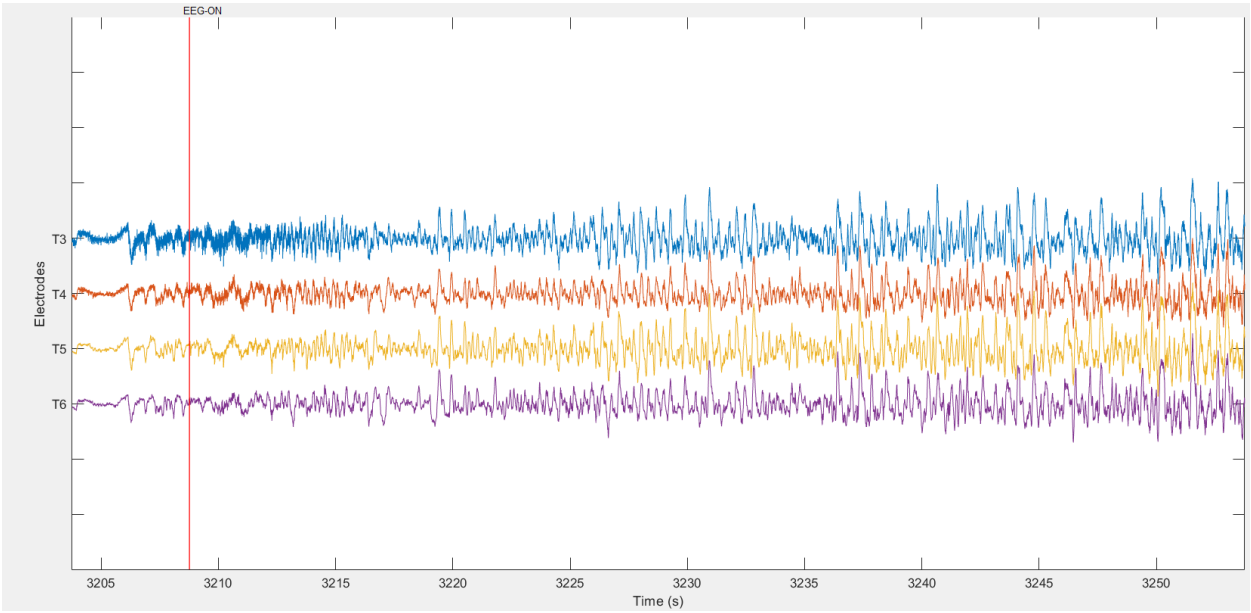

Figure 13: Ictal segment showing a prevalence of rhythmic sharp waves near the onset, from patient #114902. Screenshot taken from Epilab.

10. Cessation of interictal activity (only): Labeled as 'c' in the EPILEPSIA database.
11. Polyspikes: Seizures that begin with a pattern characterized by multiple spike waves (figure 14). Labeled as 'p' in the EPILEPSIA database.

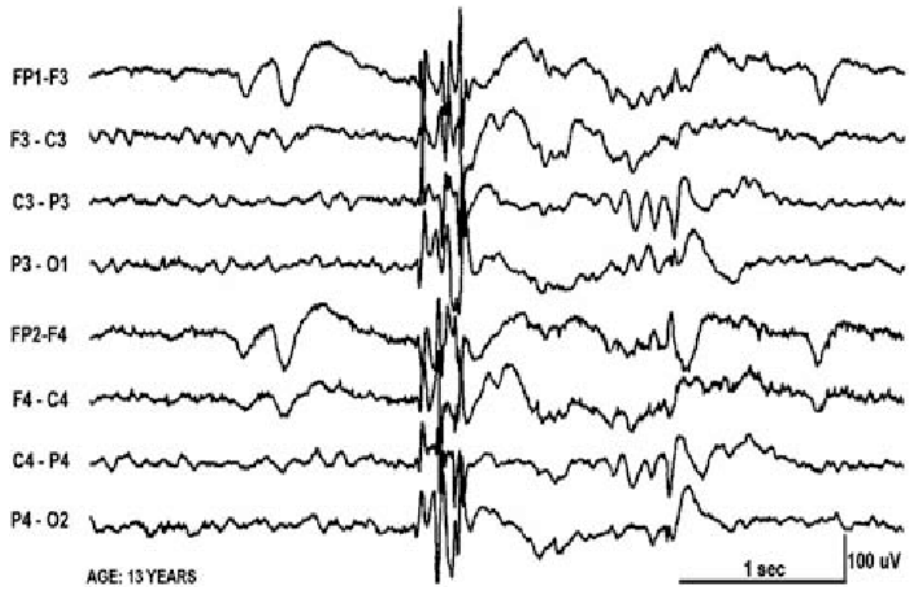

Figure 14: Polyspike wave patterns in an EEG recording. Source: [108]

12. Unclassified: some seizures do not have their seizure pattern recorded in the database. In this thesis document, they will be labeled as 'u'.

2.8 Quantitative EEG

Quantitative EEG (QEEG) is a field that is concerned with applying computational techniques and numerical analysis to EEG [55], such as Fourier analysis and wavelet analysis. The analog EEG signal is first acquired at a certain frequency (256 Hz or more, preferably) and some sort of discrete time-series analysis is applied to it to allow the extraction of features such as, for example, the relative spectral power density of each type of brain wave we have so far described. With a multi-channel EEG recording, what is commonly known as brain mapping (spatial analysis) may also be performed, and this is the main goal of this thesis project.

2.9 Noise and artifacts in EEG

Not everything on an average EEG reading is signal. In fact, EEG is known to have a particularly poor signal to noise ratio (SNR). The main problems here are that the electrical activity generated by the brain is of very low magnitude and the EEG recordings easily get contaminated by recordings of other bodily functions and from noise from outside sources or electrical devices. These non-cerebral interferences are called **noise** or **artifacts**. Artifacts of extra-bodily origin are called extraphysiologic and artifacts of bodily origin are called physiologic [30].

Extraphysiologic artifacts stem from noise sources in the environment. Radio waves, electromagnetic instruments, even movements of people and objects nearby the patient may produce some noise that will be recorded by the electrodes, so EEG should be recorded in an as much as possible isolated environment. Here are some of the most common or noteworthy extraphysiologic artifacts [32]:

- **Alternating current artifacts**: These artifacts stand at 50 Hz or 60 Hz since this is the typical frequency of alternate current that is used. In Europe and the USA, respectively. A Notch filter suffices to remove this artifact.
- **Electrode related artifacts**: There many common electrode artifacts, such as electrode popping, which is identified by a single sharp wave on the specific electrode. Other artifacts may be related to changes in scalp resistance, etc.

Physiologic artifacts are trickier to deal with and often require more complex methods to remove them. Here are some of the types of physiologic artifacts that one may find in an EEG recording:

- **Muscle artifacts (electromyogram)**: These are the most common artifacts and result from muscular activity. Tremors will produce rhythmic low-frequency activity, whereas contractions will produce higher frequency activity. Artifacts like these, as shown in Figure 15 will generally appear during motor seizures.

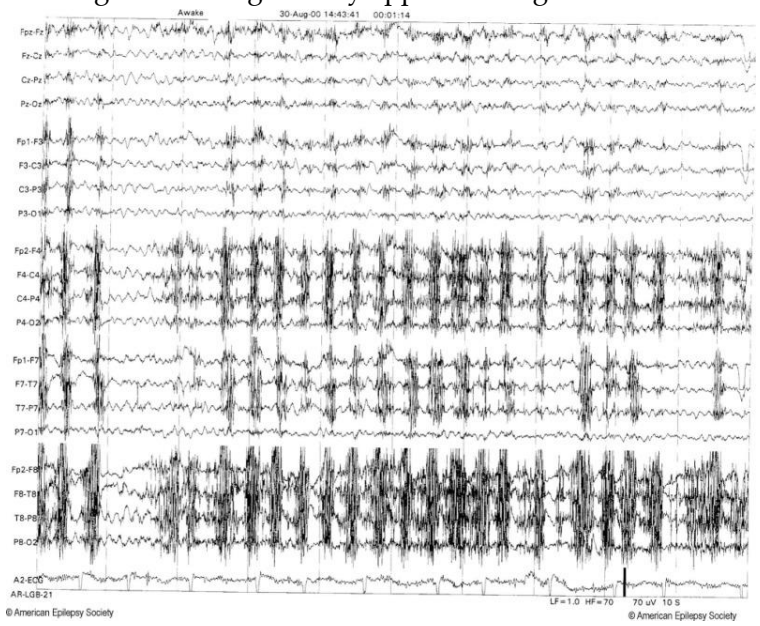

Figure 15 – Chewing artifacts [31]

- **Glossokinetic artifact**: This refers to EEG artifacts produced by thong movements. The thong functions as a dipole with its base being positive in relation to the tip. This will produce a visible effect on EEG.
- **Eye movements artifacts** (Figure 16): Eyes, just like the thong, are dipoles. Eye movements in EEG are useful for identifying sleep stages as they create visible patterns in EEG recordings.

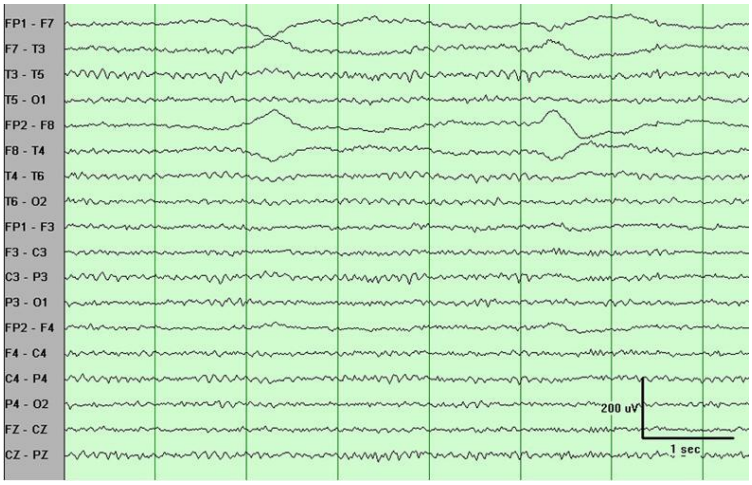

Figure 16– Eye movement artifacts are typically observed in the frontal electrodes. The phase reversals in F7 and F8 indicate lateral eye movements [32].

2.10 Artificial neural networks

An artificial neural network (ANN) is a computational structure that roughly imitates a biological brain. It is a collection of various interconnected nodes, known as **artificial neurons**, each of them able to receive one or more inputs, assigning them a weigh, and generating an output through a transfer function to pass to another neuron or be the value for the final classification. In practice, this allows an ANN to work as collection of classifiers, rather than only one classifier, as each of its neurons and layers can be seen as an intermediate classifier.

Neural networks with various layers of neurons are known as **deep neural networks**. In those networks, neurons are separated in layers, whose number represents the **depth** of the network (akin to the depth of the graph), and the number of neurons in each layer is regarded as the **width** of that layer.

There are currently many different structures for neural networks that can be used to solve problems like the one we have here. We will now be going through some of the proposed ones and discuss the advantages and disadvantages of using each one.

2.10.1 Multilayer perceptron

Multilayer perceptrons (MLPs) are the earliest form of deep neural networks. They are constituted by an input layer, one or more hidden layers and an output layer. They work as feed-forward neural networks, which is the same as saying that they have no cycles, so the output of a neuron from one layer can only go to the next layer. These networks learn through backpropagation.

MLPs learn through **backpropagation of** the error, which is a supervised learning algorithm that basically consists in computing the final classification error obtained in one iteration of the learning process, computing that error into a loss function and updating the neural network weights based on the value obtained from that loss function.

- **Advantages:**
  - Fast training, allowing for more iterations;
  - Easy to implement;
  - Relatively simple final model;
  - Can serve as a starting model and then be customized.
- **Disadvantages:**
  - The vanishing gradient problem [38] can keep these networks from reaching optimal performance;
  - For time series analysis, temporal evolution or causal analysis become especially hard, as these networks don't take into account past or future events, unless given features that explicitly model chains of events, which may not be obvious or hard to obtain;
  - Not designed to deal with any specific type of problem, so may require some reworking to produce significant results for problems that are complex to model.

2.10.2 Deep belief neural networks

A Deep Belief Network (DBN) is simply an MLP with a different training algorithm that consists in training each layer to classify the input from the previous layer with the minimum possible error. This attenuates considerably the vanishing gradient problem, as each layer is now optimized independently. DBNs work as stacks of feed-forward networks.

In terms of advantages and disadvantages, they are akin to those of an MLP, except for the fact that the vanishing gradient problem is basically solved, so they generally outperform those.

2.10.3 Convolutional neural networks

A Convolutional Neural Networks (CNN) is a form of feed-forward neural network with some different hidden layers, called convolutional layers. The neurons in these layers organize their inputs into a matrix and then apply convolutions with certain filter matrixes to those matrixes. Obviously, this only improves the learning process if the data provided to the network makes sense to represent in matrix form.

- **Advantages:**
  - Good performance when processing data that can be represented by a matrix, such as an image or a video;

- The feature extraction and selection may be simplified or even skipped when using CNNs, as using the raw matrixes or part of them as input may suffice.

- **Disadvantages:**
  - If unidimensional vectors of holistic features that represent the dataset can't be produced, and one must resort to images or videos to serve as an input, they need to be produced or extracted, which can take time to process;
  - The training phase is expected to be slow, as processing matrixes has higher complexity that processing unidimensional features, and convolutions take more time than applying transfer functions;
  - For the same reasons, classification is also expected to be slow, unless the neural network is regularized;
  - Temporal evolution and causality are also difficult to model in strictly spacial CNNs, because of the reasons explained above.

2.10.3.1 Temporal convolutional neural networks

Temporal convolutional networks (TCNs) are a form of CNNs, that applies convolutions temporal data, essentially doing the same as RNNs in a more efficient way. These networks are fairly recent and have the potential to becoming state of the art in solving many problems that LSTMs are currently used for [40, 41].

2.10.4 Recurrent neural networks

Recurrent neural networks (RNNs) are neural networks with a built-in feedback loop, that is, the output of a neuron of a certain layer can be added to any other layer in the next iteration. These networks receive a sequence of values as input and output a sequence of values as well.

The training method here is slightly different and is called backpropagation through time [39].

- **Advantages:**
  - These networks can model sequential behavior quite easily, as, when calculating an output for a certain time step, they can take into account any output from another previous time step, making them good choices to model temporal evolution and causality;
  - For the same reason, the number of false positives and false negatives, when trying to detect a preictal state, may be reduced, as previous preictal or interictal classifications may be used as a way of encouraging or deterring the classifier from classifying a certain time period as preictal, respectively.

- Disadvantages:
  - Extra connections mean that extra weights need to be corrected in each training step, so these networks take longer to train and the final model is very

complex, producing a slower classification (this can be attenuated using regularization);
    - The vanishing gradient problem and the exploding gradient problem are harder to solve in an RNN.

2.10.4.1 Long short term memory neural networks

A long short-term memory neural network (LSTMs) is a type of recurrent network that has a memory cell and a forget gate that allow the network to select information from previous iterations to be used on further iterations and create a classifier based on that. Compared to regular RNNs, LSTMs can not only store a previous output, but also a previous input.

- **Advantages:**
    - Sequential analysis is now enhanced, allowing signals or events that depend on a previous input to be correctly modeled; if there is a relation of causality in the system that is independent of the output of the system (such as the previous value of a certain feature), these neural networks are able to incorporate such a relation in the classification process;
    - The temporal evolution of a signal may be modeled without needing to extract specific features for that purpose;
    - Designed to deal with the exploding and vanishing gradient problems of RNNs
- **Disadvantages:**
    - Very heavy computationally, both in training and classification (in this case, regularization can help), even more than a regular RNN;

2.10.5 Attention-based mechanisms

Attention is a fairly recent development in neural networks. It allows the algorithm to only focus on certain important parts of the input that is to be classified, making training far more efficient. This is especially interesting for brain mapping, as it allows our model to focus on specific regions of the brain or scalp, that can be either predefined or figured out by the network. For more information, refer to [42].

2.10.6 Adaptive resonance theory-based neural networks

Adaptive resonance theory (ART) refers to a theory on how the brain recognizes patterns. It proposes that pattern recognition occurs as a result of the interaction of 'top-down' observer expectations with 'bottom-up' sensory information [43]. This model postulates that the brain stores memories as templates for a certain pattern and compares them with objects detected by the senses. As long as the difference between the expected pattern and the object does not exceed a certain threshold, the object

is classified as being of the same class of the said pattern. If no expected patterns are similar enough to the object in question, then a new template pattern is created based on the features of said object. This theory offers a plastic and stable base for unsupervised learning. Networks based on this theory, in their simplest form, deploy one neuron for each pattern and, when they receive a new input, check which neuron has the closest model for that new input and choose it, perform a check to see if that pattern is similar enough to the input and, if it is, classify it as such and update the weights, if it isn't, create a new neuron for that pattern.

This type of neural networks is interesting as, in this problem, it is definitely not guaranteed that all preictal or ictal patterns are even similar in the same patient, let alone across different patients. The same is true for the duration of the preictal state. An unsupervised learning method like this one can at least help with mapping, classifying the various ictal and preictal states found and tell us when they start, if not allow for an accurate classification as well.

Chapter 3

State of the art

3.1 Earlier approaches to seizure prediction

The first approaches to seizure prediction date back to the 70s [59] when Viglione and Walsh [57] decided to try to predict absence seizures with linear approaches which were followed by Sigel et al in 1982 [58], who noted that absence seizures could be predicted by analyzing the power spectrum density of the EEG signal one minute before absence seizures with 64% to 84% accuracy. Rogowski et al. [60], in 1981 and Salant et al. [61] in 1998 reported significant pre-ictal changes six seconds before seizures using auto-regressive modeling.

During the 90s and early 2000s, various seizure prediction attempts by analyzing certain features in pre-ictal data [59], such as Lyapunov exponents [62], spatiotemporal correlation density [63] and dynamical similarity [64, 65] were performed, however, this studies did not take into account interictal data, having no controlling mechanisms, which makes it impossible to access the specificity of these proposed approaches.

The first, controlled studies testing preictal data against interictal data using measures such as correlation dimension [66], dynamical entrainment [67] and accumulated signal energy [68] showed the capability of distinguishing preictal data from interictal data.

However optimistic these early results might seem, as more extensive databases became available, reassessment studies were performed on measures such as correlation dimension [69], similarity index [70] and accumulated energy [71] that found substantially poorer predictive performance than was led to expect from previous studies. Due to these studies and others, the reproducibility of earlier studies was put into question in [72], as well as the very suitability of the aforementioned non-linear measures for temporal analysis of EEG [73, 74].

In 2002 the First International Collaborative Workshop on Seizure Prediction [75] was held. In this workshop, various methods of seizure prediction were compared on a joint dataset. Bivariate and multivariate measures were found to outperform univariate measures [59], suggesting that a combination of factors must be studied in order to predict seizures. The pre-ictal changes in EEG were also found to be restricted to certain channels.

Shortly after these events, the first seizure prediction algorithms [76, 77, 78] were developed, which unfortunately produced sensitivity and specificity results that were unacceptable on a clinical level.

3.2 Modern day approaches to seizure detection and prediction

Modern day approaches to seizure detection and prediction are tendentially keener on building classifiers or classification models based on either features retrieved from EEG or even raw EEG. Many studies now use machine learning models such as support vector machines (SVMs) or ANNs. We will go over a few of these studies, in order to paint a diverse picture of how the state of the art of seizure detection and prediction looks like and try to expose a variety of methods and features that may prove useful to this thesis.

3.2.1 Seizure detection

Seizure detection consists in simply differentiating ictal from interictal data, disregarding the preictal and postictal states. Automatic seizure detection can be very useful to monitor patients on a clinical level as it is crucial to be able to detect all seizures that are afflicting the patients [79], to keep them as safe and healthy as possible.

Seizure detection in the time domain requires discrete analysis of consecutive EEG epochs in order to classify them as ictal or not. This can be achieved, for example, as Runarsson and Sigurdsson [80] did, by producing histograms of the epochs of the signal, taking the amplitude difference between peaks and lows of the signal and their separation in time. Using an SVM classifier, this study was able to achieve 90% of detection rate on self-recorded data. Other methods such as Principal Component Analysis (PCA), Linear Discriminant Analysis (LDA) and Independent Component analysis (ICA) have also been applied to the temporal distribution of signals to extract features for classification [82].

Treating the signal on the frequency domain is more common. These methods trend to exploit the phase and magnitude of the various frequency components of the signal being measured, obtained by applying a Fourier transform, and various higher level features that can be obtained using them. An example of this is the work of Khamis et al. [81] that uses moments of power spectral densities of EEG signals as features to perform classification, obtaining 91% of detection rate and 0.02 false positives per hour in a total of 618 hours.

Entropy, largest Lyapunov exponents, Hurst exponents and other non-linear measures can also be used to exploit the stochasticity, non-linearity and non-stationarity of EEG signal for seizure detection, despite their apparent past failures in seizure prediction. A good example of success using these measures applied to different frequency bands of EEG is the study from Martis et al. [83] that obtained 99.5% of sensitivity and 100% of specificity using SVM classification.

Wavelet-based methods have also been used for seizure detection quite extensively. One interesting and successful study was performed by Orhan et al. [84] who used discrete wavelet transforms (DWTs) to decompose EEG signal in sub-bands, clustering the wavelet coefficients using K-means and feeding them as input to a multilayer perceptron (MLP). This study obtained values for accuracy

ranging from 95% to 100%. This isn't the only study using wavelet analysis that obtained this level of performance, showing that wavelet analysis is suitable for this problem.

Another very interesting and worth mentioning study in seizure detection is the study of Weng and Khorasani [85] that uses Adaptive Resonance Theory based neural networks to create an automatic adaptive model that is able to effectively discover new patterns of seizures automatically and attribute to them a certain classification. The study managed to obtain 94.9% sensitivity and 100% specificity. This study can serve as a base to build predictors that are able to adapt themselves to each patient, which has always been something that researchers on seizure prediction have struggled with, given the heterogeneous nature of seizures.

Spatial analysis using Convolutional Neural Networks (CNNs) has also been performed by Wei et al. [86] This study uses a three-dimensional matrix with multichannel EEG as input of a CNN, achieving 88.90% of sensitivity and 93.78% of specificity.

When it comes specifically to the use of topographic maps for seizure detection, there is not much work available. However, it is worth noting that it makes sense to analyze most EEG features on a topographic/spacial basis, as brain currents propagate from electrode to electrode, making the signal in one electrode dependent on signals of close by electrodes, and brain signals are particularly well known to display some lateralized behavior, amongst many other reasons. One study that used topographic maps for seizure detection was conducted by Min Jing and Saeid Sanei [92] who came up with a method that they called topographic independent component analysis (TICA) which, to put it in simple terms, consists in applying a version of ICA that considers a certain degree of dependency between electrodes depending on how close they are to each other.

Plenty of more work with similar results has been done when it comes to seizure detection. One can say that, overall, seizure detection models have rather good performance. However, it is worth noting that the majority of these studies were done in datasets that are not particularly extensive, since the extensive ones, like the EPILEPSIA one, are fairly recent. Thus, their performances may be a result of overfitting the studied dataset and not such good usability in a clinical set.

3.2.2 Seizure prediction

Prediction of epileptic seizures is a more complicated problem than detection due to the fact that preictal states are more similar to interictal ones than ictal ones are. For this reason and despite the fact that the literature on prediction of seizures is more extensive than the one on detection, the performance of prediction models trends to be a lot lower than the one of detection models, especially when it comes to specificity. However, there are still studies that yield promising results and, as stated before, there are statistically significant differences between the preictal and interictal states [25, 36, 37], even if less than the ones between the ictal and interictal states, making it very important to have long interictal periods when testing seizure prediction models [88]. Many measures, features and methods used for seizure detection are also used for prediction.

One of the most basic and intuitive ways to approach this problem is to exploit the envelope of amplitude of the signal. This is what Li et al. [87] did, by applying averaging filters and morphological operations to transform the signal's envelope into a series of spikes and setting a spike ratio threshold to distinguish ictal, interictal and preictal states. This method was able to achieve a sensitivity of 75.8% and a false alarm rate of 0.09/hour.

Non-linear measures continue to be used for seizure prediction. One example of that is the study from Aarabi and He [89] which created a patient-specific time-domain rule-based predictor that combines various non-linear measures such as: correlation entropy, correlation dimension, Lempel-Ziv complexity, noise level, largest Lyapunov exponent and non-linear independence. The tests were only performed one or two patients, which is clearly an insufficient number of patients to determine the real accuracy of the implemented method. However, patient one obtained 90.0% sensitivity and 0.06 false positives per hour, while patient two obtained 96.5% sensitivity and 0.055 false positives per hour.

Studies based on the frequency domain are more common when it comes to seizure prediction. One of those studies is the study from Bandarabadi et al. [90] done by researchers in CISUC which use the relative power spectrum density between brain waves. This study was performed on the EPILEPSIA database, which provides certain advantages on evaluation due to the various extensive recordings that it contains. The obtained 75.8% sensitivity and a false prediction rate (FPR) of 0.1/hour.

Wavelet-based analysis is also one of the ways that one can find in the literature when it comes to seizure prediction. Elgohary et al. produced a study using the zero-crossings of the wavelet transform coefficients of EEG as features for a binary SVM classifier that distinguishes between interictal and preictal sates. This study obtained a sensitivity of 96% and a specificity of 90%. This study, has the particularity of only selecting 10 minutes of data for training, in order to try to build a predictor that does not require long term data recordings. This study shows that this feature has great potential when it comes to predicting epileptic seizures.

Studies using multiple different features both on time and frequency domains have also been performed in CISUC. One by Direito et al. [91] has compiled a set of features available in EPILAB [46] that include auto-regressive modelling prediction error, decorrelation time, signal energy, Hjorth exponents of mobility and complexity, relative spectral power of the various brain waves, spectral edge power and frequency, mean, standard deviation, skewness and kurtosis and six decomposition levels of Daubechies wavelet coefficients. The most relevant features were selected for each patient and classification was performed using SVMs. The study obtained only 38,47% sensitivity and 0.20 false positives per hour. The poor performance of this study is due to the fact that it was designed for the testing to approach as much as possible a real environment, something that is not very common in the literature. 216 recordings of patients from the EPILEPSIA database prefacing 16,729.80 hours of inter-ictal data and 1206 seizures were used for testing this study. This study clearly shows that sometimes promising results by studies performed in smaller datasets are not reproducible in a real or close to real environment and that much work still needs to be done in this area.

When it comes specifically to exploiting topographic maps for seizure prediction, not much has been done. However, there is a particularly interesting study from Direito et al. [37] who performed seizure prediction using topographic maps of spectral power densities of brain waves. Their method consists in finding points of interest in the maps and tracking those points over time. A Hidden Markov Model (HMM) was used to perform classification by distinguishing between the ictal, preictal, postictal and interictal states. This study was performed in 10 patients suffering from focal seizures and obtained an average of 94.59% sensitivity and 92.22% specificity, highlighting the potential of topographic maps to be used for seizure prediction and detection.

In terms of spatial analysis, quite a few studies were published recently that show promising results for seizure prediction. One of those studies dates only to the end of last year and was performed by Hisham Daoud and Magdy Bayoumi [96]. Their method consists in producing tridimensional matrixes in which two dimensions represent the spatial distribution of electrodes over the scalp and one has the raw (yet denoised) EEG data of each electrode. These matrixes are then used as input for a CNN. In the first layers of the CNN, the matrix is convolved in the spatial dimensions to find a region of interest. Then it is feed into a network that also possesses an LSTM module that allows it to take into account matrixes corresponding to previous time frames to allow the neural network to also study the temporal evolution of the EEG signal. This method has been able to produce 99.6% sensitivity and an FPR of 0.004/hour and, even more interestingly, a prediction time of 1 hour. This certainly one of the most successful studies on this field and showcases the ability of both spatial features and temporal evolution to produce results that are clinically acceptable. However, this study was performed with raw EEG data and, for this reason, there is extremely high overload on the classification process.

Seizure prediction, despite all the efforts done on this area, is still an issue that needs further study, yet the results obtained from researchers are promising. This is a very complex and difficult problem that can be explored in many different ways. Studies like the one of Direito et al. [91] show that the models and algorithms for seizure prediction need to be tested in an environment that emulates as much as possible a real one in order to really evaluate their prospects for clinical use. Studies like this one are, unfortunately, more an exception than a rule.

Chapter 4

Materials and methods

The work that will be developed in this thesis will require data and various methods and processes that should also be explained. In this section, we will go through the data, the framework, and the methods and technical artifacts that need to be taken into account to work on this thesis.

4.1 Framework

Our framework (figure 17) consists on acquiring the signal, preparing it, dividing it into training a testing set, organizing it into a map, feeding it on a neural network, performing cross-validation, performing a parameter search, passing the results through a regularization process and analyzing the results. In schematic terms:

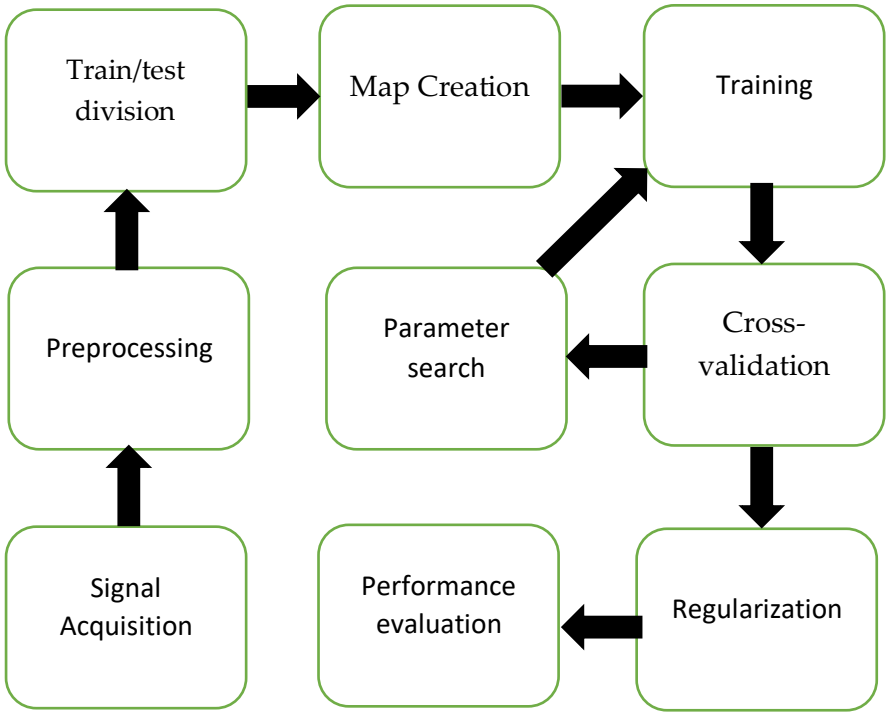

Figure 17: The framework of our project.

Each of these steps will be explained in further detail below.

4.2 Planning

The work of the first semester consisted more on studying the problem, creating topographic maps and writing the report. The topographic map framework ended up not being used.

The second semester essentially consisted of following our framework. The Gantt diagram of figure 18 illustrates this.

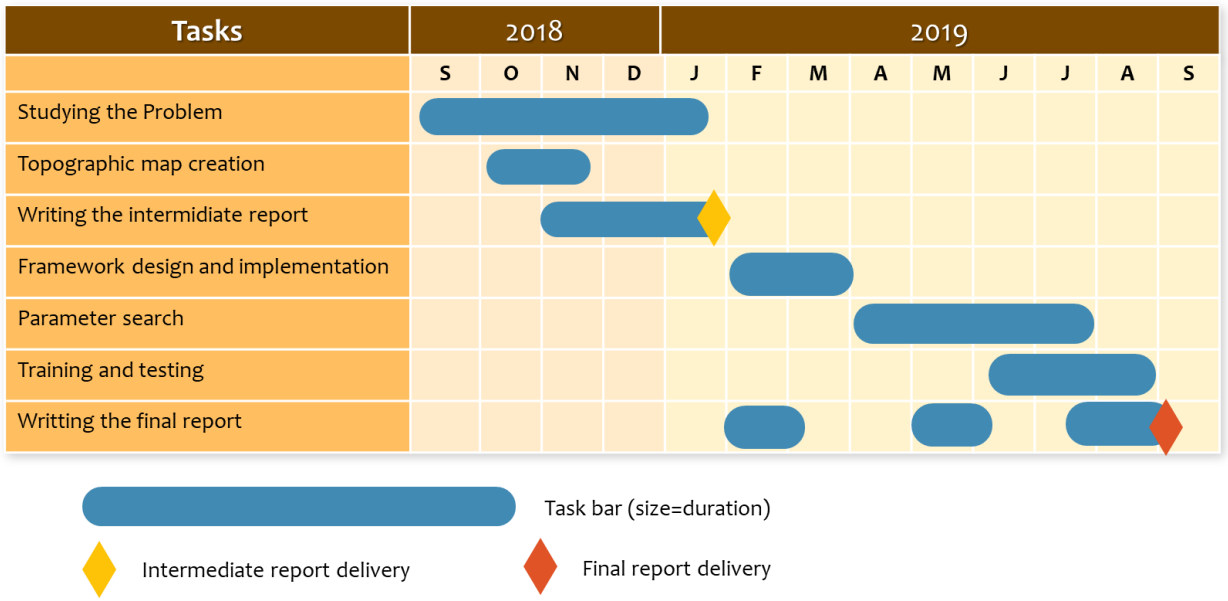

Figure 18 – This thesis' final Gantt diagram

4.3 Signal acquisition

Since the very beginning, it was proposed that I would work with the EPILEPSIA database [44], the largest epilepsy database worldwide. It contains long term EEG and ECG recordings of 275 patients that suffer from epilepsy, as well as extensive metadata and annotations, prefacing in total over 40000 hours of recording. These recordings were provided from epilepsy centers of the University Hospital Freiburg, Germany, of the University Hospital of Coimbra, Portugal, and of the Hospital de la Pitier-Salpetriere in Paris, France.

217 of these are surface recordings, while 58 are invasive EEG recordings. Some of these patients also had their EMG recorded. The surface recordings were performed using a 10-20 electrode system, sometimes with a few additional electrodes and recordings of a reference electrode and scalp resistance and invasive EEG recordings can use up to 125 electrodes. The sampling rates vary from 250 Hz to 2.5 kHz and the number of seizures recorded for each patient varies between 3 and 94 in a recording that lasts 165 hours, in average.

The annotation scheme is both based on video analysis and EEG screening made by experienced staff members and EEG signal analysis made by epileptologists. The first method was used to record the clinical onset and the second was used for the EEG onset.

Along with the EEG and seizure related data, characteristics of the patient such as his/her age, the medication that he/she was prescribed, etc. are also stored. For this work, we considered the focus of the seizure and its pattern to be the primary ones to analyze.

One of the most important advantages of this database is that it not only contains the EEG recordings of seizures and activity near them, but it also contains full sets of interictal recordings of the patients, allowing a real-time like evaluation of the detection and prediction performance.

This database is also particularly interesting for the fact that all recordings are from people who would later undergo surgery, so these patients all suffer from drug-resistant epilepsy which, for obvious reasons, is the category of epilepsy that is the most important to develop a predictor or detector for.

For more information on this database check Klatt et al. [44] or the official site of the database [45].

4.4 Preprocessing

This step consists of selecting the data we need for evaluating our model in a realistic way. In our case, we need continuous data containing both interictal and ictal samples. It is preferable that the interictal data is before the ictal data, as it can allow us to understand how our model performs when a seizure is about to begin. For reasons explained in section 4.6.2, it was decided that we would only work with seizures that had by at least one hour of continuous (or only briefly interrupted) interictal data recorded right before them.

4.4.1 Noise and artifact removal

As mentioned in the previous section, alternating current noise can be removed effectively with a Notch filter. D/C current can also be removed with a high pass filter. This proved to be unnecessary later on, as using these filters did not change the performance of our network. This is to be expected as these forms of noise are independent of ictal and interictal samples.

Other artifacts require more complex techniques to remove that are not viable in real-time, most often. Due to this, it was decided that we would try to train our neural network with the artifacts present on the EEG. This proved to be a problem in some situations, as explained in the results and discussion section.

4.5 Map creation

4.5.1 Compressed maps

Compressed maps were developed by figuring out which would be the most efficient representation that could preserve the spatial features of the input data.

We have five electrodes both in the central meridian and parallel of the head. Since we are considering a spherical head model, we can consider that both dimensions are equal in our model. Likewise, the upper and lower meridian and the upper and lower parallel of the head, we find five electrodes. Since all electrodes mentioned so far in this paragraph are supposed to have a distance from their nearest electrode either to the left, right, above or below of 10% of the front to back distance of the skull, we can simplify things and organize these electrodes in a 3x5 rectangle. We can add the three electrodes in the front (Fp1, Fpz and Fp2) and back front (O1, Oz and O2) of the head respectively centered on top and bottom of our rectangle. If recordings for Fpz and Oz are not available, we can simply compute the interpolation of the three nearest electrodes with equal weights, since they should all be equidistant from Fpz or Oz. This would suffice, however, since we want to use a CNN, a full rectangle would be more convenient. All that we need to do, in this case, is compute the bottom left and right and the top left and right values as the interpolation of its nearest electrodes, according to the expected distances. We then have a 5 by 5 square matrix with our values than can be computed into a CNN.

4.5.2 Compressed raw maps

It was decided that raw data should be tested before features. There are various reasons for this, such as neural networks being expected to work on raw data without problems, CNN filters in practice already retrieve and select features and with raw data we are giving the classifier the maximum possible quantity of information. Also feature selection in real-time may take too long, while evaluating raw data is fast enough to give a human the sensation of being instantaneous. This ended up being the only method that we could test, due to time restrictions.

The representation used consists of using a 5-by-5-by-x matrix where x corresponds to sampling rate times the temporal window size. The values on this extra dimension correspond to the temporal values of the electrodes or interpolation of these values, according to our map model. We can call these maps “Compressed raw maps”.

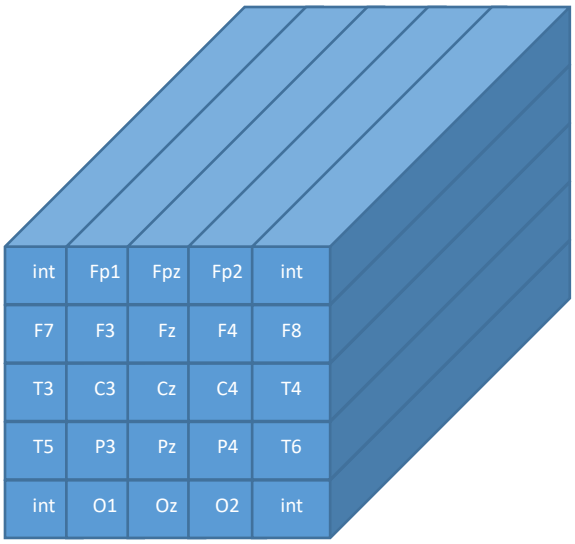

Figure 19: Scheme of our neural network input.

4.6 Model

4.6.1 Artificial neural network

For seizure detection, a typical CNN was chosen as the model. This is due to the fact that CNN's, as explained previously, are state of the art for image processing and we can treat our maps as tridimensional images. Since it was decided that raw data was to be used, tridimensional convolutional layers are necessary to process the input. Apart from this, the rest of the architecture of the neural network and its parameters must be selected. But first, we must take a look at what kind of input is going in our neural network.

4.6.2 Input

Given the fact that this is a highly imbalanced problem since there are far more non-ictal samples than ictal ones, there has to be a strategy to prevent our model from tuning itself to perform well only for the more common class. There are two typical paths to solve this problem:

1. Balance both datasets, simply by using just as many non-ictal samples as ictal ones, in this case;
2. Apply a higher misclassification cost to the class that has the least number of samples.

Since the first approach would result in too few samples to use a CNN reliably, the second was chosen.

At first, a window of 5 seconds was chosen and every 5 seconds of sample were compiled without any overlap. It took very little to realize that this did not produce enough samples for machine learning

processing and the few tests done resulted in good performance on the training set, and very poor performance on the testing set, which is a clear sign of overfitting.

This problem was solved by using an overlap of 80% (4 seconds) in the same 5 seconds window. This allowed the upsampling of seizure cases and resulted in solving the problem of overfitting.

Apart from this, there were two input methods considered:

1. Use only cases where, for the whole duration of the five seconds, either the sample corresponded to an ictal event or an interictal/preictal time for its full duration, that is, either all five seconds are identified as ictal or not.
2. Use only fully interictal/preictal samples for the samples labeled as non-ictal and use both fully ictal and partially ictal (starting as preictal and ending as ictal) samples for the ictal time. In this case, the first sample to be classified as ictal in each batch would have four seconds classified as interictal and one classified as ictal, the second would have three classified as interictal and two as ictal and so on until all seconds of the sample are classified as ictal.

Both cases were tested, yielding similar results, with the only difference being that the first case took about 3 times the number of iterations to train the neural network to a value of loss equal to the second case. Since time and computational capabilities were major technical restrictions in this work, it was decided that the second option would be taken.

The preictal/interictal time before each seizure to go into the neural network was also briefly tested. Two options were considered: seizure and non-seizure time for each seizure prefacing 1 hour and an analogous method but with 2 hours of data. The tests showed very little difference between both methods in terms of performance, so 1 hour was considered sufficient to represent a time long enough to simulate interictal temporal sample evaluation in real-time. So, for each seizure, we will be taking the ictal period and enough interictal data before the seizure to make one hour in total. This will be what our neural network will receive in each batch. As a consequence, only seizures which have an interictal time of at least one hour before it recorded will be possible to use. This may sound like a disadvantage, and it can be, for the reason that some seizures will be inevitably excluded, but it allows us to create measures that will be uniform for each seizure, facilitating comparison between them and, as a consequence, between each patient.

With the input method defined, we can now search a few possible architectures.

4.6.3 Network architecture

Only CNN's were chosen as they have the ability to extract both spatial and temporal features in their convolutional layer.

Since it would be too lengthy of a job to search the network architecture extensively, a few alternatives were chosen to be tested with one patient, with similar parameters. Those alternatives were:

1. 1 convolutional layer and 3 feedforward layers;

2. 1 convolutional layer and 4 feedforward layers;
3. 1 convolutional layer and 5 feedforward layers;
4. 2 convolutional layers and 4 feedforward layers;

After each convolutional layer, there exists a pooling layer performing a max-pooling operation and after each convolutional layer, an RLU (rectifying linear unit) is used.

The parameters of the networks were selected so that the total number of neurons was similar in all the tests and, in the case of the last architectural option, a few different parameters were tested for the convolutional layers, and the best result will be the only one presented.

Architectural option	Convolutional layer parameters	Feedforward layer parameters
1	3,3,48,1	78,16,2
2	3,3,48,1	39,39,13
3	3,3,48,1	30,30,10
4	[2,2,16,1] x 2	39,39,13

Table 1: Architectural options for our neural network

4.6.4 Base parameter search

Since a full grid search would take far too long, the parameters were searched using a bottom-up approach, meaning that the parameters that define the structures that the initialization method was the first parameter to be searched and then we proceeded to search the parameters for the structures of the neural network by the order in with they transform the input. The parameters on which this pseudo grid search was applied were:

1. Initialization method;
2. Size of convolutional filter dimensions;
3. Number of filters being trained;
4. Maximum width of the layers of the feedforward neural network;
5. Seizure misclassification penalty.

Each network configuration was run five times to provide statistical significance.

4.6.4.1 Initialization method

The weights, biases and filter parameters must be initialized in some way, in order to lead the learning process in the right direction and prevent the gradients from exploding or vanishing. The initialization methods considered were:

1. Initializing everything as ones;
2. Random normal distribution 1: a typical Gaussian distribution of mean 0 and standard deviation 1;

3. Random normal distribution 2: a typical Gaussian distribution of mean 0 and standard deviation 5;
4. Random uniform distribution 1: a uniform distribution with a minimum value of 0 and a maximum value of 1.
5. Random uniform distribution 2: a uniform distribution with a minimum value of -100 and a maximum value of 100.
6. Glorot normal distribution: an initialization method based on normal distributions of mean 0 and setting the variance of the weights to a value that preserves the variance and gradient from layer to layer [102].
7. Glorot uniform distribution: analogous to the previous method but using a uniform distribution and setting the maximum and minimum values of the weights in a way that preserves the variance and the gradient from layer to layer [102].
8. Orthogonal distribution with the biases initialized as ones: The initializer generates an orthogonal matrix. Since the biases are column matrixes, they have to be initialized differently.
9. Truncated normal distribution: a truncated normal distribution at 2 standard deviation values with mean 0 and standard deviation 1.
10. Uniform unit scaling distribution: an initialization method that aims to preserve the scale of the input variance from layer to layer in the network by initializing the weights in the interval:

$$\left[\frac{-\sqrt{3}}{\sqrt{dim}}, \frac{\sqrt{3}}{\sqrt{dim}}\right]$$

    Where dim is either the number of neurons in the respective layer in the case of a feed-forward layer or the product of the first 3 dimensions in the case of a convolutional layer.
11. Variance scaling distribution: Also attempts to preserve the scale of the input variance, but this time through computing a truncated normal distribution with an average of 0 and a standard deviation of:

$$\sqrt{\frac{factor}{n}}$$

    Where factor, in our case, is set to 2 and n is the number of input connections in each layer.

4.6.4.2 Convolutional layer

Our tridimensional convolutional layer receives 4 different parameters, apart from the initialization method, which are the sizes of the three dimensions of the layer's filter and the number of filters. It was decided that the first two dimensions would be the same, due to the fact that it would not make sense to search each of them independently from each other, as they both relate to the spatial component of the EEG and it would take far too much time to perform a grid search on all their possible combinations. However, the author highly recommends that this is done if there would be future attempts to turn the presented model into a real medical support system

We considered the following parameters in each layer:

- First and second dimension: we considered all the possible dimensions from 1 to 5;
- Third dimension: we considered the parameters 16, 24, 32, 48, 64 and 88;
- Number of convolutional filters: we considered a number of filters from 1 to 5.

4.6.4.3 Feedforward network

Our feedforward network has four layers: one input layer, two hidden layers and one output layer. Since we are using one-hot labels, our output layer will be the size of the output space, which is 2. Due to time and resource restrictions on the parameter search, it was decided that the input layer and the first hidden layer would have the same size and the last layer would have 1/3 of their size. Given this, we decided that the maximum width parameters of our feedforward network would be: 12, 18, 24, 33, 42, 54, 66, 81 and 99.

4.6.4.4 Misclassification penalty

Misclassification penalty or misclassification cost is the extra penalty applied to classifying a seizure sample as interictal. This is applied on the backpropagation algorithm for rectifying the weights, in each iteration, to the error calculation, to all the ictal samples. So if we have a misclassification penalty of 5, it means that the error calculation on the backpropagation algorithm will be multiplied by 5 for each seizure sample, causing the model to consider each ictal sample as 5 times more important than each interictal sample to the final result for the weights of the corresponding iteration. As stated before, this was the chosen way to solve the high unbalance in the data.

The misclassification cost could simply reflect the proportion of interictal to ictal samples, which would always leave us with possible penalty values over 100. However, we want to minimize, first of all, the false positive rate, since, in practice, a seizure only has to be detected as early as possible, giving room for some false negatives afterwards and many and possibly long streaks of false positives should be avoided, as that would make our model too unreliable and the generated seizure alerts would have no meaning. Due to this, our search focused on slightly lower values. The values chosen were: 30, 40, 50, 60, 75 and 90.

4.6.4.5 Other parameters

Other necessary parameters were left out of the search, due to time restrictions. Those include:

1. Number of iterations: set to 400 during the tests;
2. Lower bound for loss: set to 0.05;
3. The learning rate was set to 0.0005, since this was the lowest value found, after some testing, that did not make the gradient explode;

4. The optimizer chosen was the ADAM optimizer [103], as it is currently considered the state-of-the-art optimizer;
5. Max pooling used on the tests was set to:

$$\left[6 - cx, 6 - cy, floor\left(\frac{1280 - cz}{104}\right)\right]$$

   With cx as the first dimension of the convolutional filter, cy as the second and cz as the third. This gives us a final result of [2,2,12];

6. Strides for the convolutional layers were set to [1,1,8];
7. No padding was used.

4.6.5 Training methods

Using the parameters obtained in our search as base, we trained and test our model with more patients. In various cases, a further small parameter search was performed, as is represented in the flow diagram in figure 17.

The chosen way to validate our model's performance was through cross-validation, since, in a real environment, seizure cases to be detected would obviously not have been part of the training set, so we divided our data into training and testing sets

Our neural network was trained using three approaches: standard, progressive and mixed.

4.6.5.1 Standard approach

The first approach consisted in, for each patient, training is performed using the parameters that were obtained in the parameter search on its the training set and then testing the resulting model on the testing set. Seizures are divided into training and testing in chronological fashion, using the oldest for training and the newest for testing. This is a very standard approach when performing cross-validation, so that is exactly what we will be calling it.

4.6.5.2 Progressive approach

The second approach used in this thesis project consisted in training and testing with our data by progressively adding new seizures to the training set, in chronological order, and testing only with the immediately next seizure to the last one added to our training set. To put this in a simple way, we start with 3 seizures for the training set in each patient, train a model, and test it with the 4^{th} oldest seizure; then, we add that testing seizure to the training set, retrain the model and test with the 5^{th} seizure. This keeps going on until there are no more seizures to test. This is expected to improve our results, as there are now more seizures on the training overall.

4.6.5.3 Mixed approach

What we call mixed training here consists of picking a group of patients with similar characteristics and dividing it into train and test groups. The patients on the training group are used to produce the model, by training a neural network with the architecture and parameters selected with their ictal and interictal data and the analogous data from the patients in the testing set is used to test the model.

The purpose of this training method is to evaluate if it is possible to use data from already existing databases to detect seizures of new patients, that is, creating a ready-made seizure detection system without having to subject patients to a data collection and model creation process.

We are not expecting results that can compete with the results from previous methods, as we are now dealing with a much more difficult problem.

4.6.6 Regularization

Since one second being classified as ictal or non-ictal is hardly relevant, as it can easily be a false positive or false negative, triggering or stopping an alert based on just that would lead to a very inconsistent, flawed and highly erroneous system. Due to this, there must be some form of regularization.

The chosen form consists of triggering a series of alerts based on how many instants/seconds were classified as ictal consecutively. The alerts go as follows:

1. Yellow alert: When 2 consecutive instants are classified as ictal;
2. Orange alert: When there is an instant classified as ictal right after a yellow alert;
3. Red alert: When there is an instant classified as ictal right after an orange or red alert.

Each time there is an instant classified as interictal right after an orange alert, a yellow alert is triggered, effectively lowering the alert's importance. In the same way, a red alert may be dropped to orange.

The only actually relevant alerts in this model end up being the red alerts, as yellow alerts are rather weak and can easily be a result of localized noise and orange alerts usually appear as a transition to red alerts. However, orange and yellow alerts are useful to measure when red alerts will be triggered.

Chapter 5

Results and discussion

5.1 Network architecture

One patient, a patient from the EPILEPSIA database labeled with the ID 58602, was used to search for the optimal architecture. 10 seizures of this patient, and previous non-ictal time, as explained above, were selected for training, and other 10 for testing.

The false positive and false negative rates were tabled for each of these architectures, producing the following results:

Architectural option	Convolutional layer parameters	Feedforward layer parameters	FPR	FNR
1	3,3,48,1	78,16,2	0.04544	0.26221
2	3,3,48,1	39,39,13	0.00400	0.21507
3	3,3,48,1	30,30,10	0.02238	0.28338
4	[2,2,16,1] x 2	39,39,13	0.21288	0.58958

Table 2: Parameters for the various options for our network architecture

Given this, option 2 was chosen as the architecture to work with, giving us a network that can be summarized by the following figure:

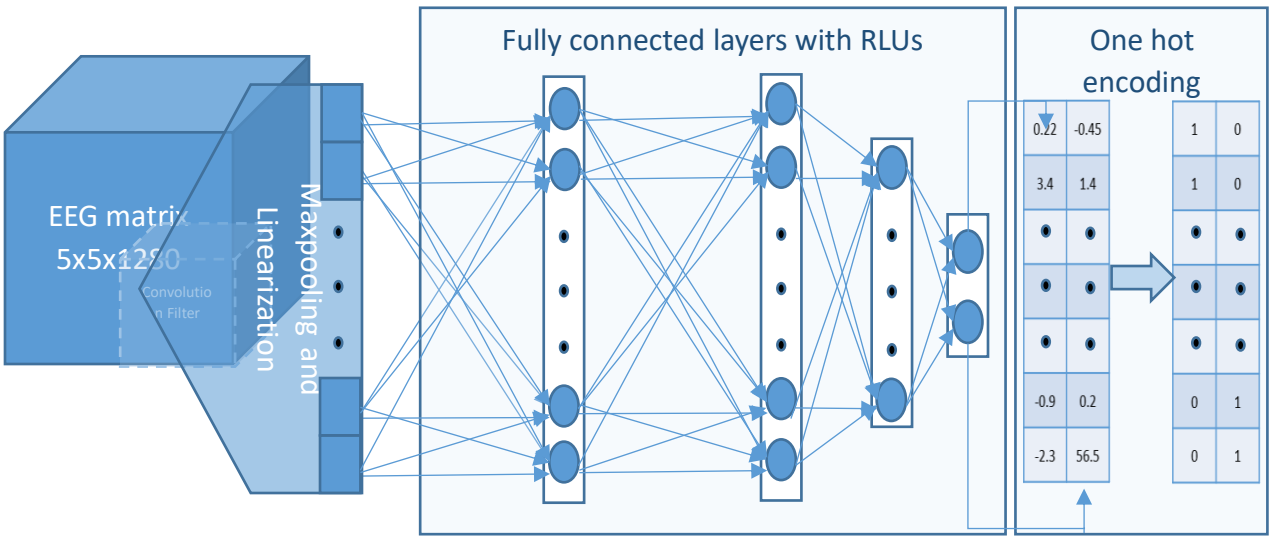

Figure 20: Scheme of the neural network architecture that will be used.

5.2 Base parameter search

The best parameters were chosen based on both the FPR and the FNR, since our purpose here is to minimize both. Once again, data from patient 58602 was used in the same fashion.

5.2.1 Initialization method

Since there were many initialization methods to consider here, and it was expected that some of them would not produce desirable results, and thus would be a waste of time to run all of these, one primary run throughout all of these methods was performed with the following results (Figure 21)

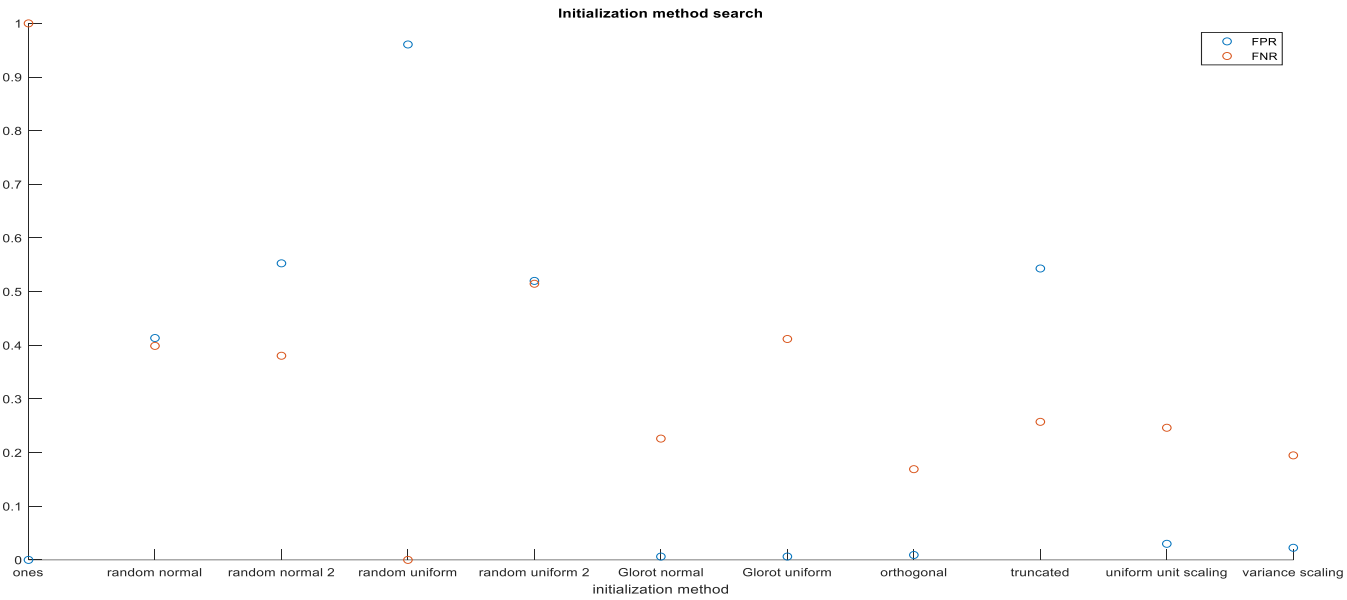

Figure 21: Preliminary initialization method search

The best performing methods were then selected for further evaluation, involving 4 more runs of each. The results were the following (Figures 22 and 23):

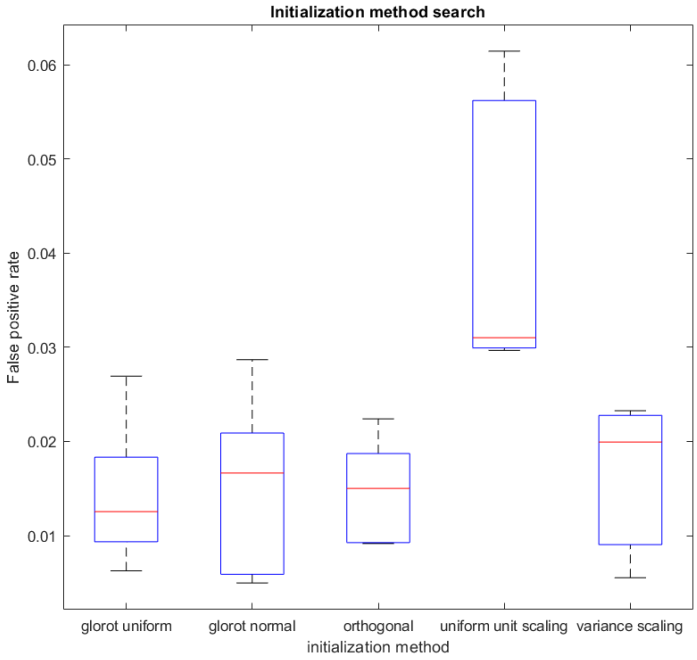

Figure 22: Box plots for the false positive rate of each pre-selected initialization method.

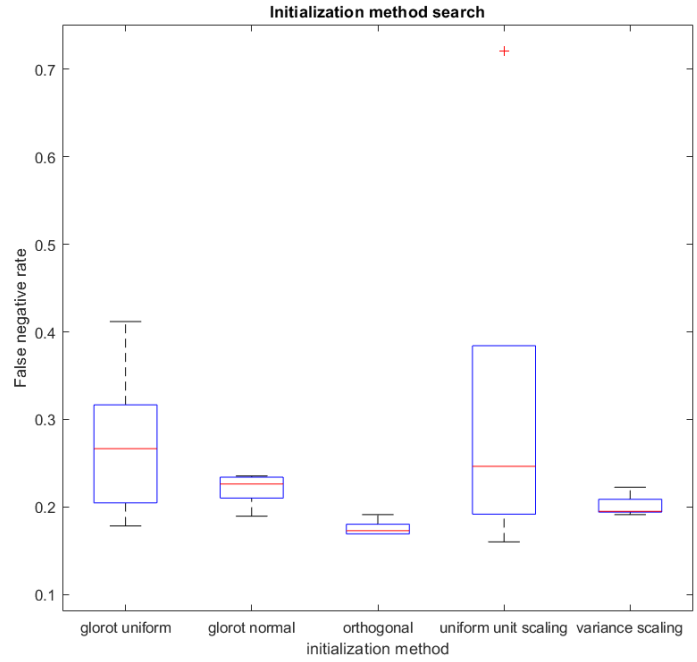

Figure 23: Box plots for the false negative rate of each pre-selected initialization method.

Due to these results, we selected orthogonal initialization as our default initialization method.

5.2.2 Convolutional layer

The results for these first two dimensions were the following:

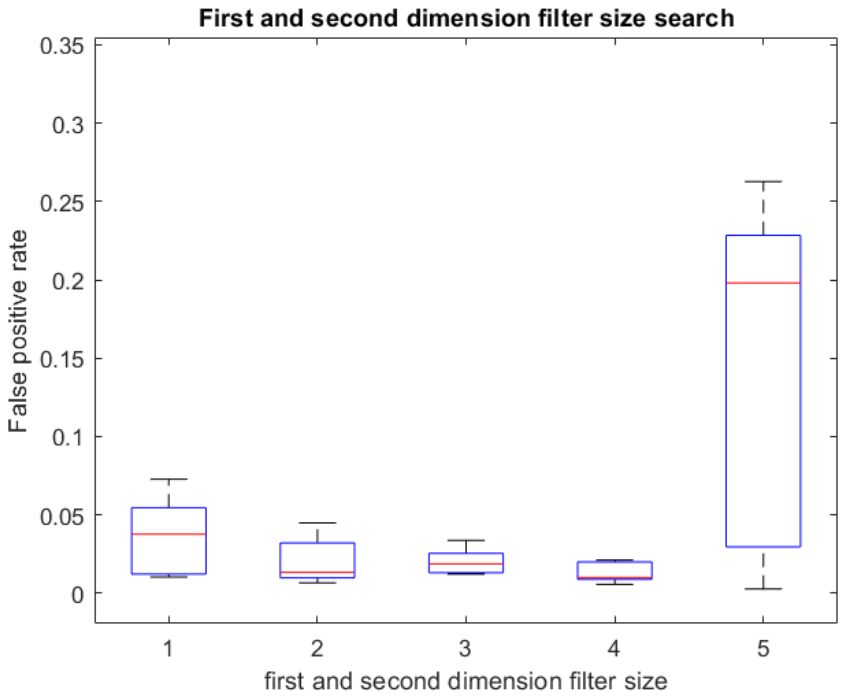

Figure 24: Box plots for the average false positive rate obtained with different first and second dimensions for the convolutional filter.

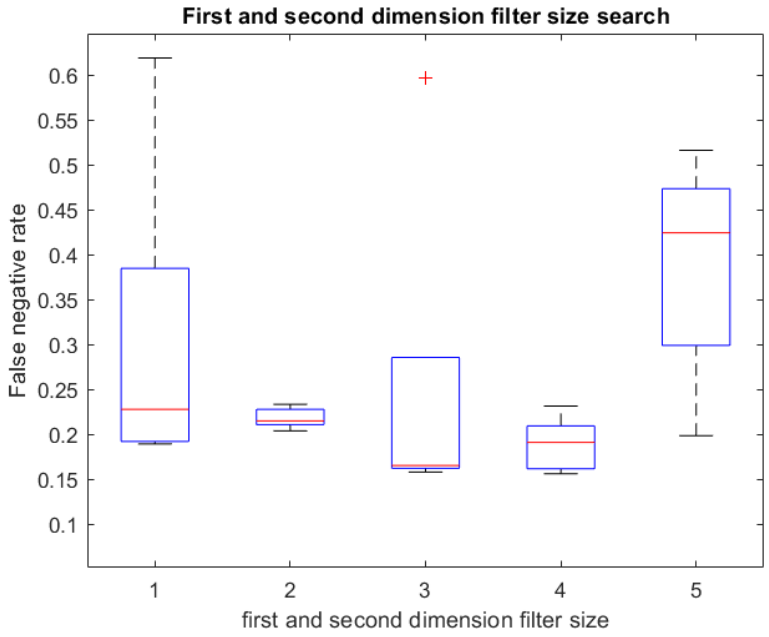

Figure 25: Box plots for the average false negative rate obtained with different first and second dimensions for the convolutional filter.

Given these results, it was decided that the value selected for these dimensions should be 4, since it presents the lowest false positive rate and the lowest dispersion, even though values of both 2 and 3 presenting promising results as well.

For the third dimension of the filter the following values were tested, producing the following results:

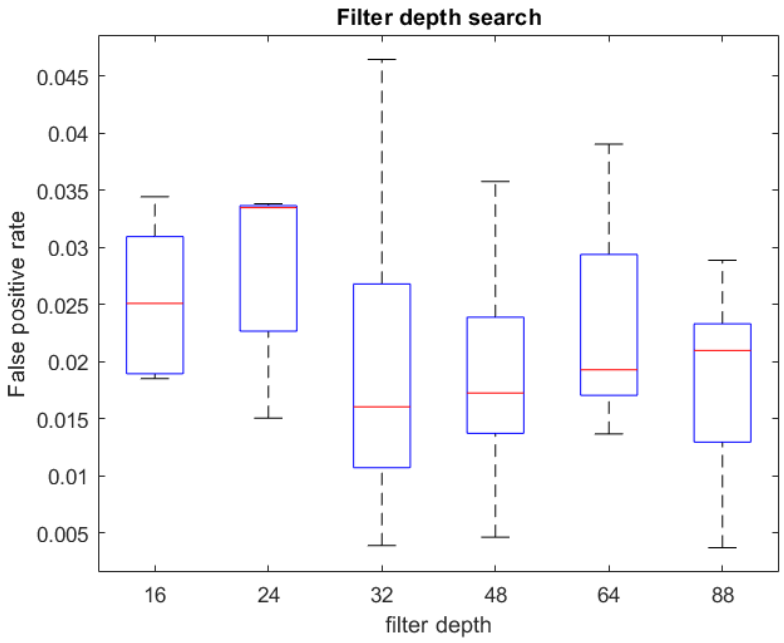

Figure 26: Box plots for the average false positive rate obtained with different values for the third dimension of the convolutional filter.

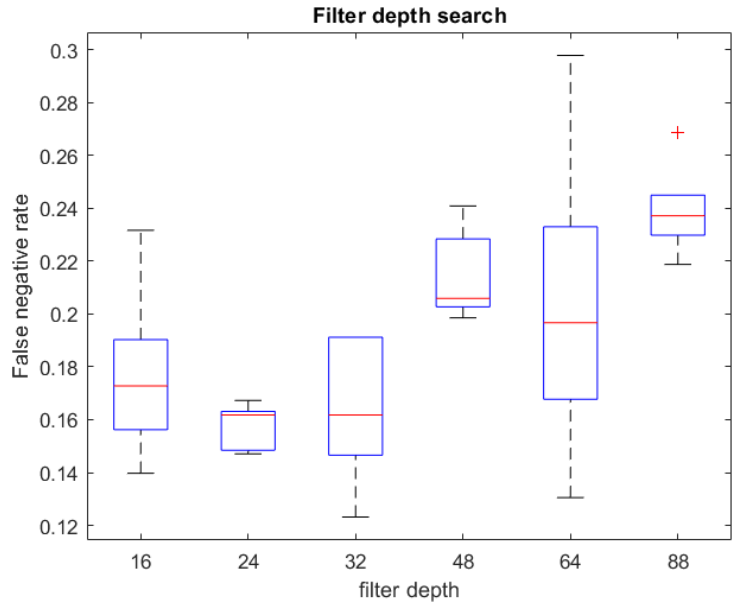

Figure 27: Box plots for the average false negative rate obtained with different values for the third dimension of the convolutional filter.

32 is definitely the overall best value, as it achieves both the lowest result for the false positive rate and false negative rate, also with a relatively low average result.

The network was tested with different numbers of filters in the convolutional layer producing the following results:

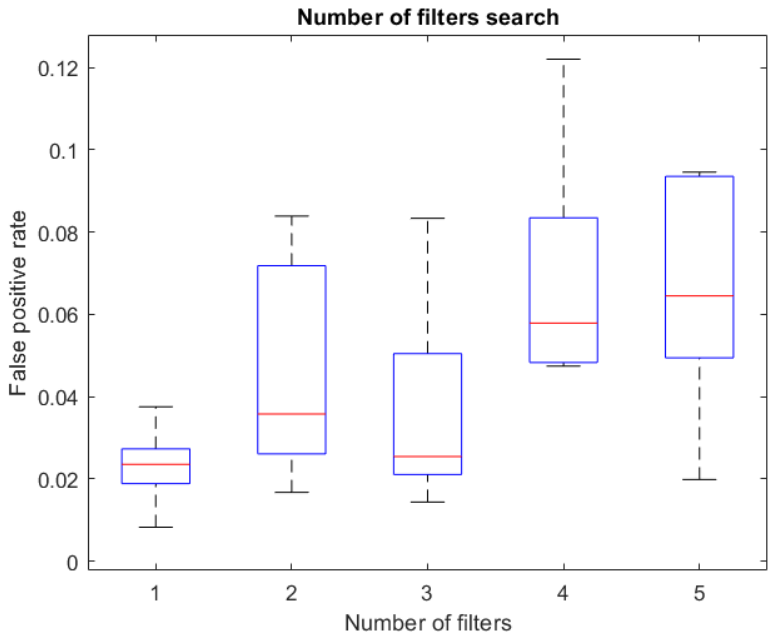

Figure 28: Box plots for the average false positive rate obtained with different values for the number of filters in the convolutional filter.

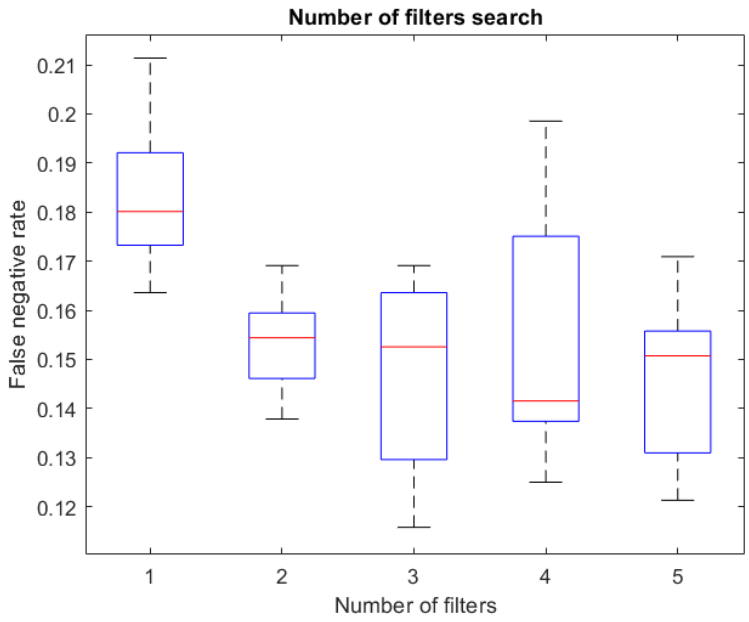

Figure 29: Box plots for the average false negative rate obtained with different values for the number of filters in the convolutional filter.

Given these results, it is clear that the training the network with 3 filters yielded the best results, therefore that is the chosen value.

5.2.3 Feedforward network

The following results were obtained during our parameter search for the maximum width of our feedforward network:

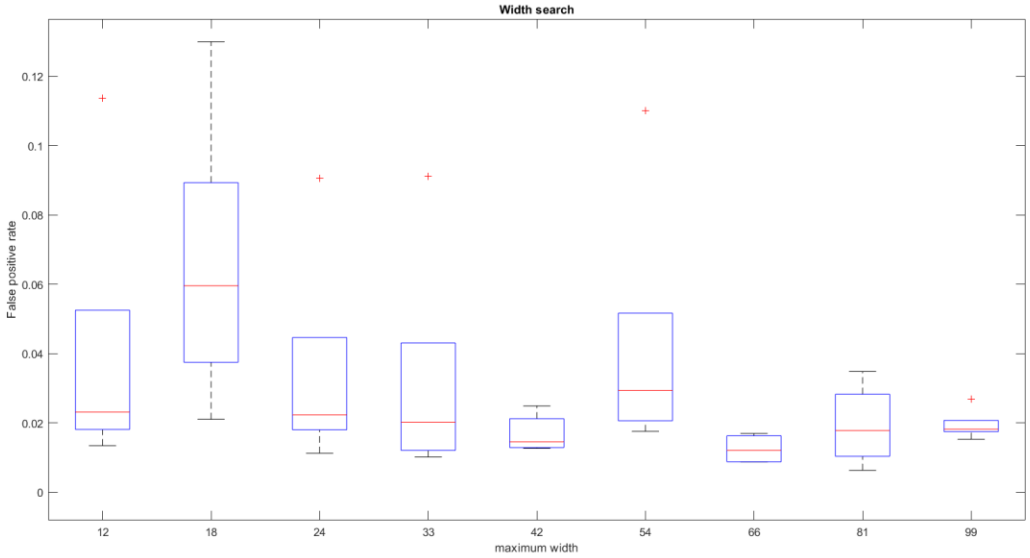

Figure 30: Box plots for the false positive rate for each value used in the maximum width (number of neurons in the first two layers) search.

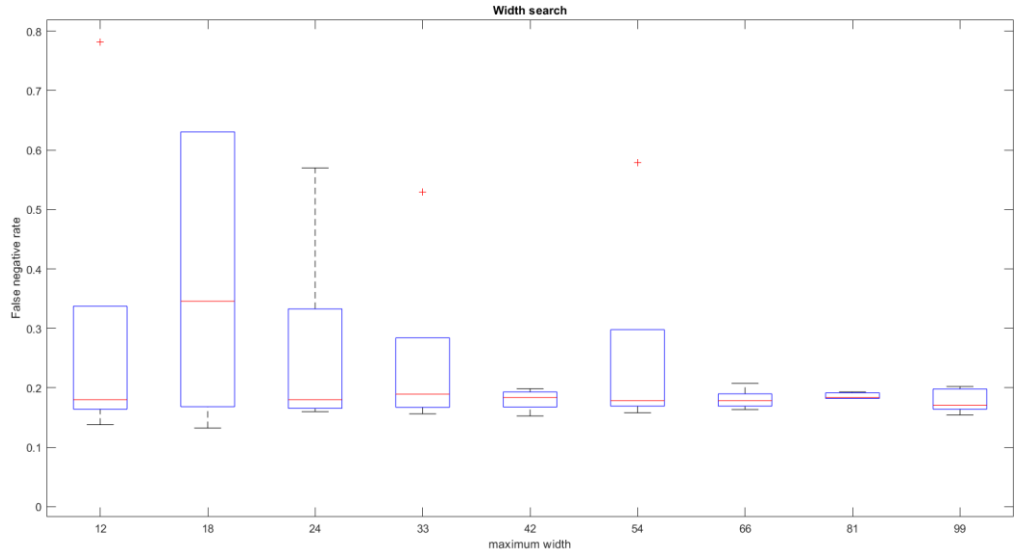

Figure 31: Box plots for the false negative rate for each value used in the maximum width (number of neurons in the first two layers) search.

Given these results, a maximum width of 42 was chosen, since even though the results for a maximum width of 66 were slightly better, since the complexity of increasing the number of neurons in the way we are doing here is of $O(n^3)$, due to the fact that we are increasing the number of neurons in 3 layers.

5.2.4 Misclassification penalty

The search for the misclassification penalty/cost produced the following results:

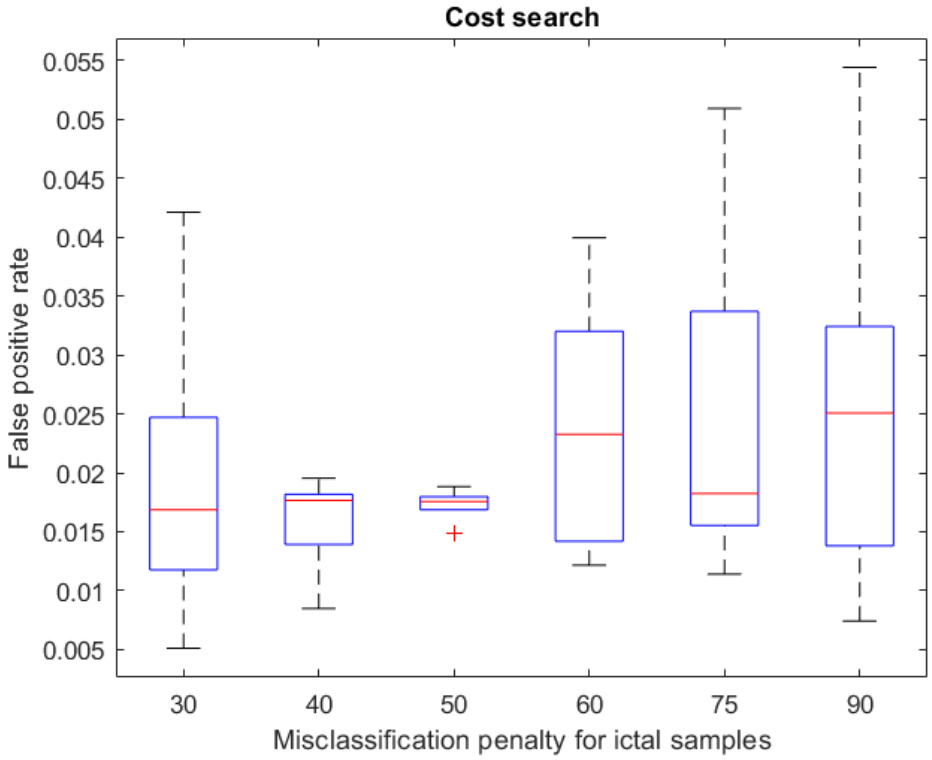

Figure 32: Results for the false positive rate for the misclassification penalty search.

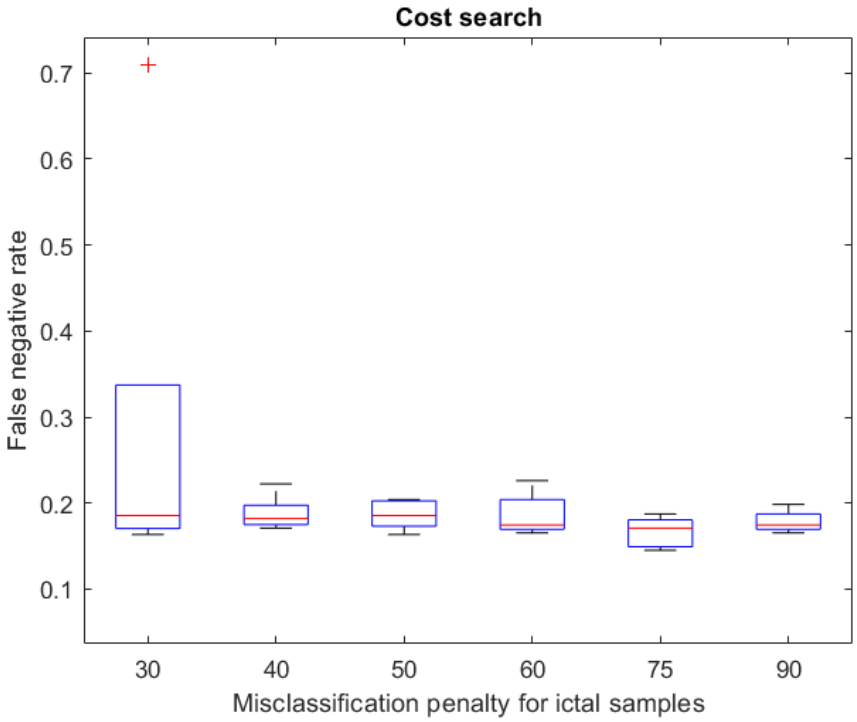

Figure 33: Results for the false negative rate for the misclassification penalty search.

Both 40 and 50 show similar results. 50 ended up being the chosen one due to having the lowest standard deviation. However, this parameter proved to be highly patient dependent in future tests.

In the end, we are left with the following network model:

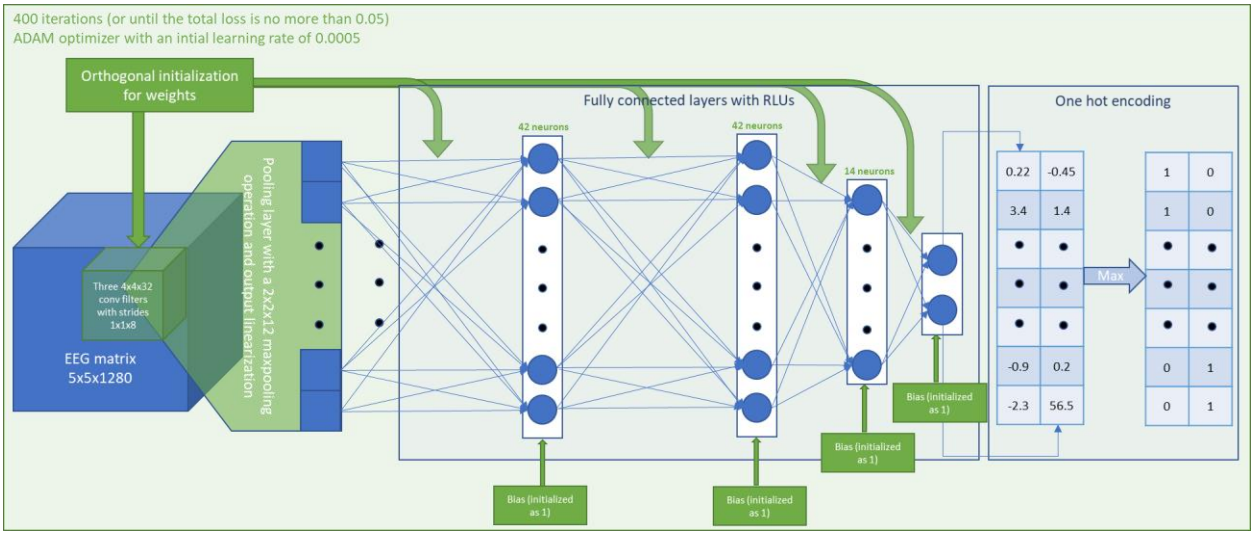

Figure 34: Our network with the chosen parameters

5.3 Performance evaluation

Various measures of performance, either standard or related to the regularization method presented before were used to statistically interpret the results obtained these measures are:

1. FPR: false positive rate;
2. FNR: false negative rate;
3. FRAR: false red alert rate, according to our regularization rules, measured by checking the ratio of interictal/preictal samples that contain red alerts to the total number of samples;
4. NSRAR: near seizure false red alert rate, measured by the ratio of preictal samples occurring five minutes before the seizure that contain red alerts to the total number of preictal samples five minutes before seizures;
5. FSFRAR: far seizure false red alert rate, measured by calculating the false red alert excluding samples happening five minutes before seizure; it can be considered the significant false red alert rate. This is equivalent to 1 minus the specificity of our model;
6. FRA/B: false red alerts per batch (using only samples far from seizures);
7. ALFRA: average length of false red alerts (using only samples far from seizures);
8. STDFRAL: standard deviation of false red alert's length (using only samples far from seizures);
9. FS: failed seizures (the numbers correspond the reference number of the failed seizure);
10. ATFTRA: average time for the first true red alert: average time that it takes for the first red alert, measured from the first EEG or clinical onset onwards.
11. ORAS: Occurrence of red alerts in a seizure: indicates how likely it is to find a red alert in an ictal sample. This is the sensitivity of our model.

5.4 Testing

5.4.1 Standard approach

We took data from 11 patients, one of which was used to perform the parameter search, in the EPILEPSIAE database and divided their seizures in training and testing set. The number of seizures in each training and testing sets for each patient varies with the number of seizures recorded for that patient. One hour of interictal/preictal time before the seizure was taken for both training and testing.

The patients selected were the following with the following traits and best performing parameters:

Patient ID	Nº train	Nº test	Patterns train	Patterns test	Focus	Initialization method	Conv. layer	Feedforward layer	Cost
58602	10	10	r,t,t,t,r,u,r,r,t,r	t,t,u,t…	t-l	orthogonal	[4,4,32,1]	39,39,13,2	48
11002	4	4	u,s,a,t	u,t,t,t	tp-r	orthogonal	[4,4,32,1]	21,21,7,2	50
30802	5	4	t,a,t…	all t	t-l, t-r	orthogonal	[4,4,32,3]	42,42,14,2	150
81102	8	4	all t	all t	t-r	orthogonal	[4,4,32,3]	42,42,14,2	100
85202	6	4	m,r,c,c,m,m	all m	t-l	orthogonal	[4,4,32,3]	42,42,14,2	50
109502	6	3	all t	all t	t-r, t-l'	orthogonal	[4,4,32,3]	42,42,14,2	12
113902	9	6	t,d,t…	t,t,a,…	t-r	orthogonal	[4,4,32,3]	42,42,14,2	40
114902	6	5	s,t,b,s,t,t	r,a,a,t,t	't-r, tll'	orthogonal	[4,4,32,3]	42,42,14,2	50
55202	6	3	t,t,d,t…	t,r,r	't-r, t-b'	orthogonal	[4,4,32,3]	42,42,14,2	150
98202	5	4	t,a,t…	all t	't-l'	orthogonal	[4,4,16,1]	42,42,14,2	12
114702	11	10	t,t,t,t,d,u,d,d,d,t,t	t,d,d,t,d,t,…	'tpr'	orthogonal	[4,4,32,3]	42,42,14,2	50

Table 3: Patient characteristics and parameters used. All patients chosen suffer from temporal seizures, and most of them present rhythmic theta waves during seizures.

In this table, we can find the following parameters:

1. Patient ID: the identification number of the patient in the EPILEPSIA database;
2. Nº train: Number of seizures used for training;
3. Nº test: Number of seizures used for testing;
4. Patterns train: This refers to the seizure pattern that the specialist found to on the EEG recorded;
5. Focus: refers to the localization of the focus of the seizure;
6. Initialization method: The initialization method used for the specific patient;
7. Conv. Layer: the parameters used in the convolutional layer in the form: [x, y, z, nº_filters];
8. Feedforward layer: The width of each layer of our neural network;
9. Cost: The misclassification cost/penalty.

The results for our first approach are summarized in the table below:

Patient	FPR	FNR	FRAR	NSRAR	FSFRAR	FRA/B	ALFRA	STDFRAL	FS	ATFTRA	ORAS
58602	0,00379	0,24749	0,00051	0,00033	0,00052	0,50	4	4,12	#3	10,33	0,67057
11002	0,02229	0,59925	0,00382	0,00667	0,00356	3,75	3	2,00	#1 #4	20,00	0,28090
30802	0,02924	0,50239	0,00662	0,01333	0,00600	3,50	6	7,00	-	16,75	0,23923
81102	0,04917	0,71429	0,00641	0,01000	0,00608	6,75	3	3,60	-	29,75	0,11058
85202	0,01461	0,39394	0,00397	0,01250	0,00318	1,50	7	7,28	-	6,75	0,45791
109502	0,05893	0,11574	0,02971	0,17556	0,01584	7,67	7	8,00	-	17,67	0,84259
113902	0,07274	0,35200	0,02066	0,03056	0,01974	14,17	5	4,00	#1	7,20	0,52800
114902	0,01114	0,29703	0,00057	0,00067	0,00056	0,60	3	3,00	-	16,20	0,63366
Average	0,03274	0,40277	0,00903	0,03120	0,00694	4,80	5	4,88	-	15,58	0,47043
55202	0,30176	0,60377	0,27099	0,15111	0,28201	21,00000	44	174,26	#1	4,50	0,31132
98202	0,20342	0,51581	0,10465	0,10167	0,10493	44,25000	8	12,73	-	16,25	0,32612
114702	0,69880	0,06729	0,69536	0,70000	0,69493	3,50000	645	952,12	-	2,50	0,91028
Average	0,13326	0,40082	0,10393	0,10931	0,10340	9,71667	67	107,10	-	13,44	0,48283

Table 4: Patients by ID and their results for each measure.

Two groups of patients were created, as they present considerably different results. The first group refers to the patients in which our model classified smoothly, while the second represents patients for whom our model found extra issues that affect classification, which will be explained and explored in the analysis. The first average refers to the first group, while the last average refers to all patients.

5.4.1.1 Individual patient analysis

5.4.1.1.1 Patient #58602

This patient was used for choosing both the neural network architecture and parameters. Naturally, it has much better results than the average.

A simulation where the results turned to have very low false red alert rate was chosen to give the idea on how the cleanest possible interictal classification would result in terms of ictal detection. In this regard, the results are very promising, since only one seizure failed to produce a red alert and only 2 false red alerts were produced, giving our model a specificity of 99.948%. However, there was one seizure that failed to produce a red alert, which was also the only seizure whose patter was not classified in the database, meaning this could very well be a different type of seizure that the model was not trained to detect.

The model takes 10 seconds, on average, to produce a red alert. This can be diminished by reducing the model's specificity, however, with such a high specificity, orange and even yellow alerts become important, so we can regard the model as producing an alert 8 seconds in the seizure on average.

Most of the false negatives are on the undetected seizure, at the end of the seizure, or at its very beginning, which is to be expected.

In an example with a lower specificity, all seizures are correctly detected. Here is an example:

Patient	FPR	FNR	FRAR	NSRAR	FSFRAR	FRA/B	ALFRA	STDFRAL	FS	ATFTRA	ORAS
58602	0,02087	0,18395	0.00531	0,03700	0,00238	1,6	5	6	-	9,4	0,74247

Table 5: A different simulation that happened to land on a local optimum that put more emphasis on minimizing the false negative rate. For reference, the ATFTRA without the previously missed seizure would be 8.

As it can be seen, the FRAR is 10 times higher in this case, corresponding to a model specificity of 99,461% and 8 times more false red alerts. Most of the false negatives are still where they were on the previous model. The red alert for the previously undetected seizure also only lasts 3 seconds, meaning it can easily be confused with a false positive, since the other seizures have red alerts during most of their time.

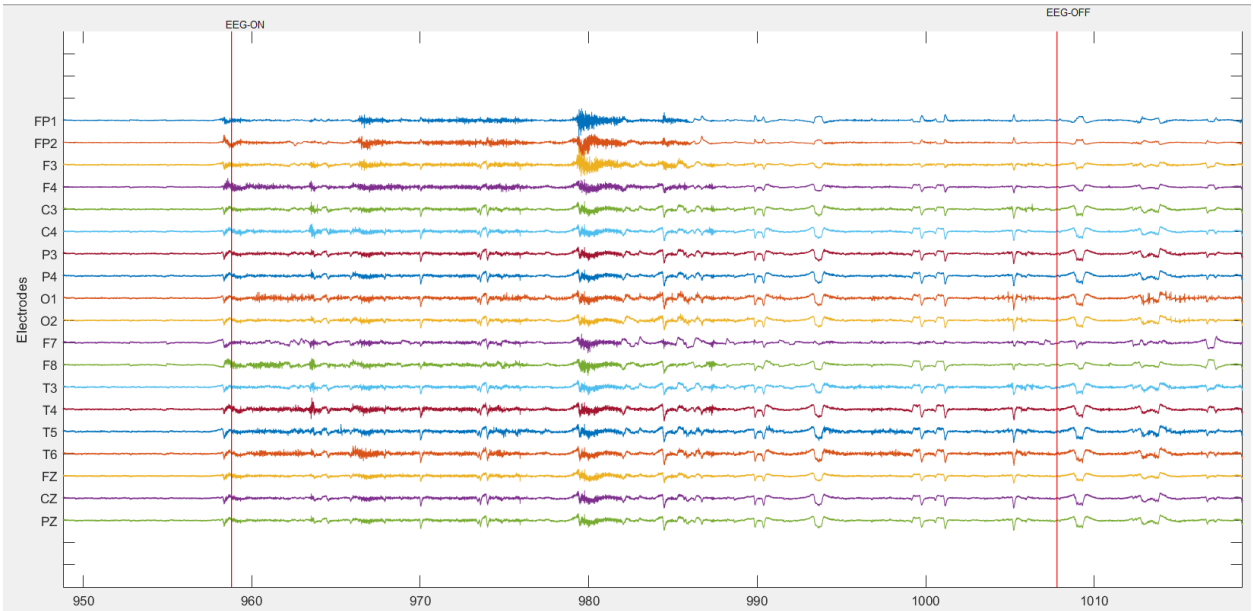

Figure 35: The elusive seizure of patient #58602. Screenshot from Epilab.

Given all this, we can note that our model was successful for this patient, despite having a hard time detecting one of the seizures.

5.4.1.1.2 Patient #11002

Our chosen parameters performed very poorly for this patient, showing that it is probably necessary to perform parameter searches for problems like this either on more patients or perform a parameter search for each patient.

While the specificity for this patient is on acceptable levels (99,644%) and false red alerts are short, meaning, once again, that even yellow and orange alerts can be significant, which is always a plus, the model fails to predict half of the seizures it was set to predict. This problem is likely due to the high heterogeneity of the seizures that affect this patient, the fact that all seizures used in the training set had been classified with different patterns and the fact there were only 4 seizures used for training the model. Due to this, the model probably lacks information to perform a generalization. This is important to note, since there has to be a minimum number of seizures required for deep learning models to perform a generalization and we can conclude that 4 seizures of different types is clearly insufficient. The low information available from this patient may also explain why reducing the size of our parameters and the number of filters produced better results, as there could have been a problem related to overfitting with the chosen parameters.

Given the above, we can say that our model was unsuccessful for this patient, but it may not be hard to improve it in a real scenario, by simply using all the seizures available of the patient for training. However, we don't have a way to perform cross-validation for that scenario.

5.4.1.1.3 Patient #30802

The misclassification penalty, on this patient, was increased to boost the model's performance, meaning the misclassification penalty has to somehow be adapted to each patient for optimal results, bolstering the idea that parameters don't work as well for all patients.

This patient shows high specificity (99.400%), making its alerts meaningful and the model is able to detect all seizures, albeit with a considerable delay of 16.75 seconds on average. These results were a lot better than expected, given that this patient was only trained with 4 seizures. However, contrary to the previous patient, this patient shows high homogeneity in its seizure patterns, which could easily be the reason why it shows much better performance at identifying seizures, while showing similar specificity.

Despite this, the model produced a very high FNR and low ORAS, which means that the seizure alerts will be intermittent. However, even intermittent alerts are significant when the specificity is high.

We can consider that our model was successful for this patient, despite the change in the misclassification penalty performed.

5.4.1.1.4 Patient #81102

We have another patient with high specificity (99.392%) and in which the misclassification penalty was increased, but this time with an even higher false negative rate. As a result, seizures take even longer to detect, (25 seconds on average) and red alerts are too infrequent during seizures, this time only being present in little more than 11% of seizure cases. However, with such high specificity, even yellow alerts may be significant.

While 11% is far more than the approximately 0.6% of FSFRAR present in this patient, making this difference undoubtedly statistically significant, and all seizures were detected, we will consider that our model is too unreliable due to the fact that it takes too long to detect seizures and the intermittent alerts might confuse both the patient and professionals that might be taking care of the patient. Therefore, we will consider the model unsuccessful for this patient, despite still being a good model to possibly help professionals study EEG and identifying seizures in it, due to the high specificity and the fact that it detected all seizures.

5.4.1.1.5 Patient #85202

This patient was trained with the exact same parameters that we obtained in our parameter search and shows remarkably good results. With a specificity of 99.682% and an average time to produce a red alert of just 6.75 seconds, while detecting all seizures, this patient arguably shows even better results than the patient #58602, used for the parameter search. The ORAS is still lower than 50%,

however, this is mainly due to the fact that the false negatives are concentrated in the last moments of the seizure, which is hardly relevant, as specificity and early detection are our priorities.

This patient has the particularity that the pattern identified it seizures is mostly amplitude depression (m), so this pattern may be more easily identifiable by our neural network, but there isn't enough information to affirm this.

False red alerts in this patient show high patterns of activity in lateral electrodes. This could signify that there is some epileptic/ictal activity happening that was not registered or could simply be typical low-amplitude fast activity arising from muscle artifacts.

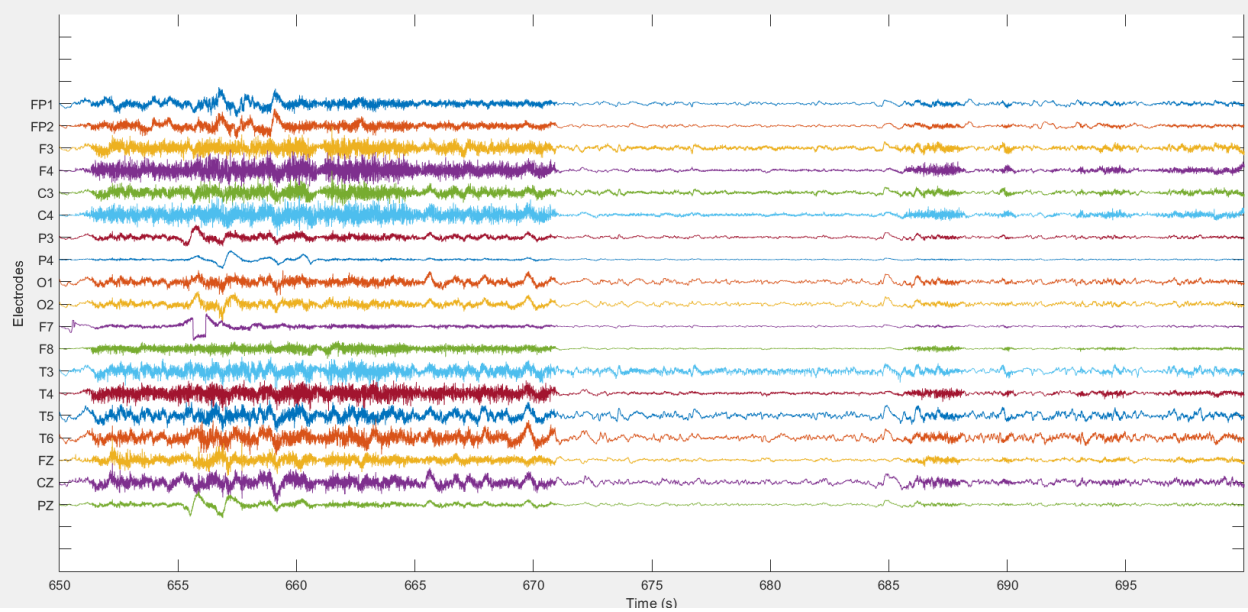

Figure 36: Example of a supposedly interictal segment that produces a red alert in patient #85202 Screenshot from Epilab.

Our model was definitely successful at classifying seizures from this patient.

5.4.1.1.6 Patient #109502

This patient presented the lowest FNR and highest ORAS while still preserving a low FSFRAR and, therefore a high specificity of 98.416%. The misclassification penalty had to be reduced during training to achieve this result. This patient has the particularity of having a relatively high when compared to other patients, NSRAR, as it shows high prevalence of red alerts right before seizures.This is considered desirable.

This patient has focal temporal seizures in both lobes, yet all of them showing rhythmic theta waves as the classified pattern, so we find a patient in which high (in this case, complete) homogeneity of seizure patterns produces good results.

Our model was successful in classifying data for this patient.

5.4.1.1.7 Patient #113902

This patient shows relatively lower specificity (98,026%) than the others, but seizures are detected earlier than usual, with only a 7,2 seconds delay on average, so our model produced a different trade-off in this case.

This patient shows three different seizure patterns, one which appears in the training set and not the testing set (rhythmic delta waves) and another one that makes up for the majority of the testing set and does not appear on the training set (rhythmic alpha waves). Despite this, it was a seizure that failed to be detected showed rhythmic theta waves, which were present in seizures in the training set as well.

The undetected seizure was detected in another simulation, but this simulation produced lower specificity and even higher false negative rate, behaving worse in both interictal and ictal samples in general. However, it is worth including it in this document for comparison:

Patient	FPR	FNR	FRAR	NSRAR	FSFRAR	FRA/B	ALFRA	STDFRAL	FS	ATFTRA	ORAS
113902	0,09841	0,43600	0,05101	0,09278	0,04716	18,66667	9,00000	11,26943	-	9,50000	0,36800

Table 6: Another simulation for the patient 113902. The only parameter changed here was the misclassification penalty, which was set to 50 in this case.

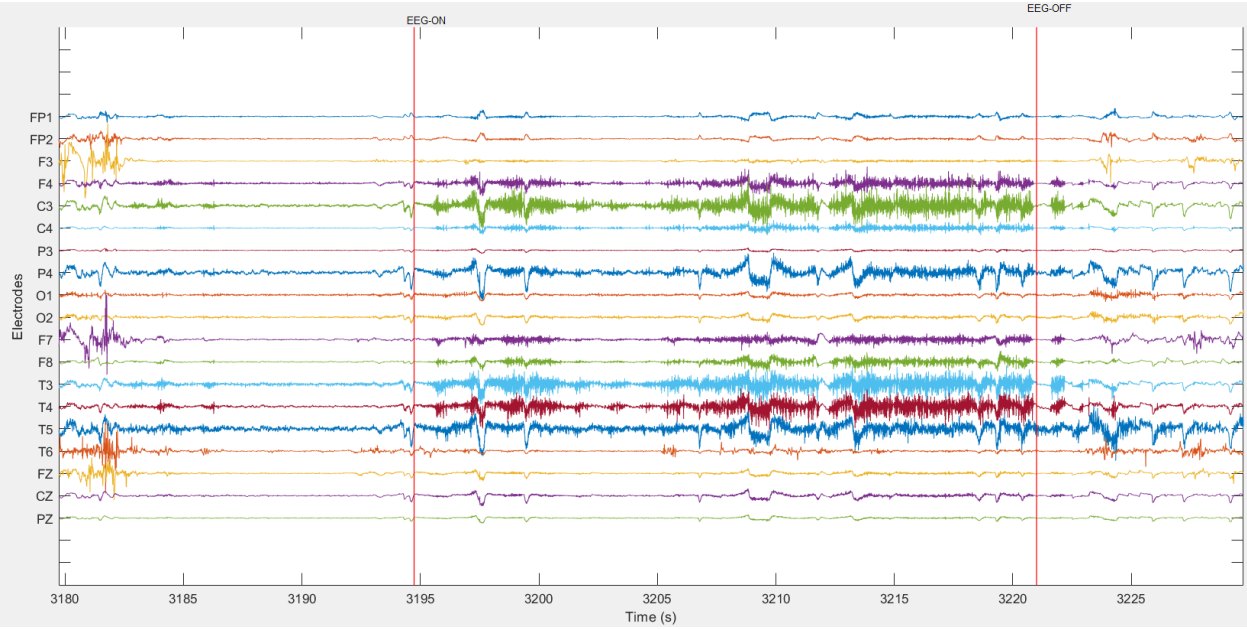

Figure 37: The seizure that proved to be hard for our model to detect. Screenshot taken from Epilab.

Despite the problems, we can consider that the early detection of seizures and still high specificity present clear signs that our model can generally classify data from this patient successfully.

5.4.1.1.8 Patient #114902

This patient presents good results with a specificity of 99,944%, despite the relatively high time seizures take to be detected on average (16,2 seconds). Neither the high heterogeneity of patterns and the fact that certain patterns are only present on the training set and others on the testing set nor the fact that this patient has two different focuses for its seizures seems to hinder the performance of our model for this patient, which is encouraging.

5.4.1.1.9 Patient #55202

Weather due to the high heterogeneity in the seizure patterns of this patient or perhaps the high occurrence of noise in recordings of this patient, or even an undetected presence of epileptic patterns in the samples classified as interictal, our model could not reliably classify data from this patient.

The first seizure of this patient is the only one not correctly identified, despite, once again, the pattern for this seizure being present in the training set, and the patterns for the other seizures not being present.

The second batch produces red alerts throughout almost the entire recording. When plotting the recordings of this batch using Epilab, we find a very interesting recurring pattern that seams to be of epileptic origin in the electrodes near the seizure focus:

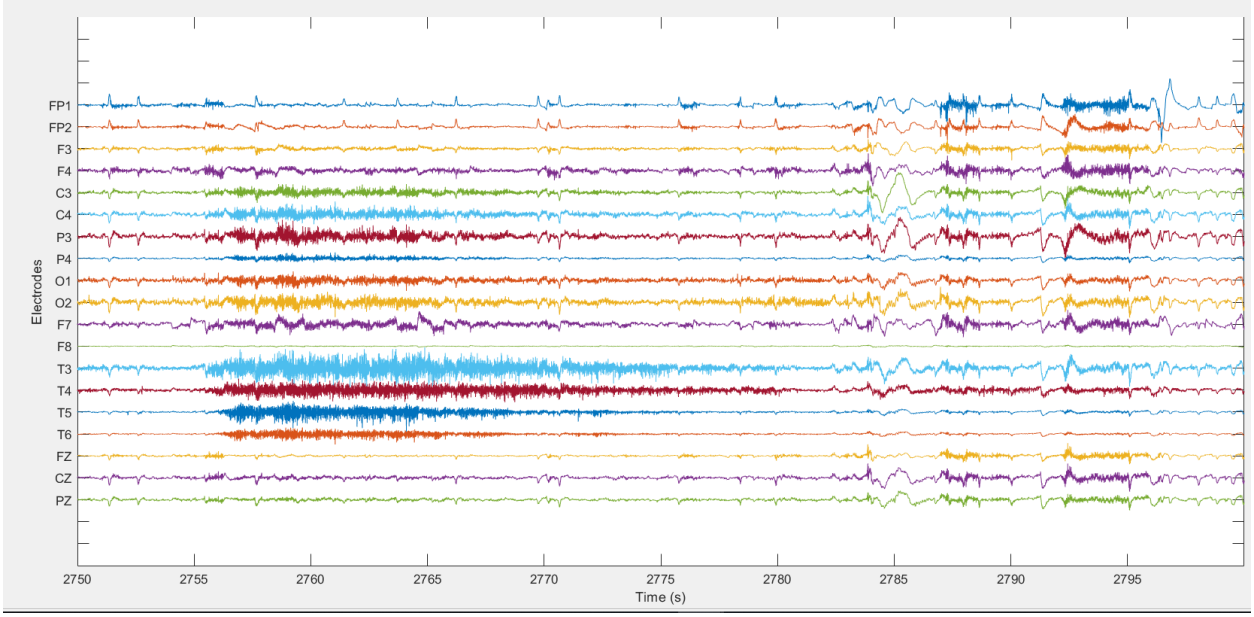

Figure 38: Recurring pattern, more noticeable in the temporal electrodes, which can be of epileptic origin. Screenshot taken from Epilab

Our neural network identifies this pattern as of ictal origin. We cannot affirm with certainty weather this pattern is actually related to any ictal or epileptic state or not.

5.4.1.1.10 Patient #98202

This patient is here to represent a patient whose recording is particularly noisy. Not even with a new small parameter search was it possible to get around the noise presented on the recording. It remains to be tested if a properly filtered recording would produce better results. However, it is still worth noting that all seizures were detected successfully in a reasonable time, so the model may still have some worth when it comes to, for example, helping a professional classify EEG segments.

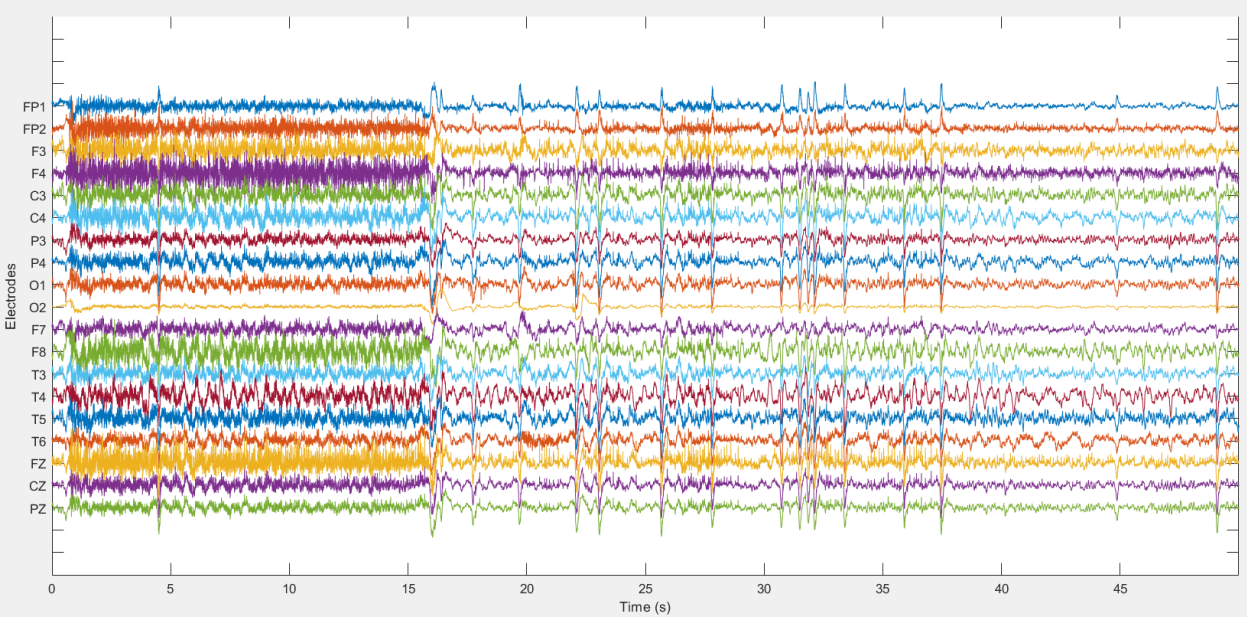

Figure 39: Typical recording of the patient #98202 where excessive activity, probably of muscular origin, produces false positives. Screenshot from Epilab.

Our model was unsuccessful for this patient.

5.4.1.1.11 Patient #114702

This patient actually presents the best results that we managed to get in the first 3 tested seizures. However, the model completely breaks and starts classifying everything as ictal in the next seizures. The next approach was though to try to solve this problem.

Patient	FPR	FNR	FRAR	NSRAR	FSFRAR	FRA/B	ALFRA	STDFRAL	FS	ATFTRA	ORAS
58602	0,00500	0,14721	0	0	0	0	-	-	-	8,33	0,80203

Table 7: Results for the first 3 seizures for the patient #114702.

5.4.1.2 General analysis

5.4.1.2.1 False red alerts

We defined three different states: one ictal, one preictal occurring five minutes or less before a seizure and one interictal/preictal occurring more than five minutes before a seizure. Our average rate of red alerts for the first group was 47.043%, 3.120% and 0.694% respectively, showing clear differences between the three states, even if our model was only trained to distinguish two of them.

However low the FSFPR is in average, it still signifies that about 5 red alerts happen in each batch on average, coincidentally lasting on average about 5 seconds and having a standard deviation of about 5 seconds relating to how long they last. The only way to improve on this would be to increase the number of samples that take to produce a red alert. However, this would affect the already high time that it takes to detect a seizure, once the ictal event starts. Here is what would happen if we only produced red alerts only each 5 samples classified as ictal:

Patient	FRAR	NSRAR	FSFRAR	FRA/B	ALFRA	STDFRAL	FS	ATFTRA	ORAS
58602	0,000310717	0,00000	0,00034	0,30	4	4,89898	#3	12,00000	0,65050
11002	0,002617986	0,00500	0,00240	2,25	3	1,73205	#1 #4	21,00000	0,26217
30802	0,005144105	0,01000	0,00470	2,75	6	7,54983	-	21,25000	0,20574
81102	0,004157272	0,00667	0,00393	3,50	4	3,74166	#4	33,33333	0,08173
85202	0,003332624	0,01000	0,00271	1,00	9	7,41620	-	12,25000	0,42761
109502	0,026716821	0,16444	0,01362	6,00	7	8,12404	-	18,66667	0,83333
113902	0,016252927	0,02444	0,01550	11,67	4	3,87298	#1	9,60000	0,50800
114902	0,000340987	0,00000	0,00037	0,40	4	2,82843	-	17,20000	0,62129
Average	0,00735918	0,02757	0,00545	3,48	5	5,02052	-	18,16250	0,44880

Table 8: Results when we increase the number of false positives required to produce a red alert by one.

With this new method, we can manage to decrease the number of false red alerts per batch by about one, but there is a price to pay when it comes to seizure detection. The ORAS decrease consistently and so does the time it takes to produce a red alert during a seizure, making this change overall undesirable.

We can, therefore, conclude that our regularization method should stay as it is and improving our method has to be done through other means.

5.4.1.2.2 Clinical onset and ATFTRA

Comparing the average time for a clinical onset to occur, after the noted EEG onset, can give us an idea of how useful our method is for early detection of seizures. A clinical onset was only noted in the EPILEPSIA database when the patient starts showing signs of having a seizure event during the film recording, so we can evaluate how long it takes for a red alert to happen once the symptoms of a seizure appear.

Patient	ATCO	ATFTRA	Difference
#58602	0,50	10,33	-9,83
#11002	0,00	20,00	-20,00
#30802	0,00	16,75	-16,75
#81102	10,33	19,67	-9,34
#85202	8,25	6,75	1,50
#109502	11,00	17,67	-6,67
#113902	0,00	7,20	-7,20
#114902	21,75	14,75	7,00
Average	6,48	14,14	-7,66

Table 9: Average difference between how long a clinical onset takes from the first recorded onset (EEG or clinical), and the time our model takes to produce a red alert for each patient. The acronym "ATCO" means "average time for clinical onset" and the ATFTRA is only taking into account seizures for which the clinical onset was recorded, hence the different values for some patients.

The average result of 7.66 seconds of delay for a red alert to be triggered after a clinical onset isn't very representative as there is a very high discrepancy from patient to patient for this difference. This is related to the fact that, in the database, some patients have their EEG onset consistently recorded after the clinical onset, while others display the opposite scenario This can be related to different epileptologists having a more or less conservative approach to pinpointing the EEG onset. Patients #81102, #85202, #109502, #114902, showing only an average delay for a red alert of 1.88 seconds, have their EEG onsets consistently before their clinical onsets, while the rest of the patients in the previous table display the opposite scenario, showing a delay of 13.45 seconds.

In conclusion, for patients who had their EEG onsets annotated early, our model performs much better, so, in a possible future application involving deep learning and seizure detection, early EEG onset annotation is a must in order to obtain an as early as possible seizure detection.

Patients #81102 and #11490 had one seizure excluded each that did not have a clinical onset recorded. In both cases, this seizure also happened to be the one that took more time to produce a red alert in our model. This may signify that epileptic events without or with little clinical manifestation can be harder to detect, but we don't have enough data to confirm it.

5.4.1.2.3 Seizure focus and performance

Our work is limited in this aspect, since only data from patients that only exhibit temporal seizures was used. We can still study if a patient displaying various focal regions for its seizures affects the performance of our neural network or not.

Average	FPR	FNR	FRAR	NSRAR	FSFRAR	FRA/B	ALFRA	STDFRAL	FS	ATFTRA	ORAS
1 focus	0,03252	0,46139	0,00707	0,01201	0,00662	5,27	4,40	4,20	-	14,80	0,40959
2 focuses	0,03310	0,30505	0,01230	0,06319	0,00747	3,90	5,33	6,00	-	16,87	0,57183

Table 10: Averages results for patients belonging to the groups that had seizures either always with their focus on the same part of the brain, or in two different parts.

Both statistical measures related to interictal and to ictal samples sometimes perform better in one case or the other. This is what we expect if or model performs independently from this trait. There isn't any clear trend that can be derived for our model to perform better or worse in each scenario.

5.4.1.2.4 Seizure patterns and performance

As we have seen in the individual patient analysis, a seizure being classified with a different pattern than the ones present on the training set is not an impeding factor for its correct identification. However, it is still worth to perform a deeper analysis on this subject.

The first thing that we can do is to pick up the patients for whom the classification was smooth and separate them into two groups: one with homogenous seizure patterns and another with heterogenous seizure patterns. A patient is considered to have a homogenous seizure pattern if, in both the training and testing set, half of its seizures have the same pattern and that pattern is the same in both the training and testing sets. It is considered heterogenous otherwise.

Heterogenous patients	Homogenous Patients
#58602	#30802
#11002	#81102
#113902	#85202
#114902	#10902

Table 11: Patients classified as either heterogenous our homogenous, relating to their seizure patterns.

The first thing to notice here is that only heterogenous patients contain seizures that failed to be detected, but, from those 4 seizures, 2 were left unclassified and the other 2 belonged to a pattern that was present in the training set. As so, no seizure that belonged to a classified pattern that was only present in the testing set failed to be detected.

If calculate the average results for this two groups, we get the following results:

Average	FPR	FNR	FRAR	NSRAR	FSFRAR	FRA/B	ALFRA	STDFRAL	FS	ATFTRA	ORAS
Homogenous	0,03799	0,43159	0,01168	0,05285	0,00778	4,85417	5,75000	6,47142	-	16,73	0,41258
Heterogeneous	0,02749	0,37394	0,00639	0,00956	0,00610	4,67917	3,75000	3,28078	-	13,43	0,52828

Table 12: Averages results for patients that were considered to display either homogenous or heterogenous seizure patterns.

The average results seem to indicate that a higher variety of seizure patterns, despite producing problems at detecting certain seizures, performs statistically much better. Even the ORAS of the heterogeneous group is higher and its FNR is lower despite the undetected seizures.

We can, therefore, conclude that a higher variety of patterns causes the model to have better differentiation but a patient displaying more heterogeneous patterns also provides a more complicated problem for our classifier, causing it to fail more. As we only have four patients in each group, we cannot affirm this with enough confidence, but it is a likely scenario that can be explored in further studies.

5.4.1.2.5 Overall viability

There are at least 3 ways that a model like this can be realistically applied:

1. Facilitate the job of an epileptologist by identifying possible seizure segments in EEG recordings;
2. Create alerts for medical personnel to allow better vigilance of epileptic patients in real-time;
3. Create a system that allows the patient or its family to be alerted when a seizure is taking place in real-time.

For the first case, the usefulness of this model would be to allow the epileptologist to, after collecting some seizure samples from a patient, identifying other regions of interest where possibly previously undetected seizures could be hiding. Our model is not 100% effective at detecting seizures and it fails for some patients, but it could still provide help and lower the amount of time and errors associated with identifying seizures in EEG recordings of epileptic patients.

In the second and third case, if our model is trained in data in which EEG onsets are pinpointed early, the model can provide with a detector of seizures that takes very little to produce a red alert and has high specificity for some patients. For others, it might simply fail completely. Also, a previous recording of seizures of a patient would be necessary each time. This makes it so that this model is unable to provide a ready-made reliable patient independent system. However it has the potential to provide accurate detection of seizures for some patients, so it might be worth trying, as epileptic seizures can be highly risky and anything that can provide earlier assistance when they occur can be critical.

5.4.2 Progressive approach

The same patients and parameters used in the previous method were used on this one. They may not be optimal, but there was no time or extra graphic cards to perform another parameter search.

The results for our progressive training method are summarized in the table below:

Patient	FPR	FNR	FRAR	NSRAR	FSFRAR	FRA/B	ALFRA	FS	ATFTRA
58602	0,01695	0,36896	0,00666	0,05412	0,00208	3,82353	0,88235	#2 #10	16,40000
11002	0,10697	0,53012	0,03833	0,03733	0,03516	8,00000	11,00000	#2 #5	36,66667
30802	0,05324	0,75743	0,02455	0,00133	0,02444	6,00000	15,20000	#2 #3	23,50000
81102	0,05873	0,57863	0,01759	0,01422	0,01639	7,80000	6,93333	#2 #4 #9	16,10000
85202	0,06680	0,50971	0,02440	0,04139	0,02085	8,91667	13,91667	-	22,66667
109502	0,33659	0,10765	0,31935	0,29190	0,29414	411,42857	3,42857	-	20,00000
113902	0,09074	0,41006	0,06669	0,08143	0,05981	8,71429	9,28571	#5	12,07692
114902	0,04602	0,22591	0,01579	0,00250	0,01558	4,37500	8,50000	-	16,87500
Average	0,14316	0,44745	0,10076	0,09503	0,09265	53,76285	14,82646	-	19,95169
55202	0,24245	0,62981	0,17732	0,11556	0,16757	10,16667	35,50000	#4	20,60000
98202	0,19301	0,53009	0,09052	0,03944	0,08708	6,33333	37,66667	-	25,33333
114702	0,36329	0,27358	0,32711	0,36611	0,29610	115,83333	20,77778	#9 #11	9,25000
Average	0,10767	0,44651	0,06710	0,06263	0,06172	51,71015	11,86815	-	21,06873

Table 13: Average results for progressive training for each patient

Considering, this time, the test set of the previous method, in order to compare both methods with more precision, the following results were obtained:

Patient	FPR	FNR	FRAR	NSRAR	FSFRAR	FRA/B	ALFRA	FS	ATFTRA
58602	0,01987	0,25460	0,01051	0,09000	0,00288	5,00000	0,90000	#3	11,44444
11002	0,09972	0,54144	0,04498	0,03333	0,04216	9,00000	12,00000	#1 #4	39,00000
30802	0,04498	0,73909	0,02256	0,00000	0,02256	5,25000	15,50000	#1	23,50000
81102	0,05362	0,60976	0,01487	0,01788	0,01335	6,63636	6,72727	#5	17,71429
85202	0,05308	0,53943	0,02229	0,03222	0,01953	11,22222	9,88889	-	23,66667
109502	0,48736	0,06601	0,48085	0,45333	0,44177	641,50000	2,75000	-	9,50000
113902	0,03246	0,34444	0,01175	0,06042	0,00665	3,75000	5,75000	-	12,87500
114902	0,07271	0,18842	0,02526	0,00400	0,02492	7,00000	13,60000	-	12,00000
Average	0,09701	0,43606	0,06417	0,06553	0,05856	57,38226	8,64333	-	20,53566
55202	0,27621	0,58572	0,23055	0,17222	0,21604	13,33333	23,33333	#1	5,00000
98202	0,21504	0,43603	0,11243	0,05917	0,10727	7,25000	37,25000	-	15,25000
114702	0,32670	0,31448	0,30092	0,37500	0,26916	118,10000	21,40000	#1 #3	5,00000
Average	0,15289	0,41995	0,11609	0,11796	0,10603	75,27654	13,55450	-	15,90458

Table 14: Average results for progressive training for each patient using the testing set of the standard approach, to facilitate comparison.

5.4.2.1 General analysis

For most patients, this method didn't show any improvements. In patient #109502, this method produced unacceptable results (a new parameter search would likely solve this).

From the first group, the only patient whose results improved by using this method was patient #113902, which has the highest number of seizures, with the exception for the patient #58602, which was used for parameter search. From the second group, we notice critical changes only in patient #114702, which now obtained completely different results, failing in seizures that it almost detected flawlessly before and solving some of the continuous false positives. However, the results for this patient are still unacceptable.

Both patient #113902 and patient 114702 showed poorer results on the last seizures in the previous method. This tendency was reverted with this new method, as expected.

Since our patients with the highest number of seizures, with exception for the patient used for the previous parameter and architecture search were the ones experiencing improvements, especially on their latest seizures, we can hypothesize that, for longer recordings, retraining the model from time to time is be good idea. However, retraining the model with each new seizure does not seem to improve results. Further research is necessary here.

5.4.3 Mixed approach

Besides the fact that all the data for all patients was retrieved at 256Hz, all the chosen patients to evaluate this model have in common the fact that they have exclusively focal seizures with their focus on the temporal left lobe. Their other characteristics are as follows:

Patient	nº seizures	Patterns
52302	6	u,u,t,d,t,t
58602	20	r,t,t,t,r,u,r,r,t,r,t,t,u,t,…
85202	10	m,r,c,c,m,…
98102	4	all u
112802	6	all t
Overall	46	-

Patient	nº seizures	Patterns
21902	6	t,t,t,t,t,b
23902	5	t,t,t,t,d,t
26102	6	m,m,t,t,m,t
50802	5	all t
Overall	22	-

Tables 15 and 16: Patients and their characteristics in both train (left) and test (right) sets for mixed training.

Using the previously mentioned measures, we can evaluate the results that our network model produced on the test set, which are.

Patient	FPR	FNR	FRAR	NSRAR	FSFRAR	FRA/B	ALFRA	STDFRAL	FS	ATFTRA	ORAS
21902	0,03250	0,59441	0,01030	0,00000	0,01125	10	4	3,00000	#1	32,80	
23902	0,18234	0,96186	0,16274	0,00030	0,17769	14,8	9	91,38381	all	-	
26102	0,25549	0,51312	0,15802	0,03118	0,16447	50,3	11	17,80449	#6	15,80	
50802	0,10052	0,20354	0,05288	0,00000	0,05783	22,8	9	13,49074	-	12,60	
Overall	0,14307	0,51370	0,09514	0,02424	0,09308	25	14	37,90778	-	22,13	

Table 17: Results for each patient on the test set for the mixed training approach

5.4.3.1 Individual patient analysis

5.4.3.1.1 Patient #21902

This patient shows results comparable to those that patients from the first method showed, however one seizure failed to be detected and the ATFTRA is excessively high. However, this is one of those patients in which the EEG onset appears before the clinical in all cases, on average 16.17 seconds earlier. This still produces a 16.63 seconds delay between the clinical onset and the first red alert. This is expected, given the analysis on the first method, since four in five patients used for training this time had their EEG onsets consistently recorded either later or at the same time of the clinical onset.

The false red alerts in this patient seem to have a common pattern:

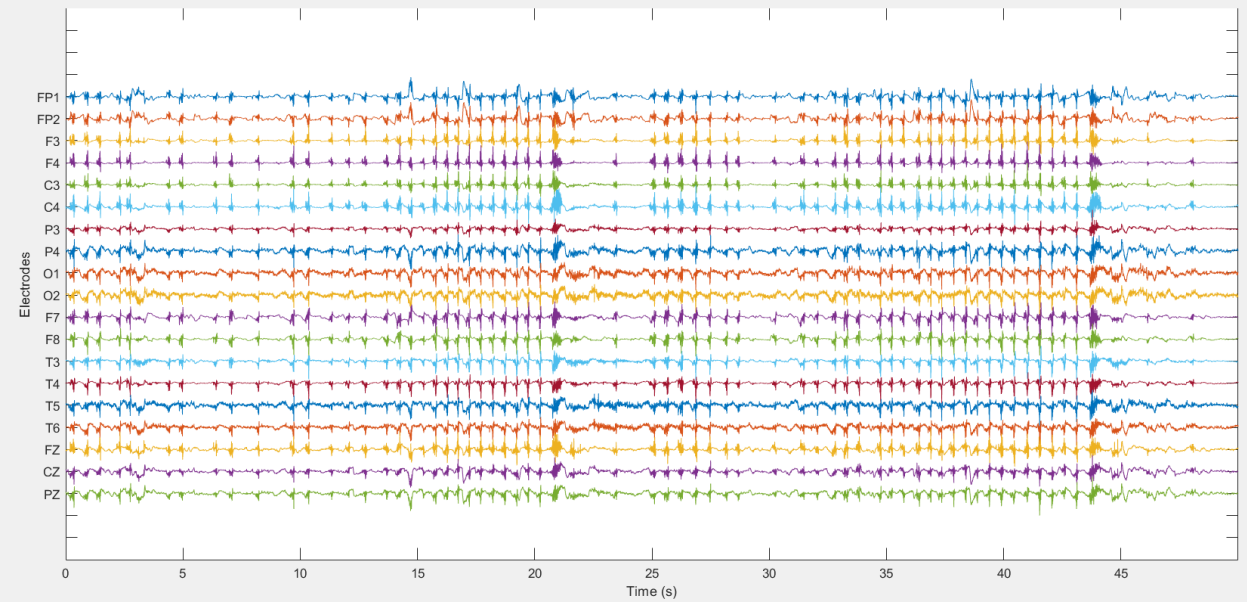

Figure 40: Pattern followed by most false red alerts in patient 21902.

5.4.3.1.2 Patient #23902

Our model completely failed to detect seizures from this patient. This shows that some patients may present seizure patterns that are completely different from other patients, making a hypothetical patient independent seizure detector a very difficult problem.

5.4.3.1.3 Patient #26102

The results for this patient were very poor, as they show a very high false positive rate. Our model seems to be confusing high-frequency activity in the patient's brain with ictal activity. This showcases one of the problems that may arise from not training a model with specific data from the patient being classified.

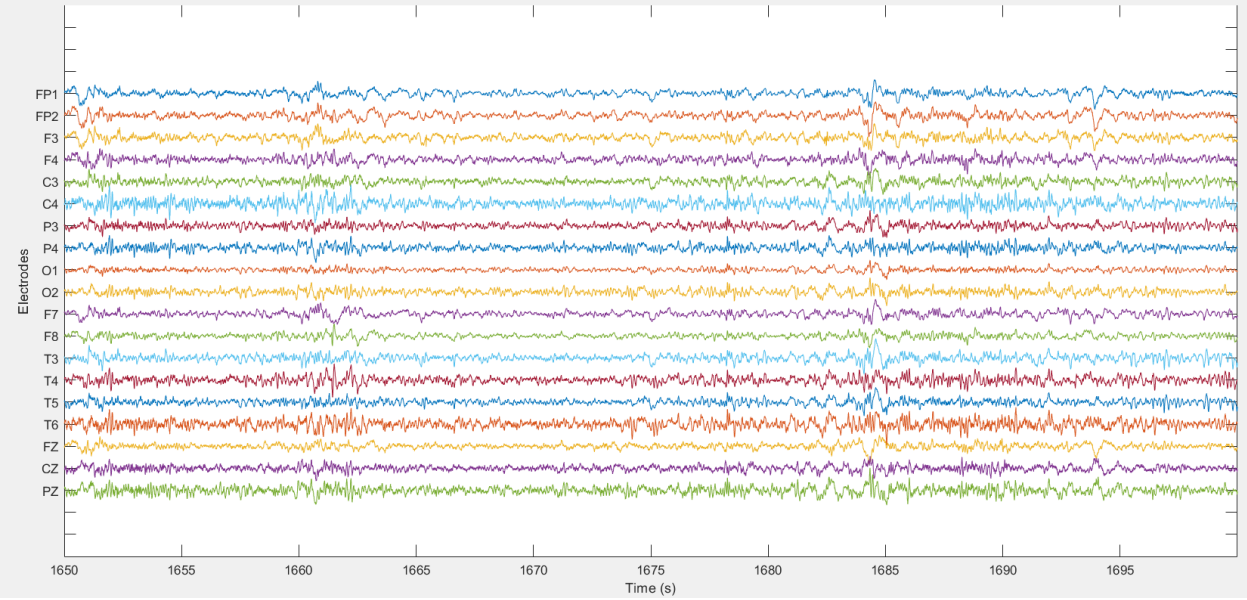

Figure 41: High activity pattern in patient #26102 producing a red alert. Screenshot taken from Epilab.

5.4.3.1.4 Patient #50802

The results for this patient can be considered somewhat successful when compared to the two previous ones but are still far from what we obtained with our first approach. A specificity of 94,217% and an average of almost 23 red alerts for each batch are not suitable results for any real application.

5.4.3.2 General analysis

This method was only successful for 1 in 4 patients. The others showed problems that were to be expected, such as the lack of ability of the model to detect seizures from a certain patient, or the low specificity given by the model not being able to interpret certain interictal samples correctly.

We can, however, conclude that if our model produced good results for one patient, it is still possible to improve it to produce better results in more patients. Since this idea wasn't explored further in this thesis project, all this serves is to point out problems and showcase what could possibly be done to put it in practice. No hard conclusions can be taken from such a superficial study.

5.4.4 Seizure prediction

Our model is easily adaptable to be trained for late prediction, however, seizure prediction ended up not being performed due to the fact that it would require a new parameter search, and this was not possible due to time and resource restrictions. It will be performed in the future.

Chapter 6

Conclusions

We have already taken a few conclusions that can be quickly summarized by:

1. Our model failed for 3 in 11 patients, so we cannot affirm that it may provide a reliable seizure classifier;
2. Parameters searched using only one patient performed comparably well when applying them to other patients, with some exceptions. The misclassification penalty, however, can not be held in the same regard, as it is highly dependent from patient to patient.
3. Red alerts have a much higher chance to appear on a seizure than near a seizure and the same goes for near a seizure than far from it, which means that there is a statistical difference between the EEG recordings produce in these three states;
4. In order to have early detection of seizures, we must also have early annotation of EEG onsets.
5. The focus of the seizure does not really affect the performance of a CNN, as even patients with focal seizures on opposite sides of the brain did not see a drop in performance. This is to be expected due to the nature of CNN's.
6. Seizures with patterns for which the model was not trained can still be identified, suggesting a high similarity between them.
7. Patients with more heterogenous seizure patterns show better statistical performance but are more prone to detection failures.
8. Our progressive training approach only provided better results for patients that had more seizures and longer EEG recordings, meaning that retraining the model for every seizure is not worth it, but retraining it after a certain quantity of seizures (more than five at least) may be worth it.
9. A patient independent classifier has to be studied in a more extensive fashion but showed acceptable results for one patient, which is promising.

Our best approach produced an average specificity of 99.306% and sensitivity of 47.043%, if we take off the failed patients. This is due to the model, a lot due to the regularization method, being heavily tweaked for sensitivity, which is a must, since, in a real environment, there is far more interictal than ictal time and our red alerts must be meaningful. With slower (taking more seconds of positive results to produce a red alert) red alerts we have seizures being identified later and, if we tune our model for poorer specificity, we have more red alerts in interictal times than is desired. Training a patient-specific model with more seizures also cannot be the solution, as it makes the model less useful in a real environment. So, with our approach, there is not much more to do. It is also worth noting that many ictal samples that are not classified with red alerts are also classified with orange or yellow ones.

6.1 Further improvements

In section 2.8 of the background concepts, we saw that many seizure patterns can be related sudden bursts of spike waves, theta activity, etc. In our model, we are assuming that all ictal samples should be classified in the same fashion, but this isn't necessarily the case. For example, we can see in figure 9, in seizures that show amplitude depression patterns, the genesis of the seizure is very different from what starts happening as it progresses. This can explain why some of our seizures take so long to be detected. A model that is able to identify the beginning of a seizure versus the preictal/interictal state, to identify the beginning of a seizure versus its end and its end versus the post-ictal, rather than then classifying the entire seizure as a unit may provide better results when it comes to sensitivity. Anyway, the difficulties of our model definitely lie on identifying whether we are in a seizure or not and where the seizure begins.

Training with more complex maps, using data from patients with different electrode setups and coupling our results with other methods like, for example, ECG classification may also provide some improvements.

Another possibility that was briefed on the background concepts was to use adaptive models to identify the various brain states. This would likely come up with various patterns for ictal, preictal and interictal states and may be worth testing.

References

1-https://epilepsymichigan.org/page.php?id=358

2 - Teixeira C. et al. (2014) Brainatic: A System for Real-Time Epileptic Seizure Prediction. In: Guger C., Allison B., Leuthardt E. (eds) Brain-Computer Interface Research. Biosystems & Biorobotics, vol 6. Springer, Berlin, Heidelberg

3 - Klatt, J., Feldwisch-Drentrup, H., Ihle, M., Navarro, V., Neufang, M., Teixeira, C. Schelter, B. (2012). The EPILEPSIAE database: An extensive electroencephalography database of epilepsy patients. *Epilepsia*, *53*(9), 1669–1676.

4 - http://www.who.int/news-room/fact-sheets/detail/epilepsy

5 - An Introduction to Epilepsy: Edward B Bromfield, MD, José E Cavazos, MD, PhD, and Joseph I Sirven, MD. West Hartford (CT): American Epilepsy Society; 2006.

6 - R, Bachu & B.K., Adapa & S, Kopparthi & Barkana, Buket. (2008). Separation of Voiced and Unvoiced Speech Signals using Energy and Zero Crossing Rate.

7 - http://hyperphysics.phy-astr.gsu.edu/hbase/electric/laplace.html

8 - https://www.verywellmind.com/what-is-a-neuron-2794890

9 - Elston GN (November 2003). "Cortex, cognition and the cell: new insights into the pyramidal neuron and prefrontal function". Cereb. Cortex. 13 (11): 1124–38. doi:10.1093/cercor/bhg093. PMID 14576205

10 - Grech, R., Cassar, T., Muscat, J., Camilleri, K. P., Fabri, S. G., Zervakis, M., Xanthopoulos, P., Sakkalis, V., … Vanrumste, B. (2008). Review on solving the inverse problem in EEG source analysis. *Journal of neuroengineering and rehabilitation*, *5*, 25. doi:10.1186/1743-0003-5-25

11 - https://en.wikipedia.org/wiki/Excitatory_postsynaptic_potential

12 - https://en.wikipedia.org/wiki/Electroencephalography

13 - http://learn.neurotechedu.com/neural oscillations/

14 -Thalía Harmony, Departamento de Neurobiología Conductual y Cognitiva, Instituto de Neurobiología: The functional significance of delta oscillations in cognitive processing. Universidad Nacional Autónoma de México, Campus Juriquilla, Boulevard Juriquilla 3001, Querétaro CP 76230

15 - http://www.scholarpedia.org/article/Neurobiology_of_sleep_and_wakefulness

16 -Christoph S. Herrmann a,b, Daniel Strüber a,b,∗, Randolph F. Helfrichc, Andreas K. Engel: EEG oscillations: From correlation to causality; Experimental Psychology Lab, Department of Psychology, Cluster of Excellence “Hearing4all”, European Medical School, Carl von Ossietzky Universität, 26111

Oldenburg, Germany; b Research Center Neurosensory Science, Carl von Ossietzky Universität, 26111 Oldenburg, Germany; c Department of Neurophysiology and Pathophysiology, University Medical Center Hamburg-Eppendorf, 20246 Hamburg, Germany

17 - Mitchell, Damon, N McNaughton, Danny Flanagan and Ian J. Kirk. "Frontal-midline theta from the perspective of hippocampal "theta"." Progress in Neurobiology 86 (2008): 156-185.

18 -Huster RJ, Enriquez-Geppert S, Lavallee CF, Falkenstein M, Herrmann CS. Electroencephalography of response inhibition tasks: functional networks and cognitive contributions. International Journal of Psychophysiology. 2013 Mar;87(3):217-33. Available from, DOI: 10.1016/j.ijpsycho.2012.08.001 19 - Functional aspects of alpha oscillations in the EEG: Martin Schürmanna Erol Başarab

20 - Britton JW, Frey LC, Hopp JLet al., authors; St. Louis EK, Frey LC: Electroencephalography (EEG): An Introductory Text and Atlas of Normal and Abnormal Findings in Adults, Children, and Infants; Chicago: American Epilepsy Society; 2016.

21 - Juri D. Kropotov, in Quantitative EEG, Event-Related Potentials and Neurotherapy, 2009

22 - Thomas F. Collura Ph.D., David Siever CET, in Introduction to Quantitative EEG and Neurofeedback (Second Edition), 2009

23 - Robert Coben James R. Evans, in Neurofeedback and Neuromodulation Techniques and Applications, 2011

24 - https://www.neurosonica.com/the-science/brainwave-types-frequencies.html

25 - Mormann, Florian, Jürgen Fell, Nikolai Axmacher, Bernd Weber, Klaus Lehnertz, Christian Erich Elger and Guillén Fernández. "Phase/amplitude reset and theta-gamma interaction in the human medial temporal lobe during a continuous word recognition memory task." Hippocampus 15 7 (2005): 890-900.

26 - https://www.epilepsy.com/article/2016/12/2017-revised-classification-seizures

27 - https://www.ilae.org/

28 - https://www.epilepsy.com/article/2016/12/2017-revised-classification-seizures

29 - https://www.epilepsy.com/learn/types-seizures/focal-onset-aware-seizures-aka-simple-partial-seizures

30 - N Sethi, P Sethi, J Torgovnick, E Arsura. Physiological and non-physiological EEG artifacts. The Internet Journal of Neuromonitoring. 2006 Volume 5 Number 2

31 - Erik K. St. Louis, MD and Lauren C. Frey, MD. Authors: Jeffrey W. Britton, MD, Lauren C. Frey, MD, Jennifer L. Hopp, MD, Pearce Korb, MD, Mohamad Z. Koubeissi, MD, FAAN, FANA, William E. Lievens, MD, Elia M. Pestana-Knight, MD, and Erik K. St. Louis, MD: Electroencephalography (EEG): An Introductory Text and Atlas of Normal and Abnormal Findings in Adults, Children, and Infants; Chicago: American Epilepsy Society; 2016. ISBN-13: 978-0-9979756-0-4

32 - Selim R Benbadis, MD: EEG Artifacts; https://emedicine.medscape.com/article/1140247-overview

33 - https://en.wikipedia.org/wiki/10–20_system_(EEG)

34 - Seeck, Margitta & Koessler, Laurent & Bast, Thomas & Leijten, Frans & Michel, Christoph & Baumgartner, Christoph & He, Bin & Beniczky, Sándor. (2017). The standardized EEG electrode array of the IFCN. Clinical Neurophysiology. 128. 10.1016/j.clinph.2017.06.254.

35 - https://www.verywellhealth.com/post-ictal-1204459

36 - Florian Mormann, Thomas Kreuz, Christoph Rieke, Ralph G. Andrzejak, Alexander Kraskov, Peter David, Christian E. Elger, Klaus Lehnertz, On the predictability of epileptic seizures, Clinical Neurophysiology, Volume 116, Issue 3, 2005, ISSN 1388-2457

37 - Bruno Direito and Teixeira, C. and Ribeiro, B. and Castelo-Branco, M. and Sales, F. and António Dourado, "Modeling epileptic brain states using EEG spectral analysis and topographic mapping", *Journal of Neuroscience Methods, Elsevier*, pp. 220-229, 2012

38 - https://towardsdatascience.com/the-vanishing-gradient-problem-69bf08b15484

39 - http://www.wildml.com/2015/10/recurrent-neural-networks-tutorial-part-3-backpropagation-through-time-and-vanishing-gradients/

40 - https://www.datasciencecentral.com/profiles/blogs/temporal-convolutional-nets-tcns-take-over-from-rnns-for-nlp-pred

41 - Bai, Shaojie & Zico Kolter, J & Koltun, Vladlen. (2018). An Empirical Evaluation of Generic Convolutional and Recurrent Networks for Sequence Modeling.

42 - Ashish Vaswani, Noam Shazeer, Niki Parmar, Jakob Uszkoreit, Llion Jones, Aidan N. Gomez, Lukasz Kaiser, Illia Polosukhin. Attention Is All You Need

43 - Stephen Grossberg. 2013. Adaptive Resonance Theory: How a brain learns to consciously attend, learn, and recognize a changing world. Neural Netw. 37 (January 2013), 1-47. DOI=http://dx.doi.org/10.1016/j.neunet.2012.09.017

44 - Klatt, Juliane & Feldwisch-Drentrup, Hinnerk & Ihle, Matthias & Navarro, Vincent & Neufang, Markus & Teixeira, César & Adam, Claude & Valderrama, Mario & Alvarado-Rojas, Catalina & Witon, Adrien & Le Van Quyen, Michel & Sales, Francisco & Dourado, Antonio & Timmer, Jens & Schulze-Bonhage, Andreas & Schelter, Bjoern. (2012). The EPILEPSIAE database: An extensive electroencephalography database of epilepsy patients. Epilepsia. 53. 1669-1676. 10.1111/j.1528-1167.2012.03564.x.

45 - http://www.epilepsiae.eu/project_outputs/european_database_on_epilepsy

46 - Teixeira, César & Direito, Bruno & Feldwisch-Drentrup B, H & Valderrama, Márcio & Costa, Rui & Alvarado-Rojas, Catalina & Nikolopoulos, Stavros & Le Van Quyen, Michel & Timmer B, J & Schelter B, B & Dourado, Antonio. (2011). EPILAB: A software package for studies on the prediction of epileptic seizures. Journal of neuroscience methods. 200. 257-71. 10.1016/j.jneumeth.2011.07.002. 47

47 - Prediction of Spike-Wave Bursts in Absence Epilepsy by EEG Power-Spectrum Signals: Armand Siegel, Cheryl L. Grady, Allan F. Mirsky

48 - Spectral and amplitude characteristics across studies Nima Bigdely-Shamlo, Jonathan Touryan, Alejandro Ojeda, Christian Kothe, Tim Mullen, Kay Robbins, Automated EEG mega-analysis I

49 - https://rewiringtinnitus.com/science-brainwave-entrainment/

50 - http://support.ircam.fr/docs/AudioSculpt/3.0/co/Discrete Cepstrum.html

51 - Boeing, G. 2016. "Visual Analysis of Nonlinear Dynamical Systems: Chaos, Fractals, Self-Similarity and the Limits of Prediction." *Systems*, 4 (4), 37. doi:10.3390/systems4040037

52 - Schlögl, Alois, Georg Dorffner, Bob Kemp, Alpo Värri, Thomas Penzel, Steve Roberts, Peter Anderer, Peter Rappelsberger, Iead Rezek, Gerhard Kloesch, Oliver Filz, Jon Wolpaw, Dennis J. McFarland and Theresa M. Vaughan. "The Electroencephalogram and the Adaptive Autoregressive Model: Theory and Applications." (2000).

53 - Yong Zhang; Xiaomin Ji; Yuting Zhang, Classification of EEG signals based on AR model and approximate entropy:

54 - Ohira, Junichiro & Yoshimura, Hajime & Morimoto, Takeshi & Ariyoshi, Koichi & Kohara, Nobuo. (2019). Factors associated with the duration of the postictal state after a generalized convulsion. Seizure. 65. 10.1016/j.seizure.2019.01.001.

55- David G. Greer, Peter D. Donofrio, Michael R. Dobbs: Clinical Neurotoxicology; Syndromes, Substances, Environments.

56 - https://nhahealth.com/brainwaves-the-language/

57 - Viglione S, Walsh G. Proceedings. Epileptic seizure prediction.

58 - Siegel A, Grady CL, Mirsky AF. Prediction of spike-wave bursts in absence epilepsy by EEG power-spectrum signals. Epilepsia 1982; 23: 47–60.

59 - Florian Mormann, Ralph G. Andrzejak, Christian E. Elger, Klaus Lehnertz; Seizure prediction: the long and winding road, *Brain*, Volume 130, Issue 2, 1 February 2007, Pages 314–333, https://doi.org/10.1093/brain/awl241

60 - Rogowski Z, Gath I, Bental E. On the prediction of epileptic seizures. Biol Cybern 1981; 42: 9–15.

61 - Salant Y, Gath I, Henriksen O. Prediction of epileptic seizures from two-channel EEG. Med Biol Eng Comput 1998; 36: 549–56.

62 - Iasemidis LD, Sackellares JC, Zaveri HP, Williams WJ. Phase space topography and the Lyapunov exponent of electrocorticograms in partial seizures. Brain Topogr 1990; 2: 187–201.

63 - Martinerie J, Adam C, Le Van Quyen M, Baulac M, Clemenceau S, Renault B, et al. Epileptic seizures can be anticipated by non-linear analysis. Nat Med 1998; 4: 1173–6.

64 - Le Van Quyen M, Martinerie J, Baulac M, Varela F. Anticipating epileptic seizure in real time by a nonlinear analysis of similarity between EEG recordings. Neuroreport 1999; 10: 2149–55.

65 - Le Van Quyen M, Martinerie J, Navarro V, Boon P, D'Have M, Adam C, et al. Anticipation of epileptic seizures from standard EEG recordings. Lancet 2001; 357: 183–8.

66 - Lehnertz K, Elger CE. Can epileptic seizures be predicted? Evidence from nonlinear time series analysis of brain electrical activity. Phys Rev Lett 1998; 80: 5019–23.

67 - Iasemidis LD, Pardalos P, Sackellares JC, Shiau DS. Quadratic binary programming and dynamical system approach to determine the predictability of epileptic seizures. J Comb Optim 2001; 5: 9–26.

68 - Litt B, Esteller R, Echauz J, D'Alessandro M, Shor R, Henry T, et al. Epileptic seizures may begin hours in advance of clinical onset: a report of five patients. Neuron 2001; 30: 51–64.

69 - Aschenbrenner-Scheibe R, Maiwald T, Winterhalder M, Voss HU, Timmer J, Schulze-Bonhage A. How well can epileptic seizures be predicted? An evaluation of a nonlinear method. Brain 2003; 126: 2616–26.

70 - Winterhalder M, Maiwald T, Voss HU, Aschenbrenner-Scheibe R, Timmer J, Schulze-Bonhage A. The seizure prediction characteristic: a general framework to assess and compare seizure prediction methods. Epilepsy Behav 2003; 4: 318–25.

71 - Maiwald T, Winterhalder M, Aschenbrenner-Scheibe R, Voss HU, Schulze-Bonhage A, Timmer J. Comparison of three nonlinear seizure prediction methods by means of the seizure prediction characteristic. Physica D 2004; 194: 357–68.

72 - De Clercq W, Lemmerling P, Van Huffel S, Van Paesschen W. Anticipation ofepileptic seizures from standard EEG recordings. Lancet 2003; 361: 971.

73 - McSharry PE, Smith LA, Tarassenko L. Prediction of epileptic seizures: are nonlinear methods relevant? Nat Med 2003; 9: 241–2.

74 - Lai YC, Harrison MA, Frei MG, Osorio I. Inability of Lyapunov exponents to predict epileptic seizures. Phys Rev Lett 2003; 91: 068102.

75 - Lehnertz K, Litt B. The first international collaborative workshop on seizure prediction: summary and data description. Clin Neurophysiol 2005; 116: 493–505.

76 - D'Alessandro M, Vachtsevanos G, Esteller R, Echauz J, Cranstoun S, Worrell G, et al. A multi-feature and multi-channel univariate selection process for seizure prediction. Clin Neurophysiol 2005; 116: 506-16.

77 - Iasemidis LD, Shiau D, Chaovalitwongse W, Sackellares JC, Pardalos PM, Principe JC, et al. Adaptive epileptic seizure prediction system. IEEE Trans Biomed Eng 2003; 50: 616-27.

78 - Iasemidis LD, Shiau D, Pardalos PM, Chaovalitwongse W, Narayanan K, Prasad A, et al. Long-term prospective on-line real-time seizure prediction. Clin Neurophysiol 2005; 116: 532-44.

79 - An Adaptive Structure Neural Networks with Application to EEG Automatic Seizure Detection.: Khorasani K1, Weng W.

80 - Runarsson TP, Sigurdsson S: On-line detection of patient specific neonatal seizures using support vector machines and half-wave attribute histograms. In The International Conference on Computational Intelligence for Modelling, Control and Automation, and International Conference on Intelligent Agents, Web Technologies and Internet Commerce (CIMCA-IAWTIC). Vienna; 673-677. 28–30 Nov 2005

81 - Khamis H, Mohamed A, Simpson S: Frequency–moment signatures: a method for automated seizure detection from scalp EEG. Clin. Neurophysiol. 2013, 124(12):2317-2327. 10.1016/j.clinph.2013.05.015

82 - Acharya UR, Sree SV, Swapna G, Martis RJ, Suri JS: Automated EEG analysis of epilepsy: a review. Knowl.-Based Syst. 2013, 45: 147-165.

83 - Martis, Roshan & Tan, Jen Hong & Chua, Kuang & Cheah Loon, Too & Yeo Wan Jie, Sharon & Tong, Louis. (2015). Epileptic EEG classification using nonlinear parameters on different frequency bands. Journal of Mechanics in Medicine and Biology. 15. 1550040. 10.1142/S0219519415500402.

84 - U. Orhan, M. Hekim, M. Ozer, EEG signals classification using the K-means clustering and a multilayer perceptron neural network model, Expert Syst. Appl. 38 (10) (2011) 13475–13481.

85 - W.Weng K.Khorasani, An Adaptive Structure Neural Networks with Application to EEG Automatic Seizure Detection

86 -Xiaoyan Wei, Lin Zhou, Ziyi Chen, Liangjun Zhang and Yi Zhou; Automatic seizure detection using three-dimensional CNN based on multi-channel EEG

87 - Li S, Zhou W, Yuan Q, Liu Y: Seizure prediction using spike rate of intracranial EEG. IEEE Trans. Neural Syst. Rehabil. Eng. 2013, 21(6):880-886.

88 - Alotaiby, Turky N., Saleh A. Alshebeili, Tariq Alshawi, Ishtiaq Ahmad and Fathi E. Abd El-Samie. "EEG seizure detection and prediction algorithms: a survey." EURASIP J. Adv. Sig. Proc. 2014 (2014): 183.

89 - Aarabi A, He B: A rule-based seizure prediction method for focal neocortical epilepsy. Clin. Neurophysiol. 2012, 123(6):1111-1122. 10.1016/j.clinph.2012.01.014

90 - Mojtaba Bandarabadi, César A. Teixeira, Jalil Rasekhi, António Dourado; Epileptic seizure prediction using relative spectral power features; CISUC/DEI, Center for Informatics and Systems of the University of Coimbra, Department of Informatics Engineering, Polo II, 3030-290 Coimbra, Portugal

91 -Bruno Direito, César A. Teixeira, Francisco Sales, Miguel Castelo-Branco, António Dourado; A Realistic Seizure Prediction Study Based on Multiclass SVM; University of Coimbra, Portugal

92 - Min Jing and Saeid Sanei: A Novel Constrained Topographic Independent Component Analysis for Separation of Epileptic Seizure Signals Centre of Digital Signal Processing, Cardiff University, Cardiff CF24 3AA, Wales, UK

93 - http://desktop.arcgis.com/en/arcmap/10.3/tools/spatial-analyst-toolbox/how-natural-neighbor-works.htm#GUID-81A67F31-5180-4721-AF52-BCE7B6AFB761

94 - http://mathworld.wolfram.com/VoronoiDiagram.html

95 - Hallez, Hans, Bart Vanrumste, Roberta Grech, Joseph Muscat, Wim De Clercq, Anneleen Vergult, Yves D'Asseler, Kenneth P. Camilleri, Simon G. Fabri, Sabine Van Huffel and Ignace Lemahieu. "Review on solving the forward problem in EEG source analysis." Journal of NeuroEngineering and Rehabilitation 4 (2007): 46 - 46.

96 - H. Daoud and M. Bayoumi, "Deep Learning based Reliable Early Epileptic Seizure Predictor," 2018 IEEE Biomedical Circuits and Systems Conference (BioCAS), Cleveland, OH, USA, 2018, pp. 1-4. doi: 10.1109/BIOCAS.2018.8584678

97 - Scott Segan, MD, Absence Seizures; https://reference.medscape.com/article/1183858-overview

98 - Buzsáki, Gyorgy & Anastassiou, Costas & Koch, Christof. (2012). The origin of extracellular fields and currents—EEG, ECoG, LFP and spikes. Nature reviews. Neuroscience. 13. 407-20. 10.1038/nrn3241.

99 - Sharbrough, F & Chatrian, G.E. & Lesser, Ronald & Luders, H & Nuwer, M & Picton, Terence. (1991). American Electroencephalographic Society guidelines for standard electrode position nomenclature. Clinical Neurophysiology. 8. 200-202.

100 - Joel E. Morgan, Joseph H. Ricker: Textbook of Clinical Neuropsychology; Taylor & Francis

101 - Siddiqui, Asra & Kerb, Reinhold & E Weale, Michael & Brinkmann, Ulrich & Smith, Alice & Goldstein, David & Wood, Nicholas & M Sisodiya, Sanjay. (2003). Association of Multidrug Resistance in Epilepsy with a Polymorphism in the Drug-Transporter Gene ABCB1. The New England journal of medicine. 348. 1442-8. 10.1056/NEJMoa021986.

102 - Glorot, Xavier & Bengio, Y. (2010). Understanding the difficulty of training deep feedforward neural networks. Journal of Machine Learning Research - Proceedings Track. 9. 249-256.

103 - Kingma, Diederik & Ba, Jimmy. (2014). Adam: A Method for Stochastic Optimization. International Conference on Learning Representations.

104 - de Curtis, Marco & Gnatkovsky, Vadym. (2009). Reevaluating the mechanisms of focal ictogenesis: The role of low-voltage fast activity. Epilepsia. 50. 2514-25. 10.1111/j.1528-1167.2009.02249.x.

105 - Pourmand, R. (1994). The Significance of Amplitude Asymmetry in Clinical Electroencephalography. Clinical EEG (electroencephalography). 25. 76-80. 10.1177/155005949402500208.

106 - Jin, Bo & So, Norman & Wang, Shuang. (2016). Advances of Intracranial Electroencephalography in Localizing the Epileptogenic Zone. Neuroscience Bulletin. 32. 10.1007/s12264-016-0035-8.

107 - Britton JW, Frey LC, Hopp JLet al., authors; St. Louis EK, Frey LC, editors. Electroencephalography (EEG): An Introductory Text and Atlas of Normal and Abnormal Findings in Adults, Children, and Infants [Internet]. Chicago: American Epilepsy Society; 2016. Available from: https://www.ncbi.nlm.nih.gov/books/NBK390354/

108 - Mader, Edward & Olejniczak, Piotr. (2018). EPILEPSY SYNDROMES *.

Appendix A

Topographic map creation

Preliminary work

This chapter explains what was done in the first semester of this thesis project. With exception for studying the problem and the state of the art, the work of the first semester consisted mostly on the creation and validation of topographic maps.

5.1 Topographic maps

5.1.1 Geometry

There are many different approaches to plot the geometry of a topographic map. A topographic map of the scalp corresponds to an approximation of the electrode positions on the scalp by creating a tangent space that fits this approximation. The approach that we have picked in this work is based on interceptions of circles, that attempt to simulate the curves of the human head. So far it assumes the head to be circular when seen from above but a correction to this may be done in the future, but it will probably yield the same classification results, since this correction will be based on the circular geometry created. Another possible geometric tool to explore here could be the transverse Mercator projection.

The geometry chosen is centered around two concentric circles: one with a larger radius for the six electrodes that are at eye level (X9 and X10) and another for those that are right above. Other auxiliary circles will be used, which will be explained below. The X and Y axis will also be used. The electrodes will correspond to some of the interceptions of this circles and axis.

In order to create the wanted geometrical pattern, it is useful to have formulas that calculate these interceptions. Since it is trivial to intercept the circles with the axis, we only need to find a formula to intercept circles with circles. To simplify this process, we will simply use the fact that any axis on a bi-dimensional plane can be translated such as they will fit two points having one with its x coordinate equal to zero and another with its y coordinate equal to zero. This is trivial to verify since, in a bi-dimensional plane, an axis can be moved in a direction perpendicular to itself, thus it is able to fit the coordinate of the other axis of one point at 0 or any other value and, since we have two axis we can fit two points, which, in this case, will be the centers of two circles. In this case, it follows that we can solve this system of equations to intercept two circles (Eq. 7):

$$\begin{cases}(x-a)^2+y^2=r_1^2\\ x^2+(y-b)^2=r_2^2\end{cases} \qquad \text{Eq. 7}$$

With one circle having its center at [a,0] and radius r_1 and the other having its center at [0,b] and radius r_2.

Isolating and replacing the terms of this equation we can obtain (Eq. 8):

$$\begin{cases} y = \sqrt{r_1^2 - (x-a)^2} \\ -4(b^2x^2 + a^2x^2) + 4(ab^2 + a^3 - ac) = -4b^2r_1^2 + 2a^2b^2 + a^4 + b^4 - 2a^2c + c^2 \end{cases} \quad \text{Eq. 8}$$

Where $c = r_1^2 - r_2^2$.

To simplify this expression, we can consider (Eq. 9, 10, 11):

$$d = a^2 + b^2 \quad \text{Eq. 9}$$

$$e = ab^2 + a^3 - ac \quad \text{Eq. 10}$$

$$f = -4b^2r_1^2 + 2a^2b^2 + a^4 + b^4 - 2a^2c + c^2 \quad \text{Eq. 11}$$

Now through the quadratic formula we can obtain (Eq. 12):

$$\begin{cases} y = \sqrt{r_1^2 - (x-a)^2} \\ \frac{4e \pm \sqrt{16e^2 - 16df}}{8d} \end{cases} \quad \text{Eq. 12}$$

With this formula we can easily compute the intersections of any two circles if we know their centers and radiuses. To solve in order to x firstly, we simply need to trade the x's for the y's, the a's for the b's and r_1 for r_2.

The main unit to consider here is the radius of the larger circle, which we will call r, which corresponds to half of the map's resolution. Since, in the 10-10 electrode position system, there are ten electrodes along each axis until the bigger circle and 8 until the smaller one, the radius of the smaller circle is *0.8r*. In order to obtain suitable positions for the electrodes that are inside and along the smaller circle we will need four more auxiliary circles.

Taking the 10-20 system, the first circle will contain the points corresponding to the Fp1, F3, C3, P3, O1 electrodes. This circle has a center at $r(tan(0.4) - 0.4)$ and a radius of $\frac{r}{\tan(0.4)}$ as this allows C3 to be half way between Cz and T3. The circle that contains the symmetrical in relation to the y axis electrodes is, obviously symmetrical in relation to the y axis to the previously mentioned circle. We will also plot the equivalent circles to this ones, but with the x and y coordinates switched. After this, we will end up with something of the kind of Figure 7.

This only places the values of the electrodes on certain positions on the plane. Now we need to find the remaining points on the plane to create a map.

5.1.2 Interpolation

Interpolation, in numerical analysis, is a method of constructing new data points in the range of previously known data points.

The interpolation method chosen at this point was the natural neighbor interpolation (93). This method creates a Voronoi tessellation [94] with the electrode values and their positions and, for each new point to be inserted, calculates the various weights based on the portions of the Voronoi tessellation that are taken from the other points. This can be expressed by the following equation (Eq. 13):

$$G(x^*, y^*) = \sum_{i=1}^{n} w_i f(x_i, y_i) \qquad \text{Eq. 13}$$

Where $G(x^*, y^*)$ is the value obtained on a new point, $f(x_i, y_i)$ is the value at a given point (x_i, y_i) and w_i is the weight assigned to a point (x_i, y_i). The greater the taken portion is, the greater the weight.

This works as a smoother form of linear interpolation. If we want a form of interpolation which is non-linear we can apply a transformation to the values that makes them linear, build the interpolator with those linear values, and then apply the inverse transformation to the final obtained values. This works because natural interpolation is a linear transformation for points that have the same weights (in the same position). The function *scateredinterpolant* from Matlab was be used to create this interpolator, but others work just as well.

5.1.3 Extrapolation

Extrapolation is necessary here for estimating the values on the scalp that are outside of the convex hull of the electrode points. This values are probably not that relevant but, for now, let's have them. I will be using nearest neighbor extrapolation, for now, which consists of assigning the value of the nearest point to values that are beyond the limit of the convex hull. It is needless to say that this method will not produce spectacular results so there is room open for improvement if need be, or, most likely, excluding this method. The function *scateredinterpolant* from Matlab was be used to create this as well.

5.1.4 Contours and coloring

First, it should be clarified that, in order to have an easy term of comparison between features, I will be plotting the Z-scores of each feature rather than the values of the feature itself. As such, the values will be plotted in a scale of -3 to 3. This is a common practice when it comes to topographic brain maps. The step chosen was 0.25 and this means the contours will mark steps of such magnitude. The jet color pallet of Matlab was chosen. In Figures 9 and 10 we have representations of the color scale and an example map

5.1.5 Map validation

In order to validate the maps, a benchmark generator that can generate signals that exclude certain bands in each electrode and then calculates their power spectrum density was created. In this way, we can simulate, for example, an electrode that only produces delta waves, or only produces beta and gamma waves. We can then produce a short video with various samples of topographic maps for the given configuration. The benchmark created is described in Table 1.

Electrodes\Waves	Delta	Theta	Alpha	Beta	Gamma
Fp1	X				
Fp2	X	X			
F7		X	X		
F3		X			
Fz			X		
F4			X	X	
F8				X	
T3				X	
C3			X	X	
Cz				X	X
C4					X
T4			X	X	X
T5			X	X	
P3			X		
Pz		X	X		
P4		X			
T6	X	X			
O1		X	X	X	
O2	X				

Table 18 – Configuration for the validation maps.

This configuration produced the following maps:

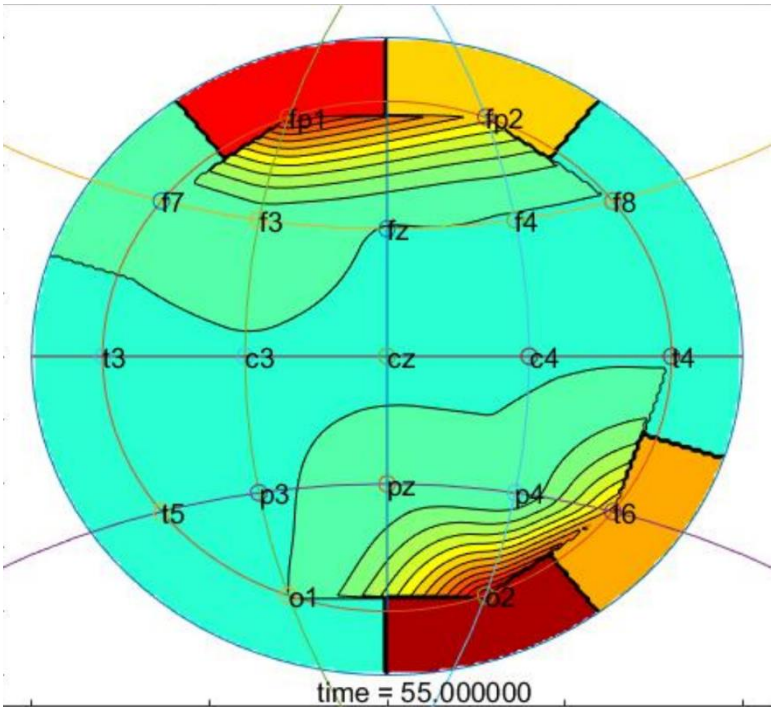

Figure 42 – power spectrum density of delta waves for time = 55 seconds.

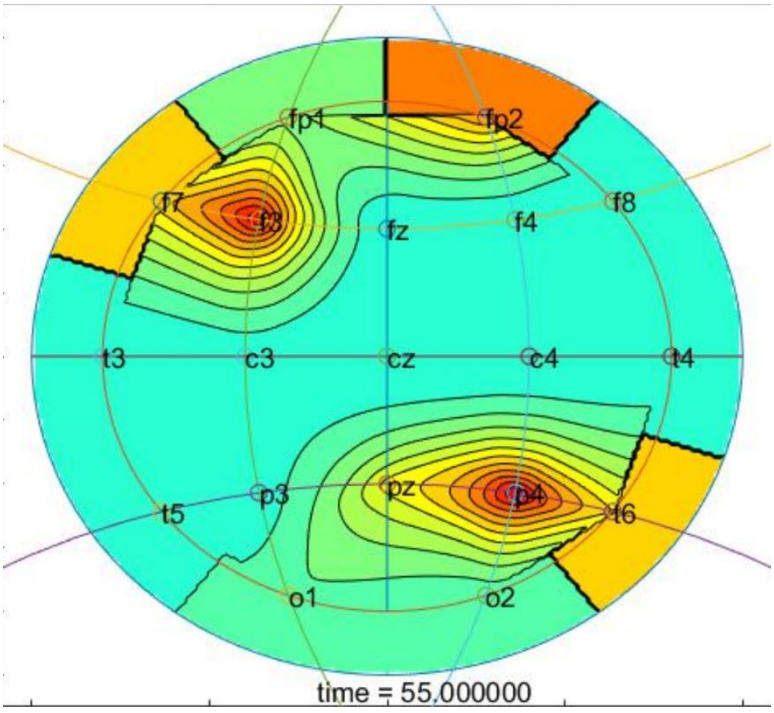

Figure 43 – Relative power spectrum density of theta waves for time = 55 seconds.

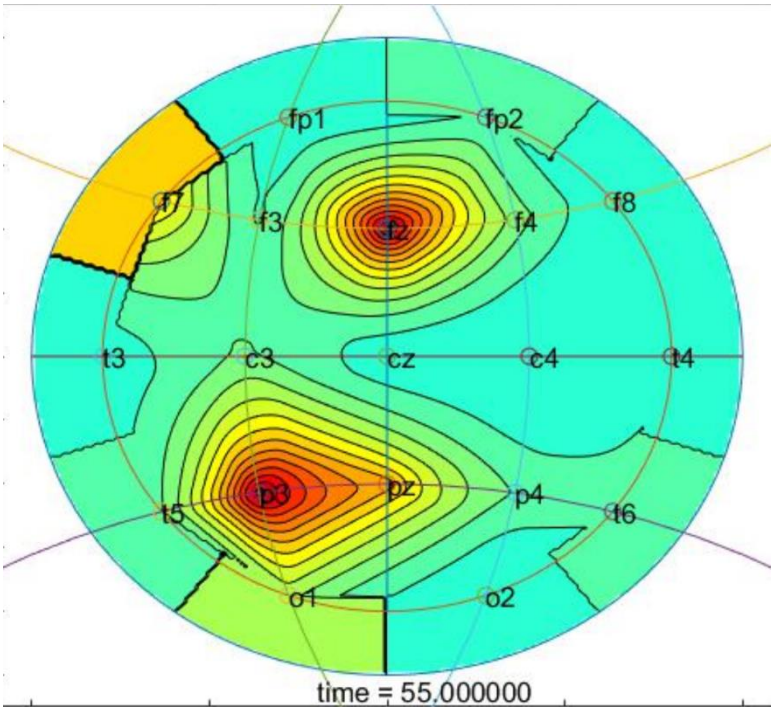

Figure 44 – Relative power spectrum density of alpha waves for time = 55 seconds.

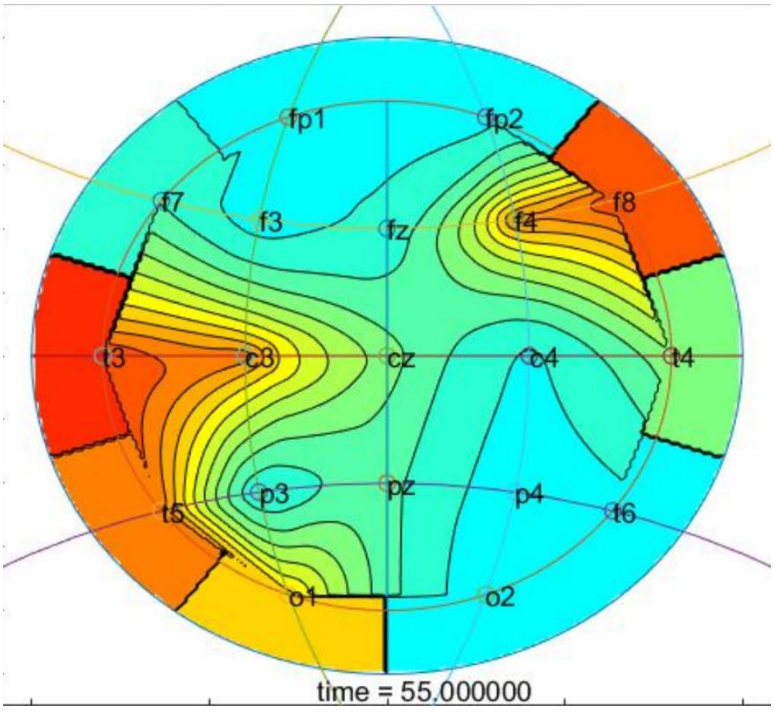

Figure 45 – Relative power spectrum density of beta waves for time = 55 seconds.

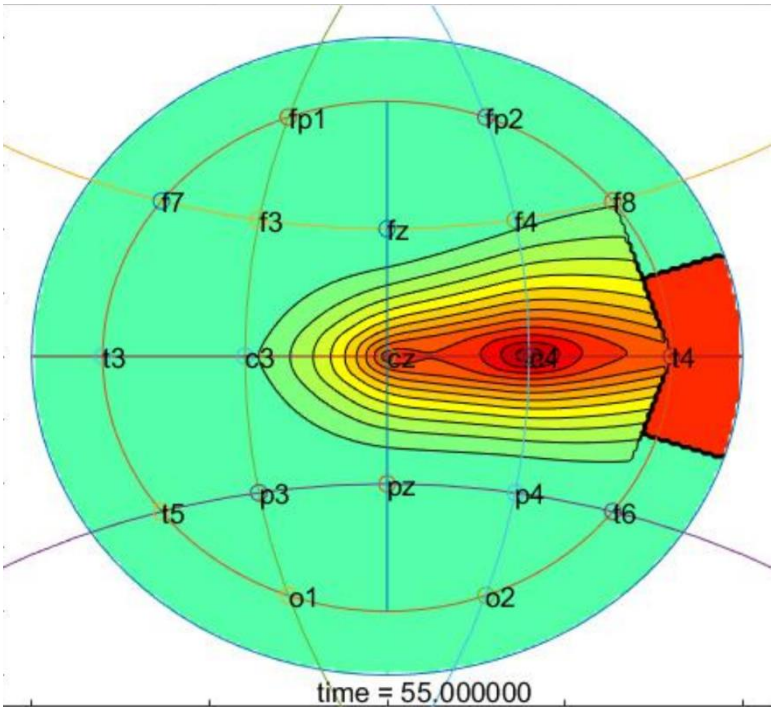

Figure 46 – Relative power spectrum density of gamma waves for time = 55 seconds.

As can be seen, this results validate the method and code used to produce this maps and so we can proceed to apply them to real data. The issue that seems to be present here is that, for example, the alpha waves seem to be made redundant by the beta waves. This is due to the frequency range of the beta waves being 4.5 times greater than the one of the alpha waves being considered. This will not be significant in real EEG data, given that the amplitude of alpha waves is of greater magnitude that the one of the beta waves, evening out this effect. However, these discrepancies in amplitude and frequency range between waves may require some attention in the future.

5.2 Preliminary conclusions

During the first semester of this thesis project, the topographic map creation toolbox was produced, validated and preliminary evaluation of relative spectral powers of the various brain waves has been informally evaluated by compiling the maps in a video for one patient and trying to look for some changes. There appear to be some pre-ictal differences in some brain wave bands in some areas of the brain, such as the theta band, but it is extremely difficult to evaluate those differences and come to any trustworthy results.

More important than that, the literature, concepts and tools necessary or useful for this thesis have been extensively reviewed and a much clearer picture of what needs to be done to produce relevant work has surfaced. The research done so far leads to a few conclusions:

1. **CNNs are likely perfectly suited for EEG spacial analysis**, as, in their convolution layers they can successfully retrieve spacial features and find regions of interest.
2. The quantity of features that provide encouraging results on seizure detection and prediction plus the fact that raw EEG also provides good results leads one to the conclusion that **there is some common ground in at least some of these features** that is discriminating the various epileptic brain states. That being said, more holistic, complementary or lower level features may produce better results.
3. **Spacial analysis of EEG looks promising to predict and detect seizures**, as various studies [37, 86, 96] achieved good sensitivity and specificity results
4. Taking into account the fact that we reached the conclusion that the signal on EEG electrodes is spatiotemporally correlated and the use of LSTMs gave promising results on seizure prediction [96], we can infer that it **may be useful to develop or use machine learning mechanisms, such as TCNs or LSTM modules, or features that express temporal or spacial evolution**, such as AR coefficients or spectral flux, to help successful classification of the various epileptic brain states.
5. **Studying the entropy of EEG signals has also yielded good classification results**, so it would be a valid choice to exploit that.

Appendix B

Illustrative charts for the test results of the standard approach (chronological order)

Patient #58602

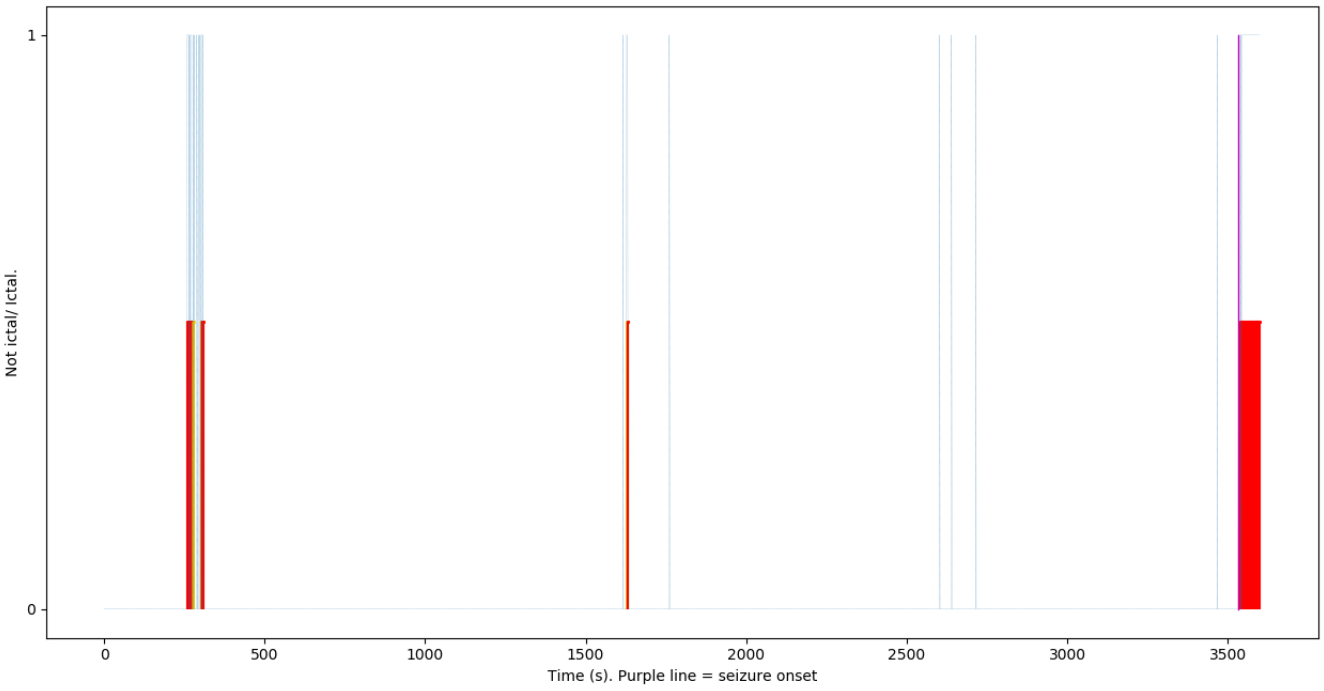

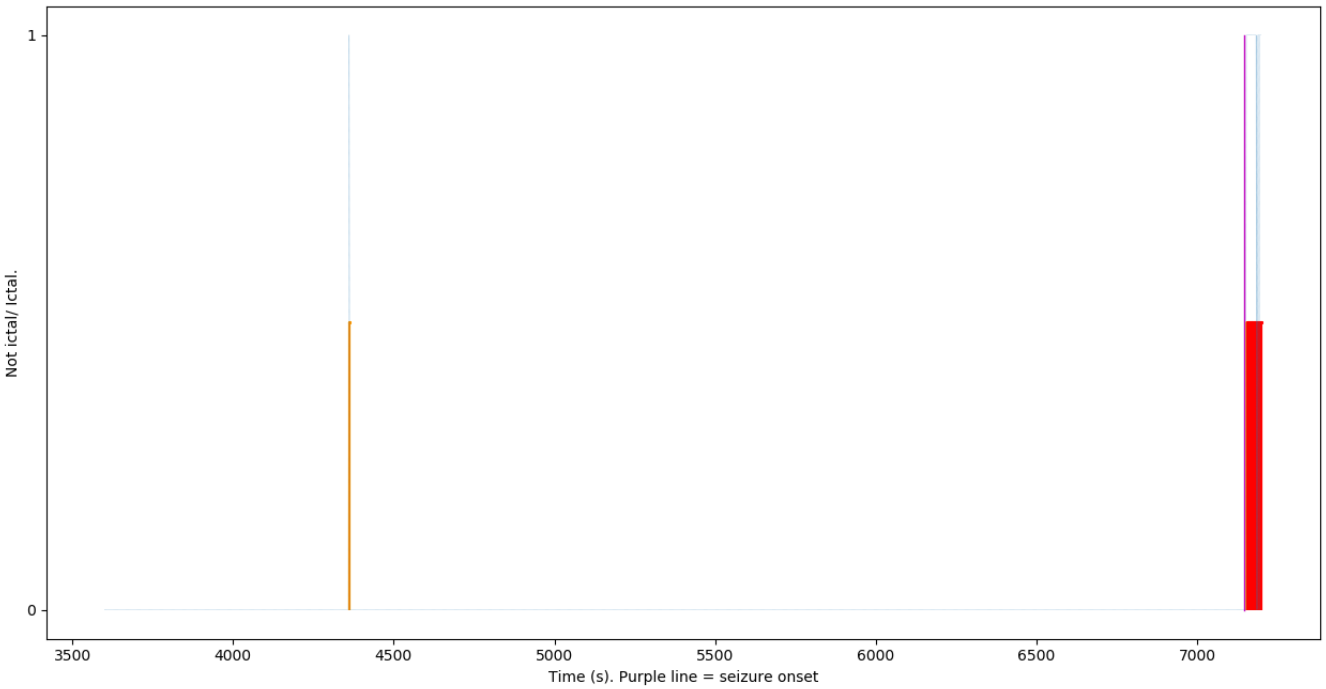

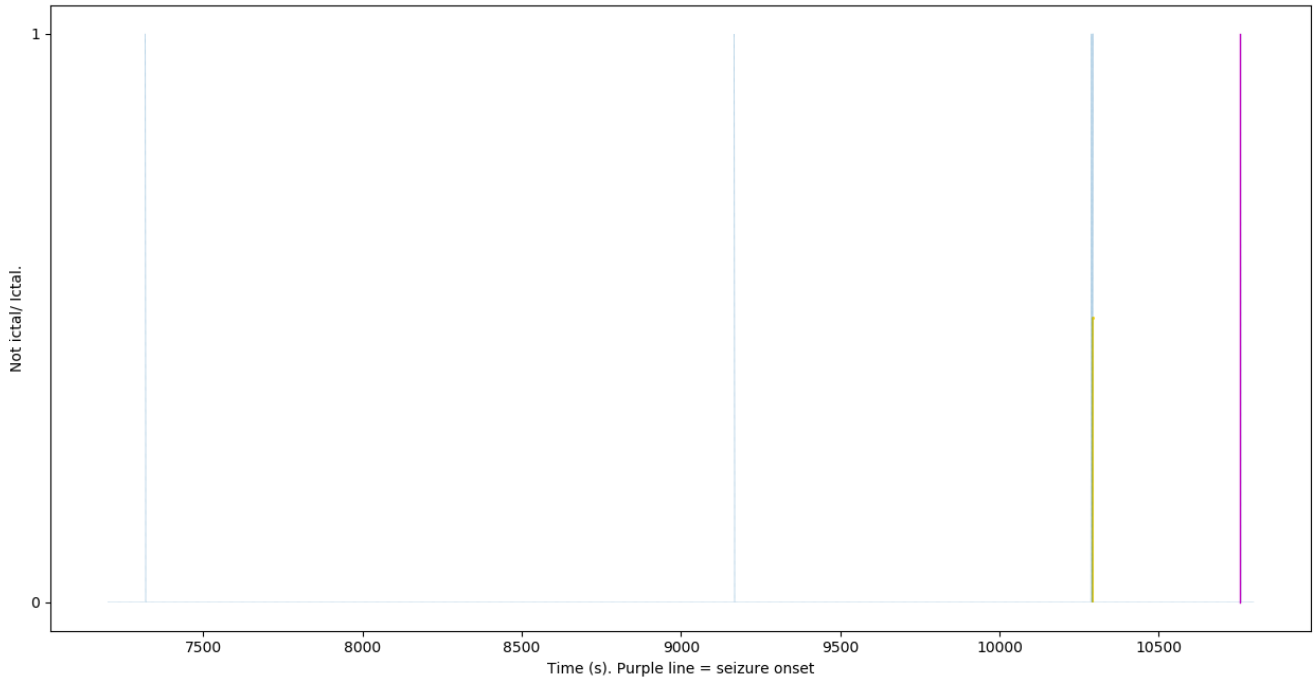
1
0
Not ictal/ Ictal.
7500
8000
8500
9000
9500
10000
10500
Time (s). Purple line = seizure onset

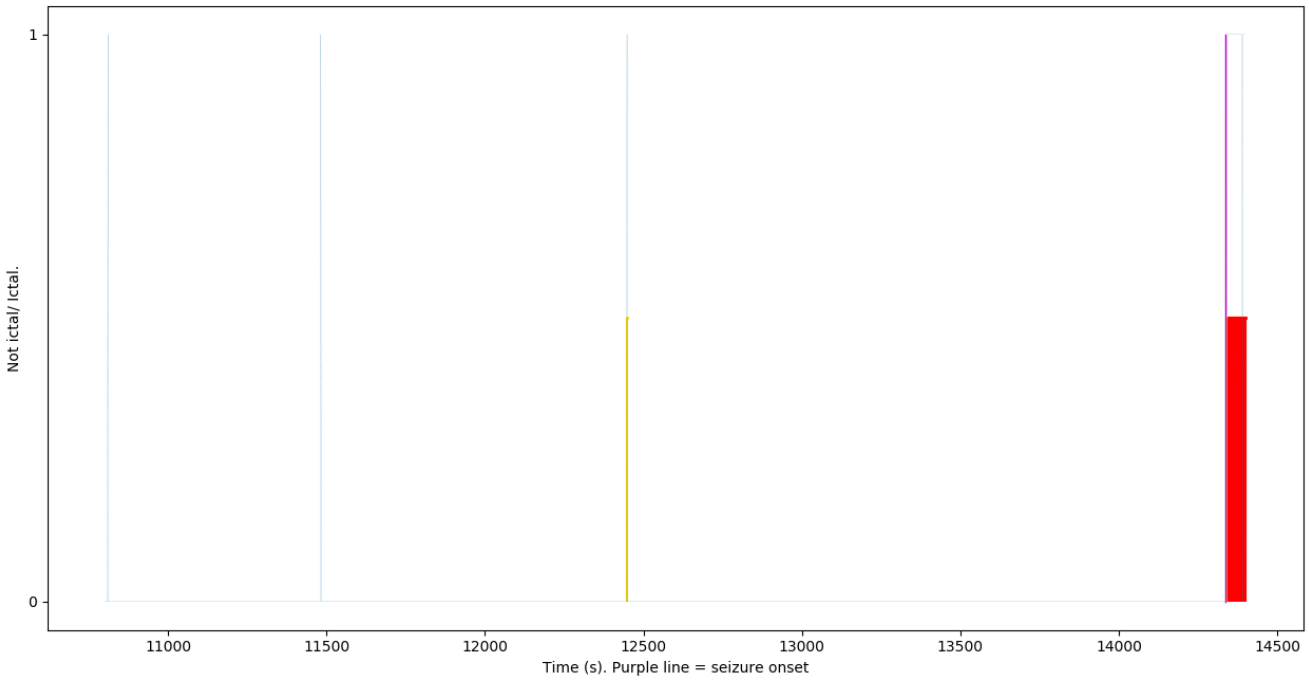
1
0
Not ictal/ Ictal.
11000
11500
12000
12500
13000
13500
14000
14500
Time (s). Purple line = seizure onset

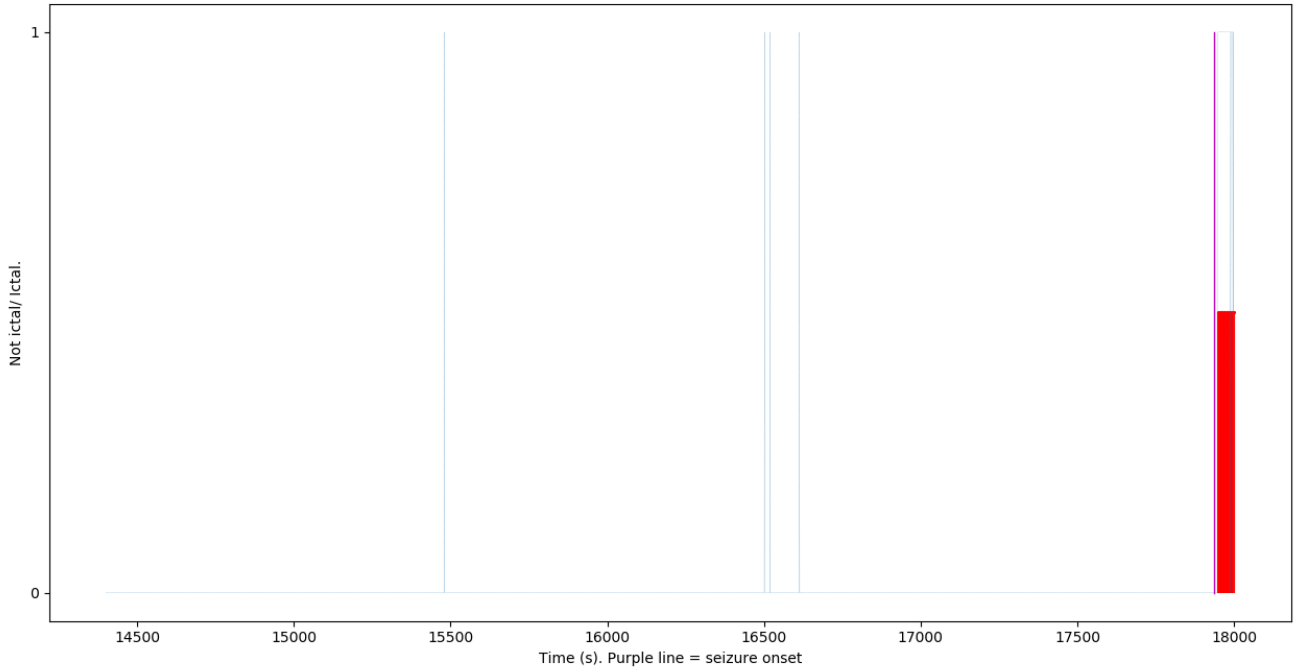
1
0
Not ictal/ Ictal.
14500
15000
15500
16000
16500
17000
17500
18000
Time (s). Purple line = seizure onset

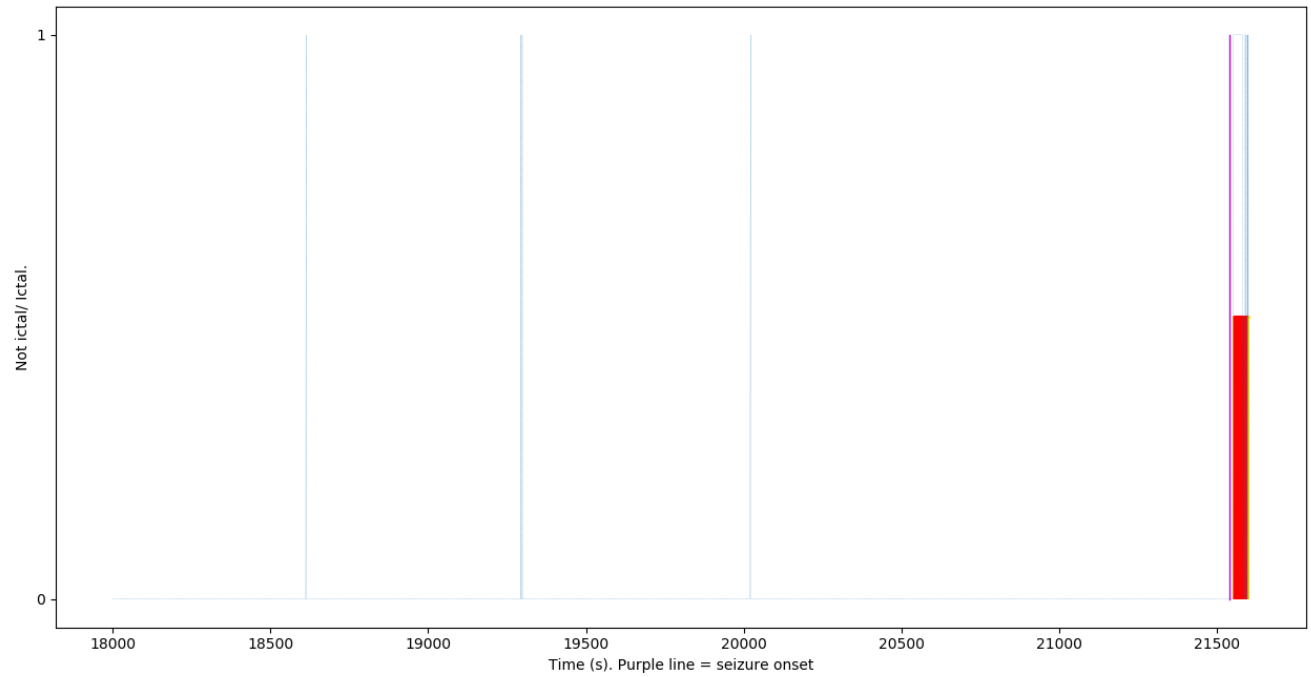
1
0
Not ictal/ Ictal.
18000
18500
19000
19500
20000
20500
21000
21500
Time (s). Purple line = seizure onset

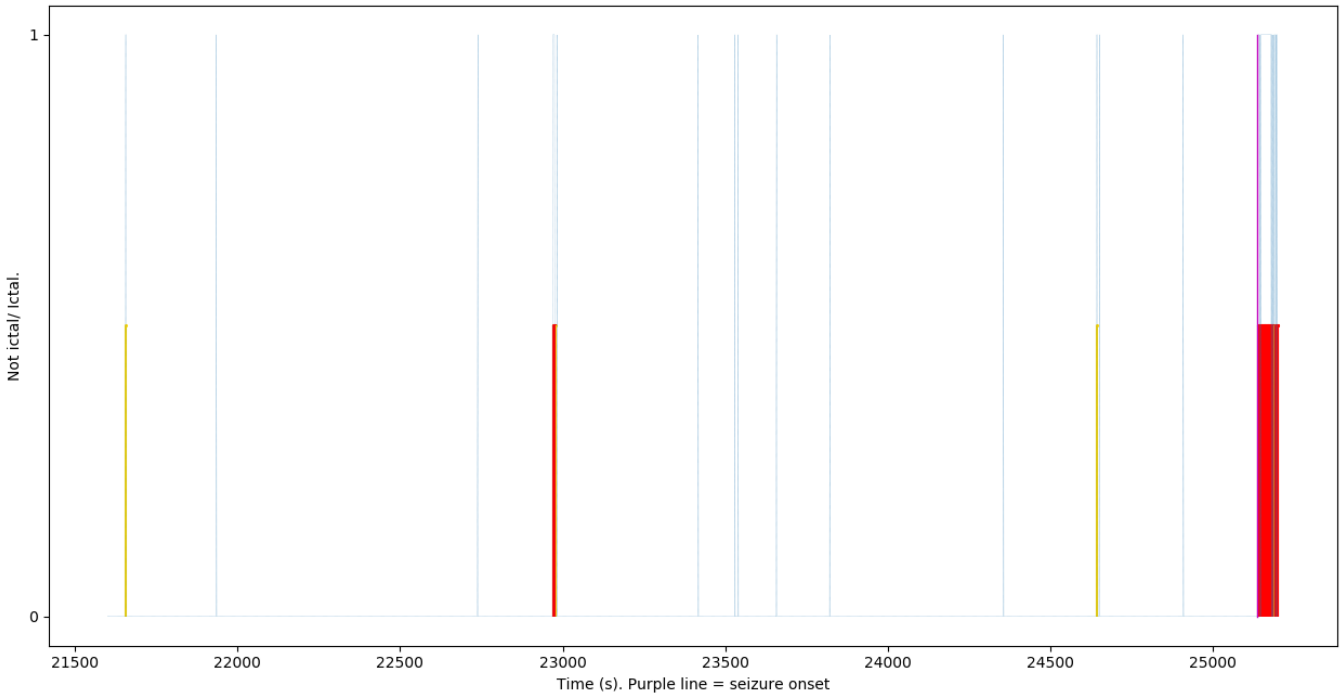
1
0
Not ictal/ Ictal.
21500
22000
22500
23000
23500
24000
24500
25000
Time (s). Purple line = seizure onset

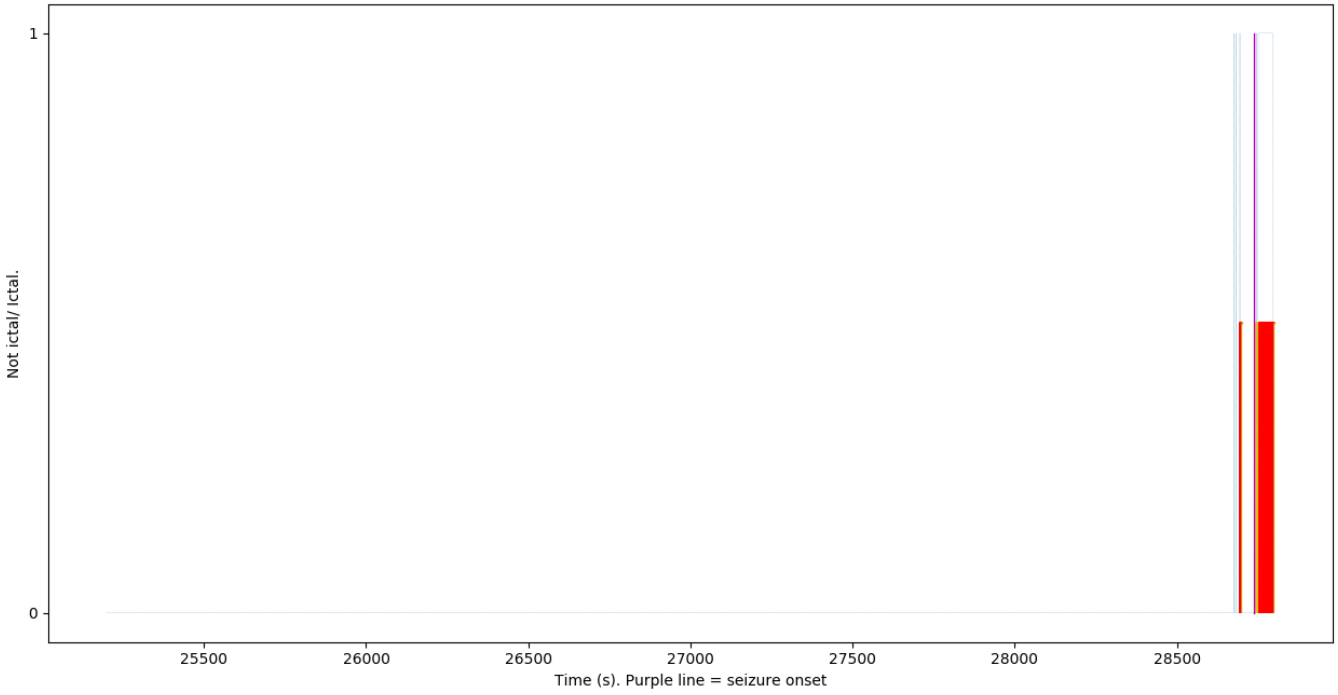
1
0
Not ictal/ Ictal.
25500
26000
26500
27000
27500
28000
28500
Time (s). Purple line = seizure onset

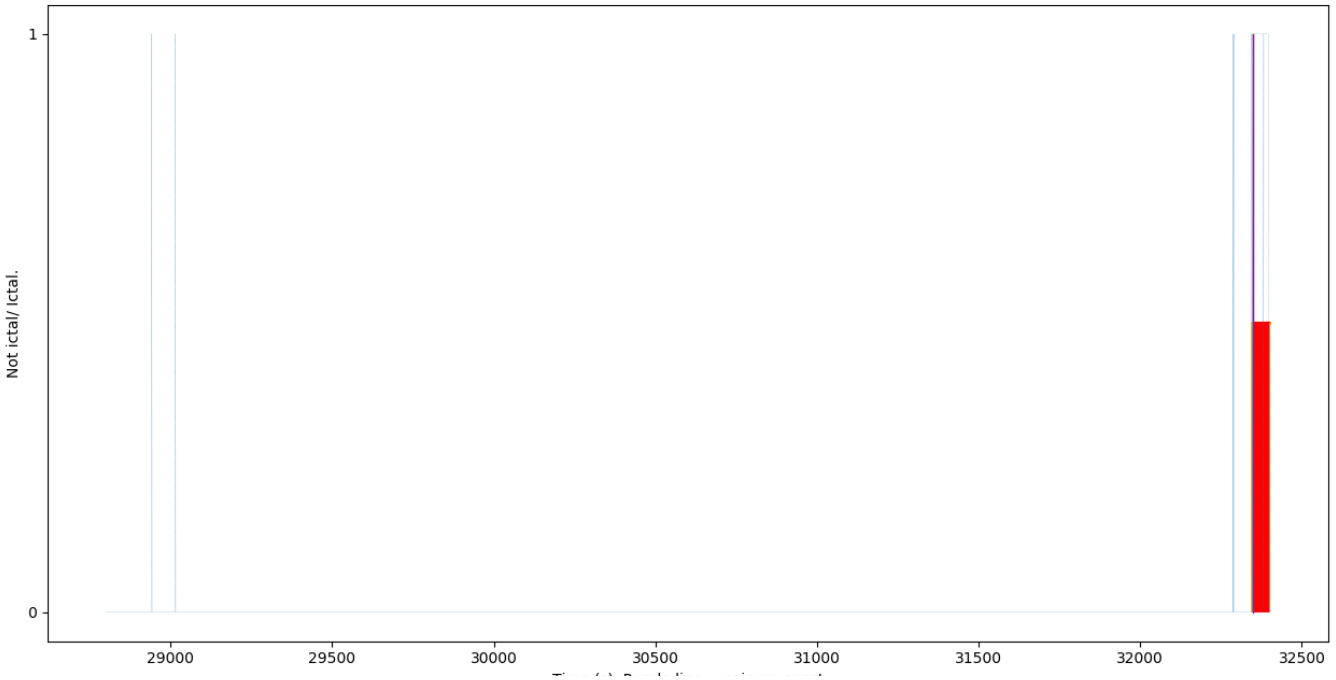
1
0
Not ictal/ Ictal.
29000
29500
30000
30500
31000
31500
32000
32500

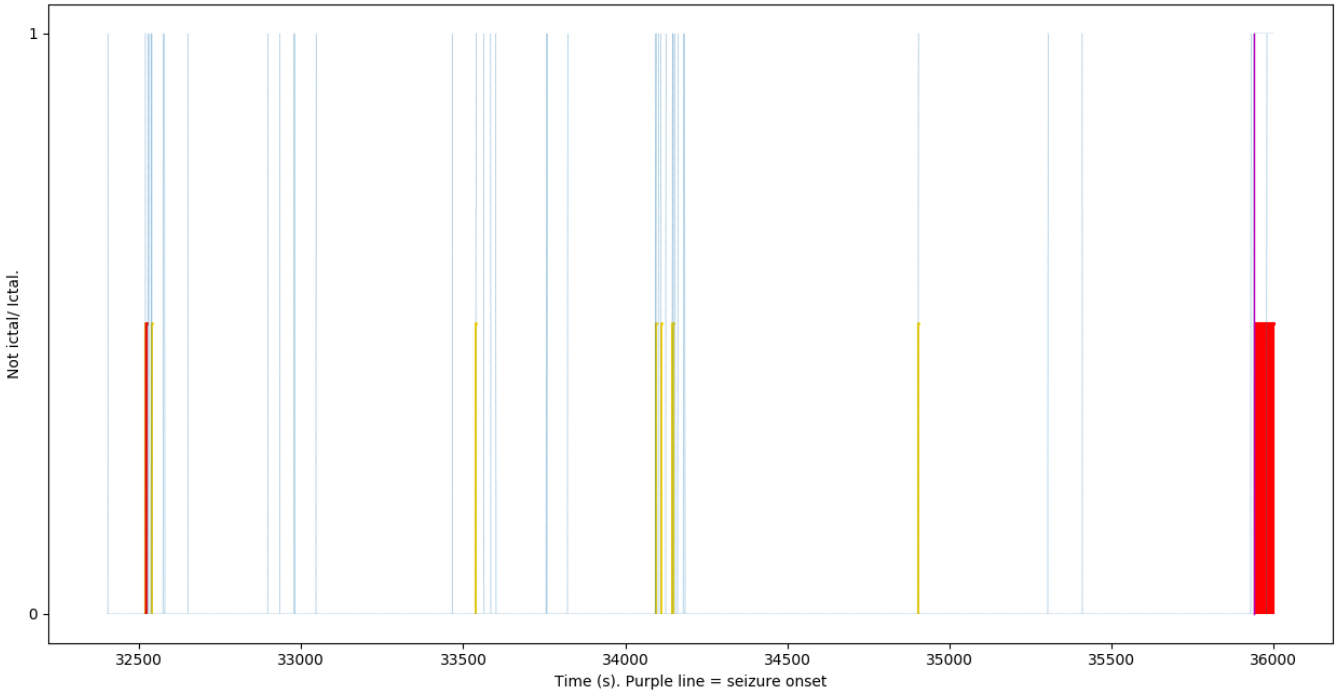
1
0
Not ictal/ Ictal.
32500
33000
33500
34000
34500
35000
35500
36000
Time (s). Purple line = seizure onset

Patient #11002

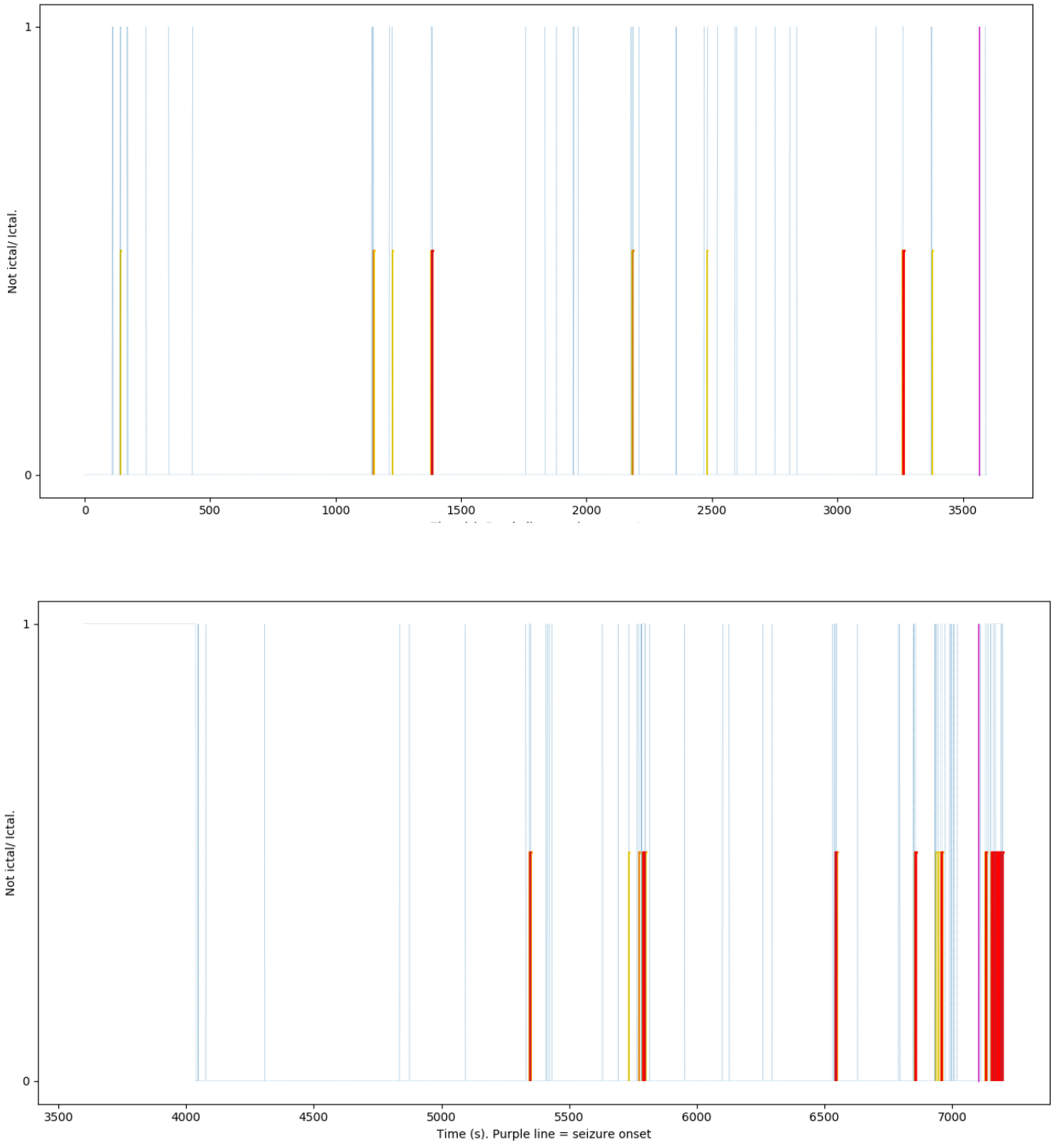

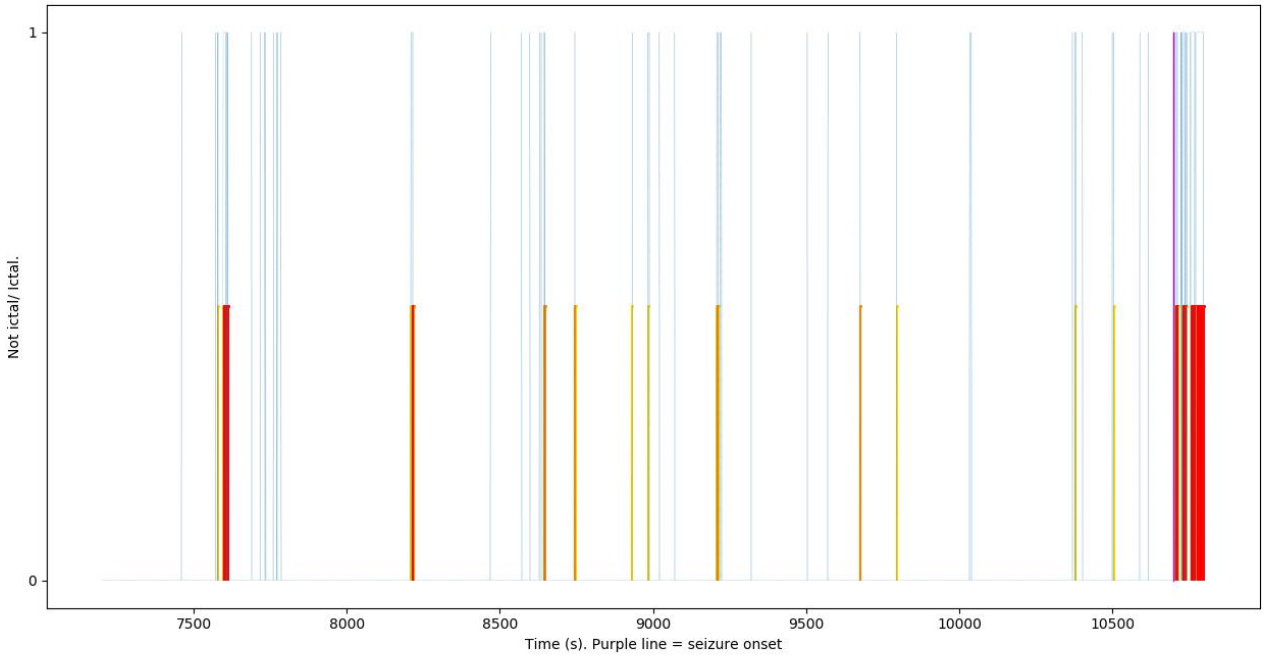
1
0
Not ictal/ Ictal.
7500
8000
8500
9000
9500
10000
10500
Time (s). Purple line = seizure onset

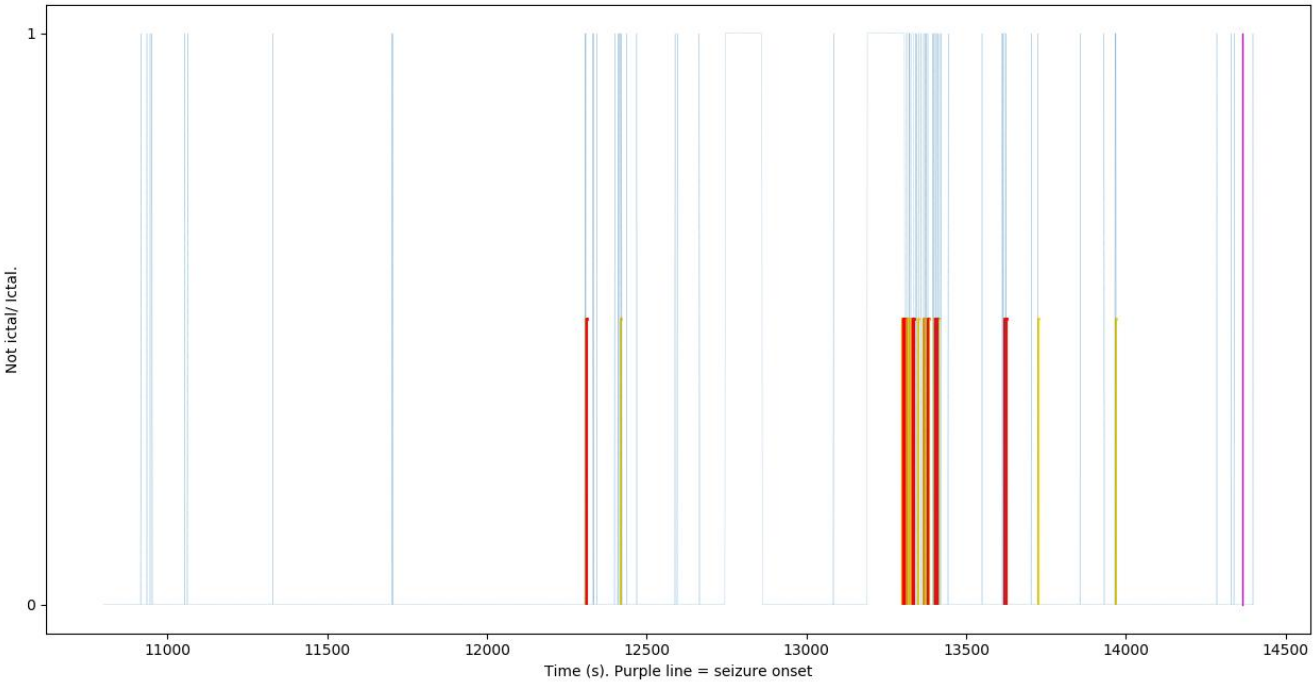
1
0
Not ictal/ Ictal.
11000
11500
12000
12500
13000
13500
14000
14500
Time (s). Purple line = seizure onset

Patient #30802

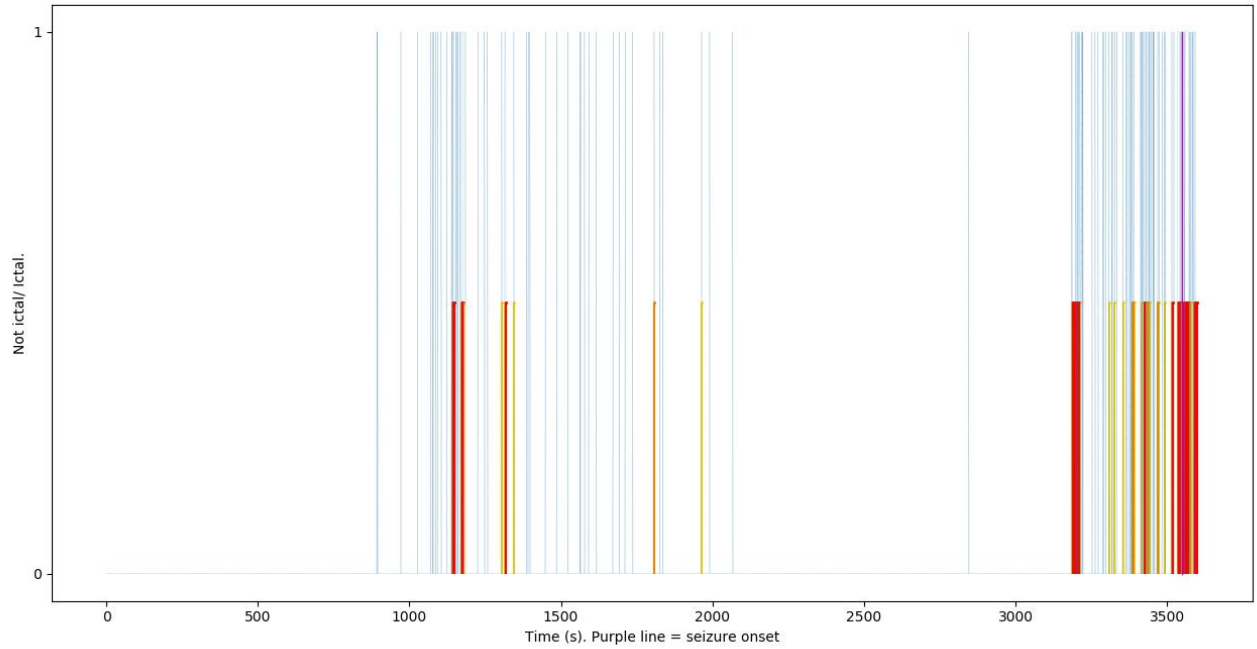

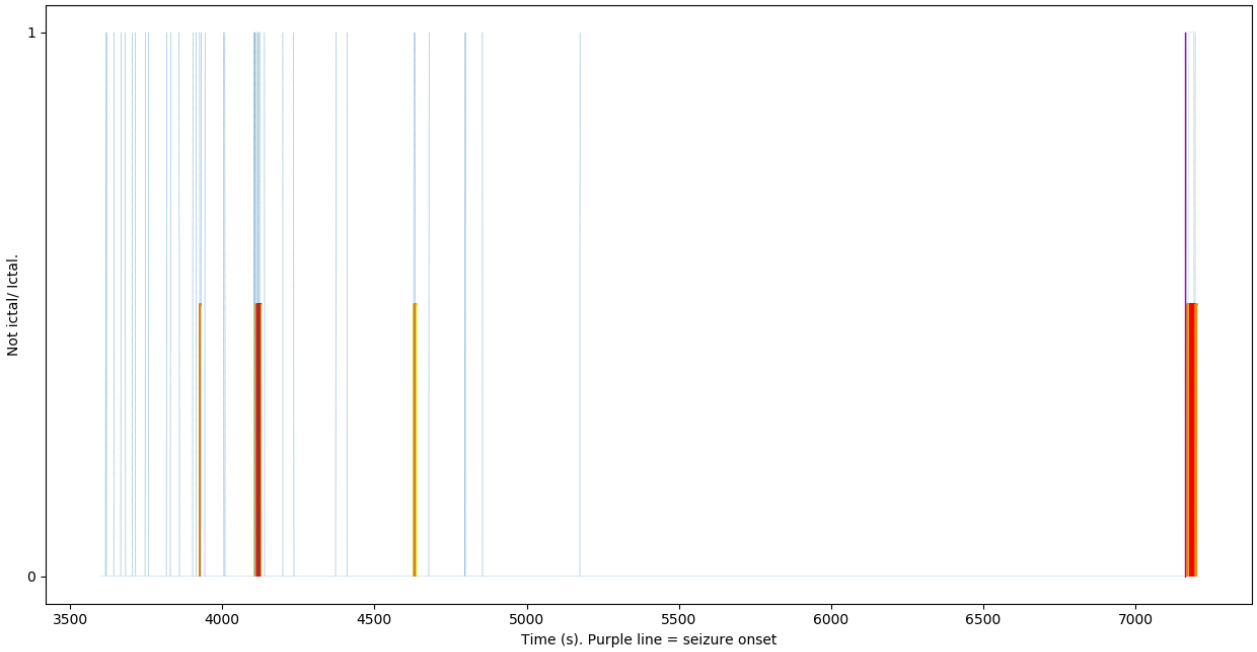

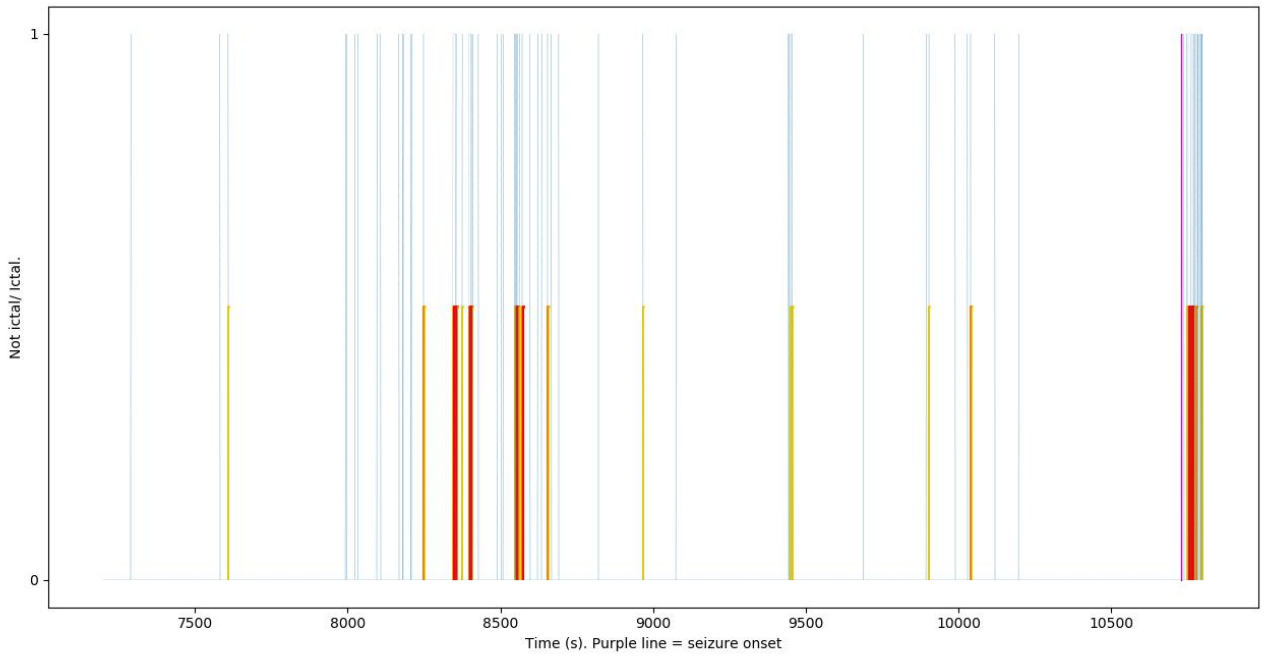
1
0
Not ictal/ ictal.
7500
8000
8500
9000
9500
10000
10500
Time (s). Purple line = seizure onset

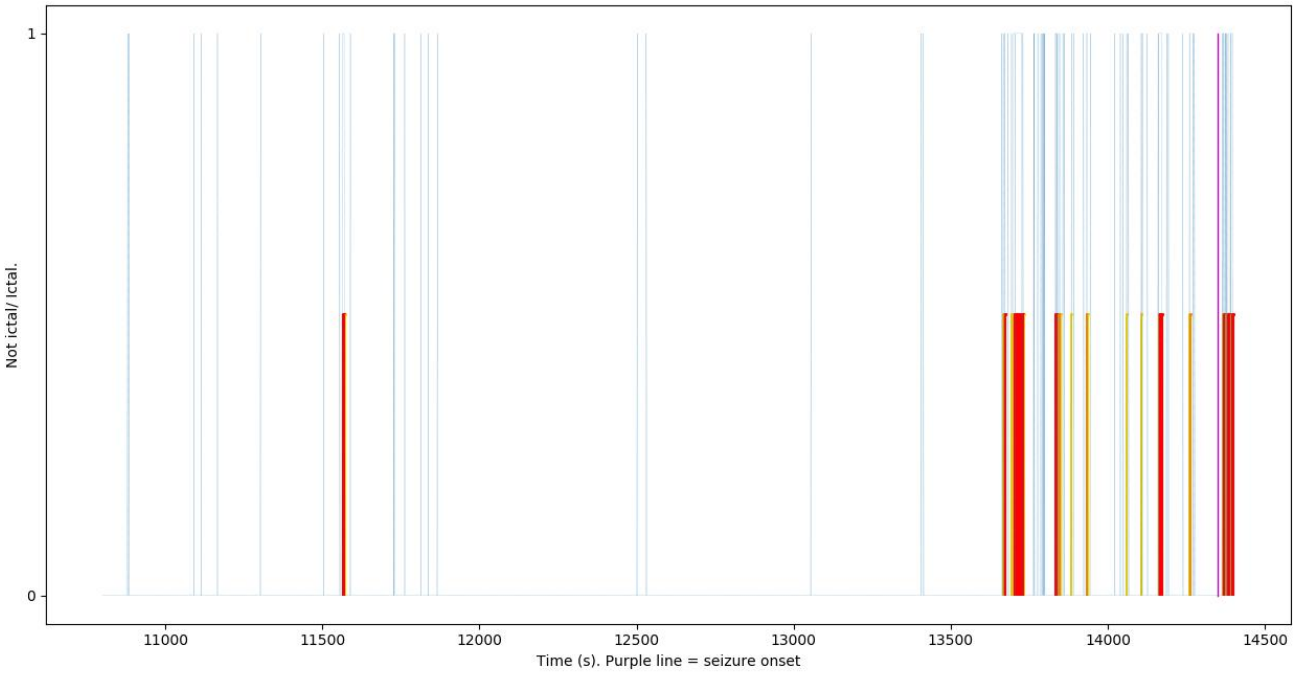
1
0
Not ictal/ ictal.
11000
11500
12000
12500
13000
13500
14000
14500
Time (s). Purple line = seizure onset

Patient #81102

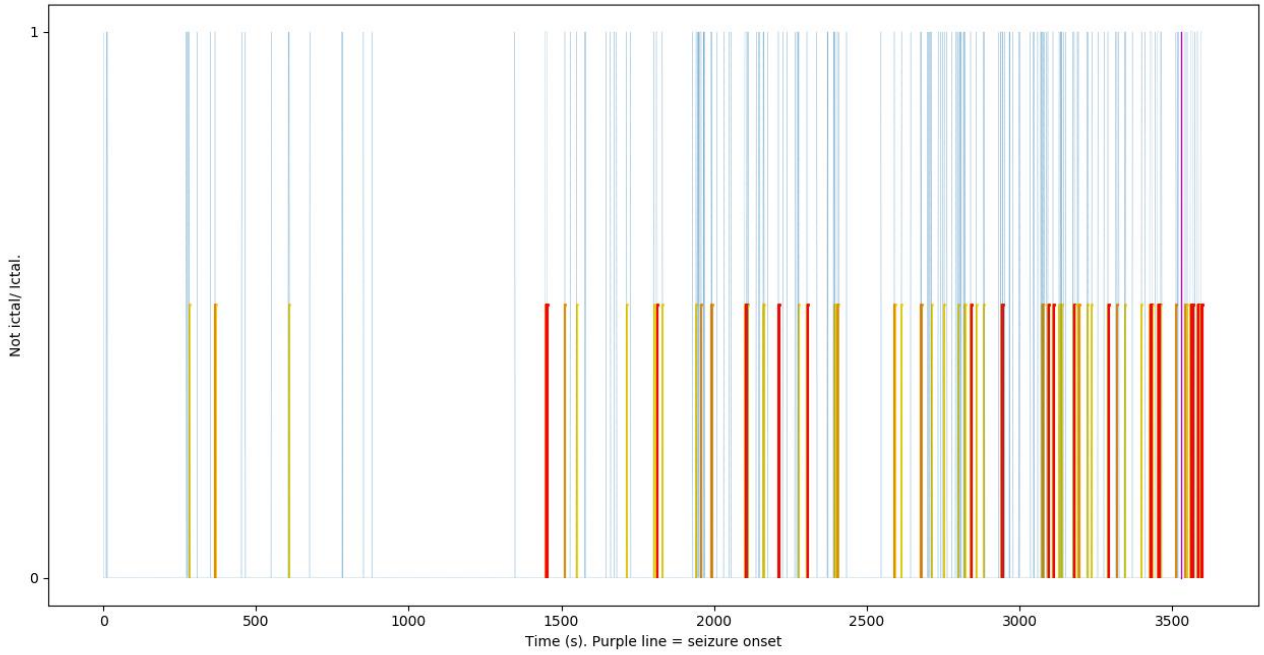

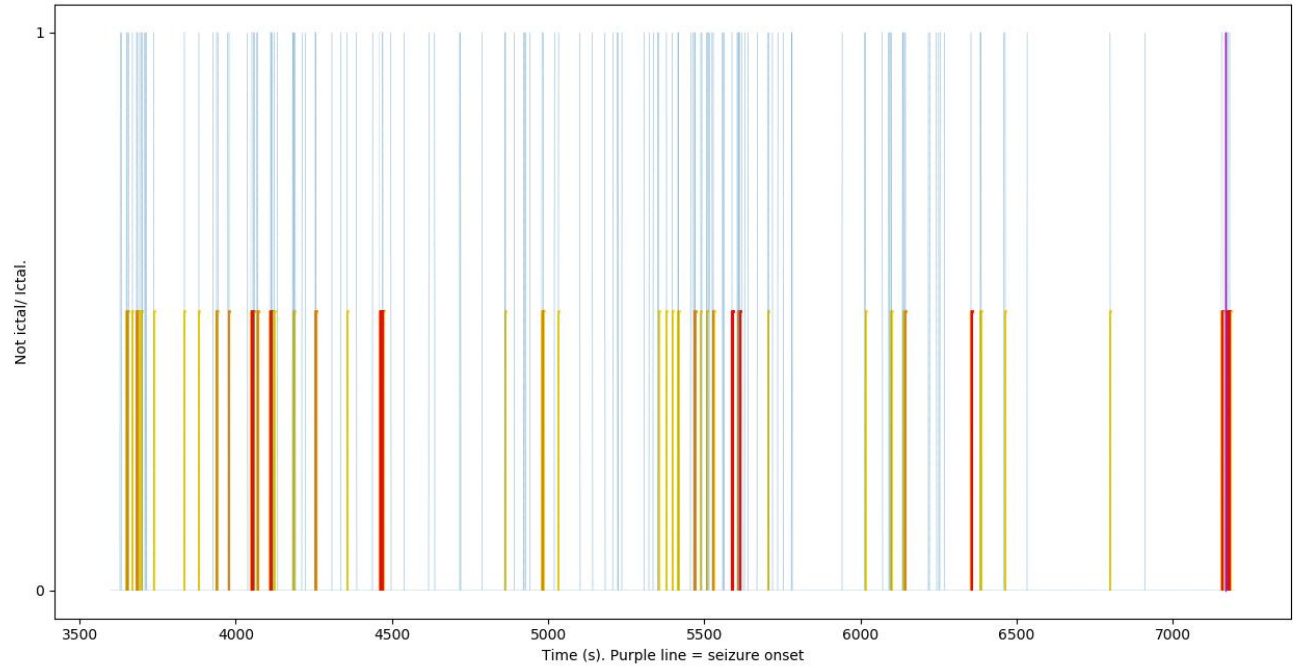

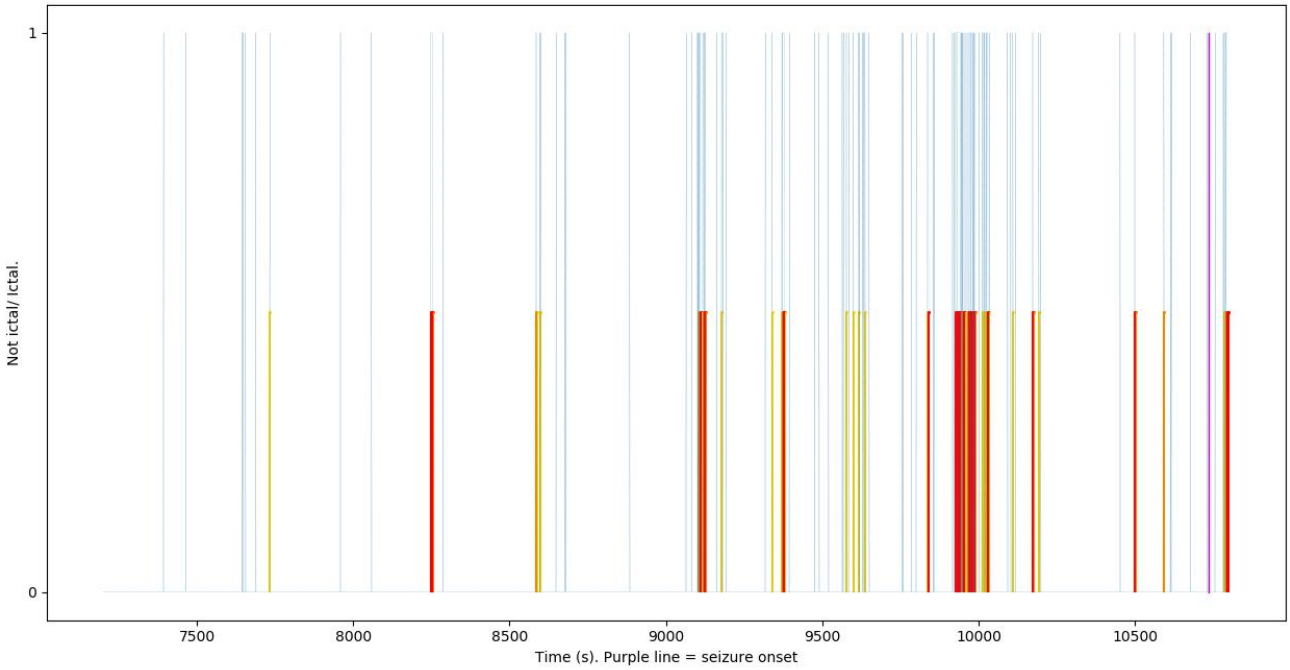
1
0
Not ictal/ Ictal.
7500
8000
8500
9000
9500
10000
10500
Time (s). Purple line = seizure onset

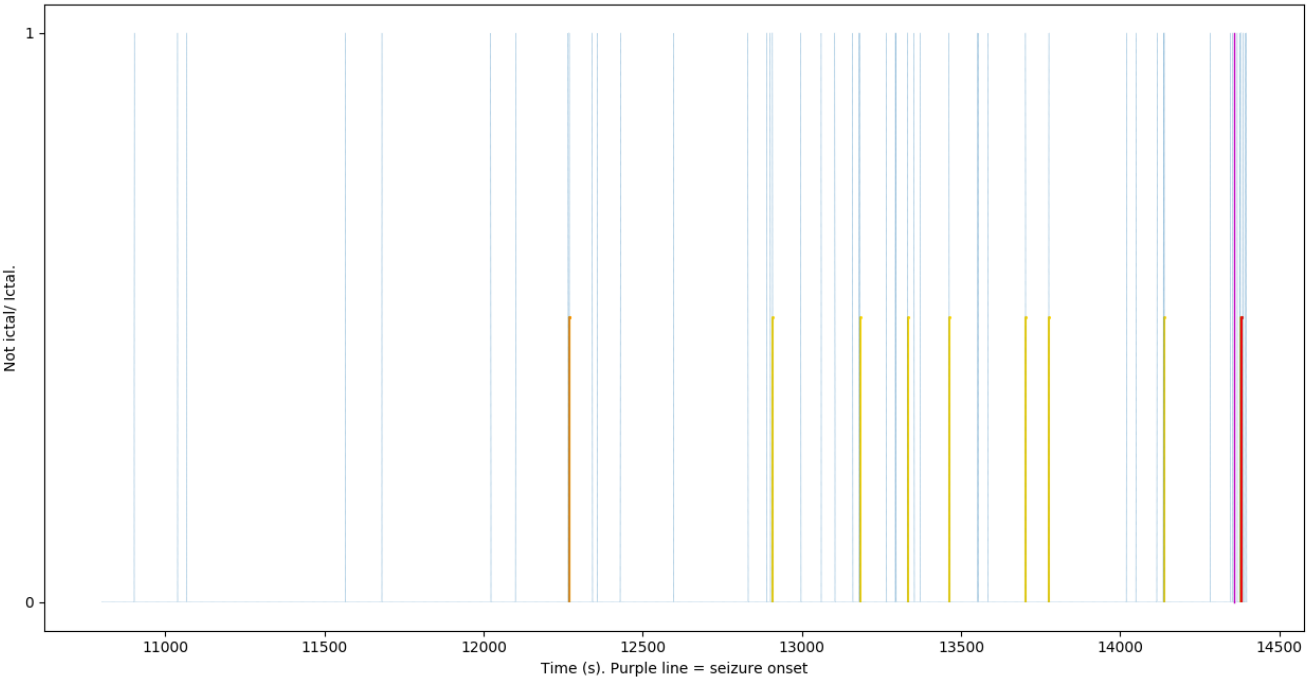
1
0
Not ictal/ Ictal.
11000
11500
12000
12500
13000
13500
14000
14500
Time (s). Purple line = seizure onset

Patient #85202

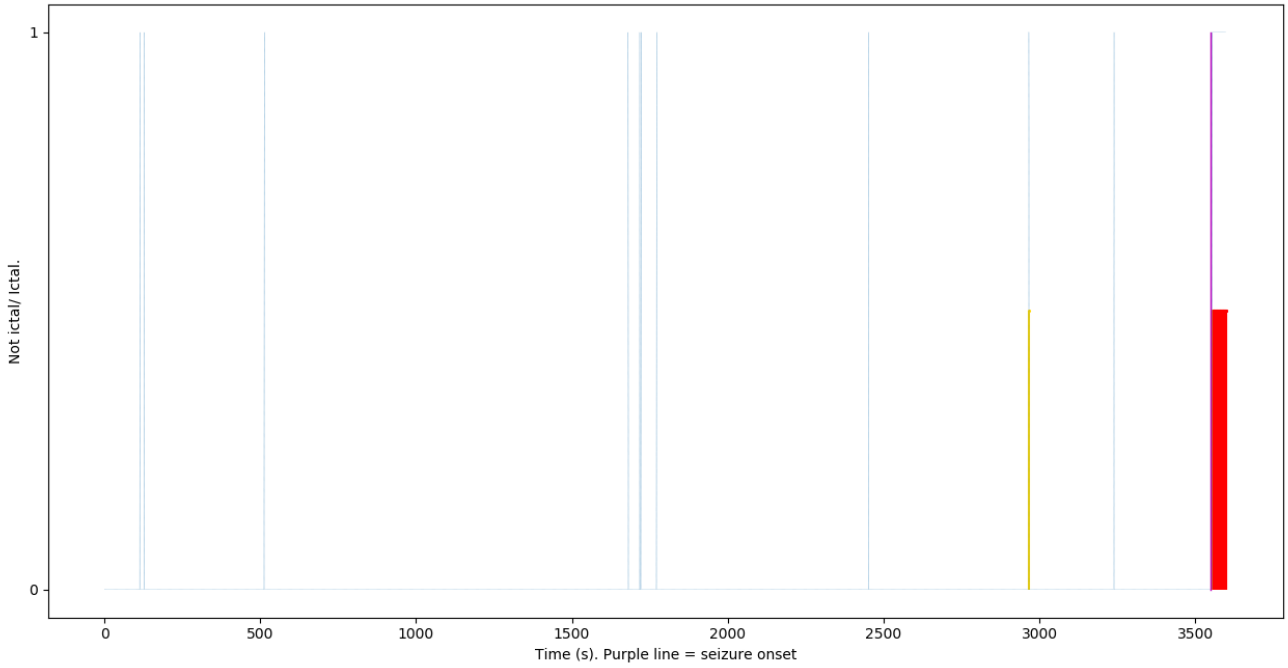

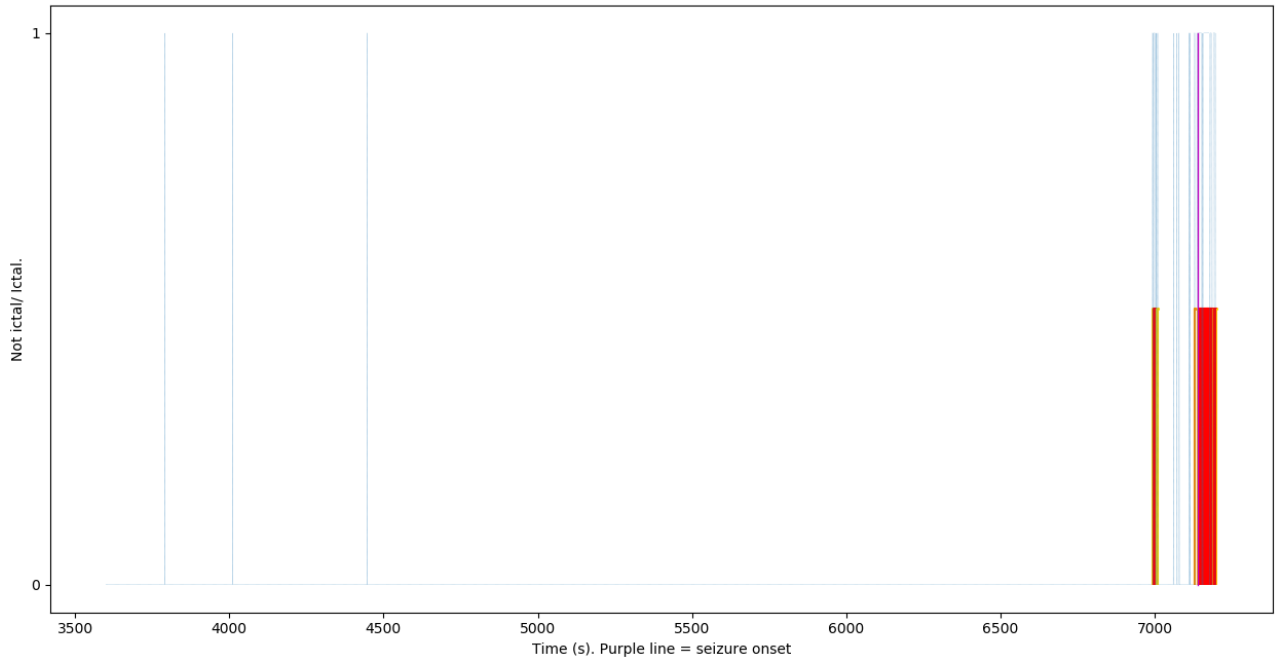

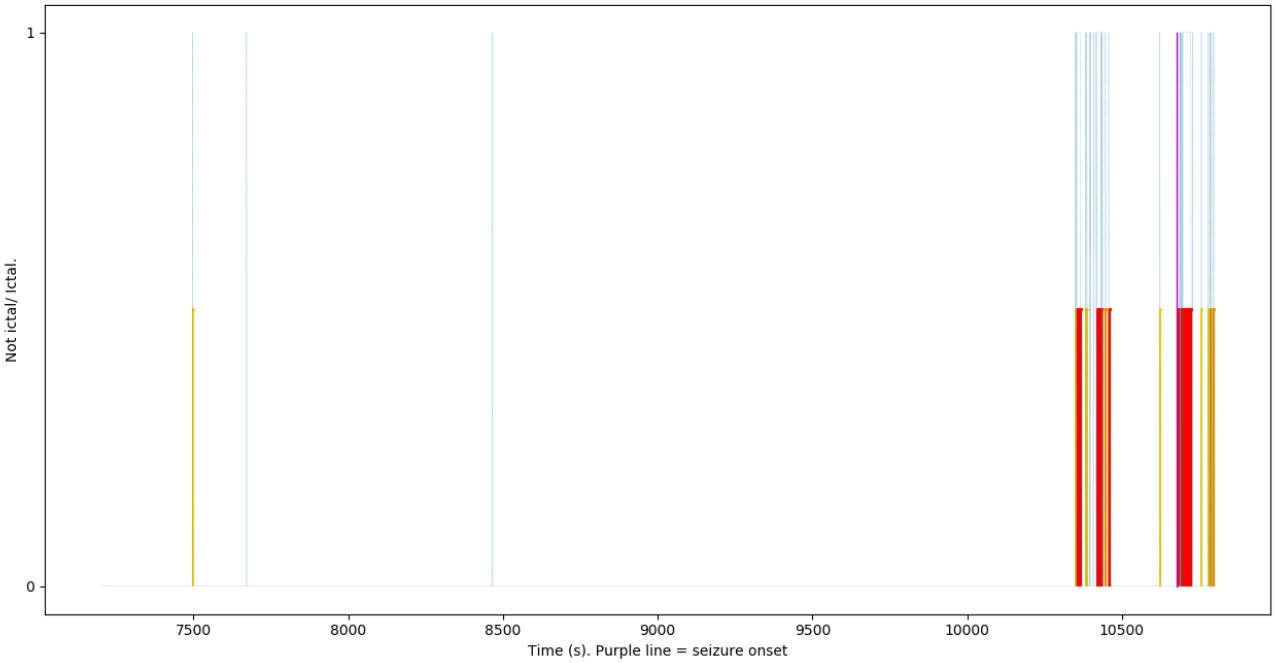
1
0
Not ictal/ ictal.
7500
8000
8500
9000
9500
10000
10500
Time (s). Purple line = seizure onset

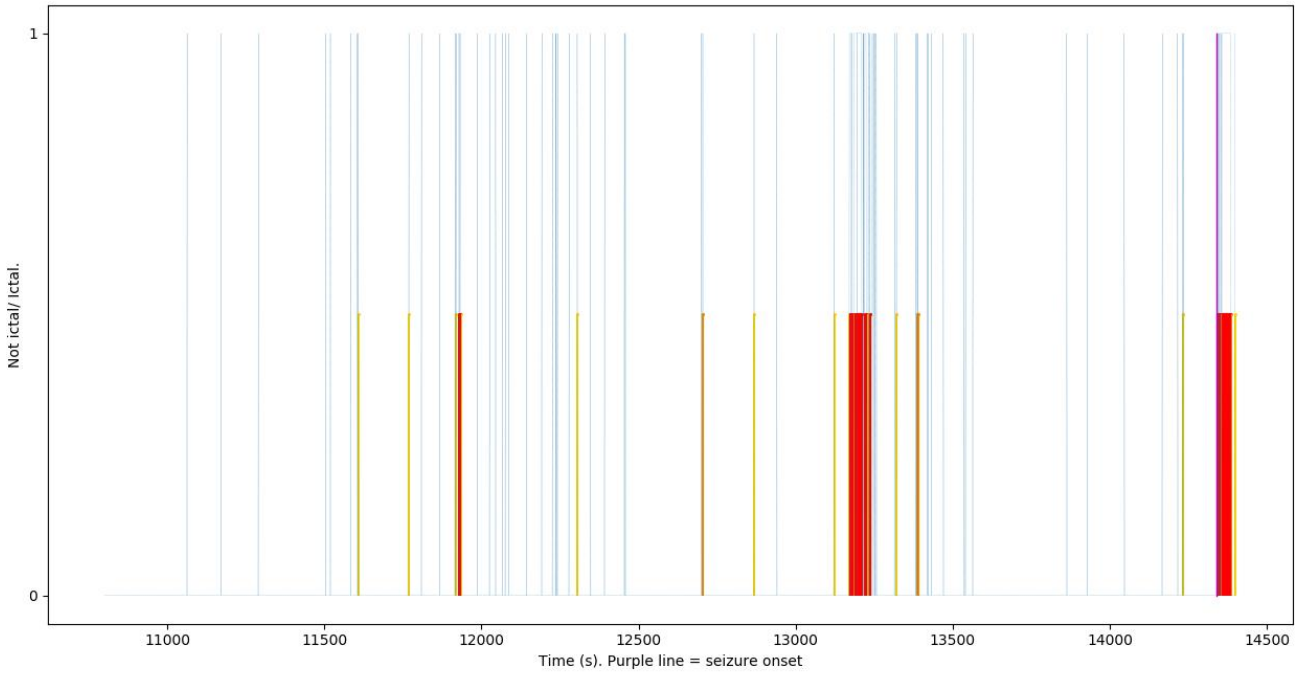
1
0
Not ictal/ ictal.
11000
11500
12000
12500
13000
13500
14000
14500
Time (s). Purple line = seizure onset

Patient #109502

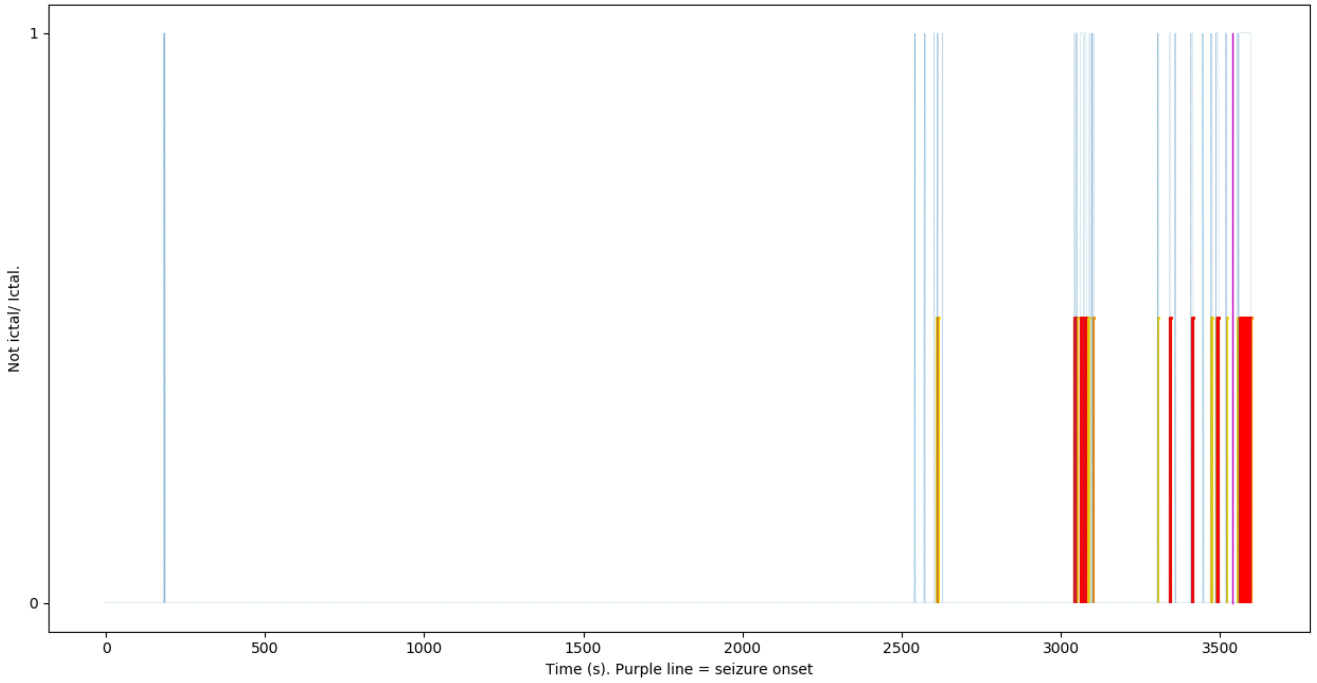

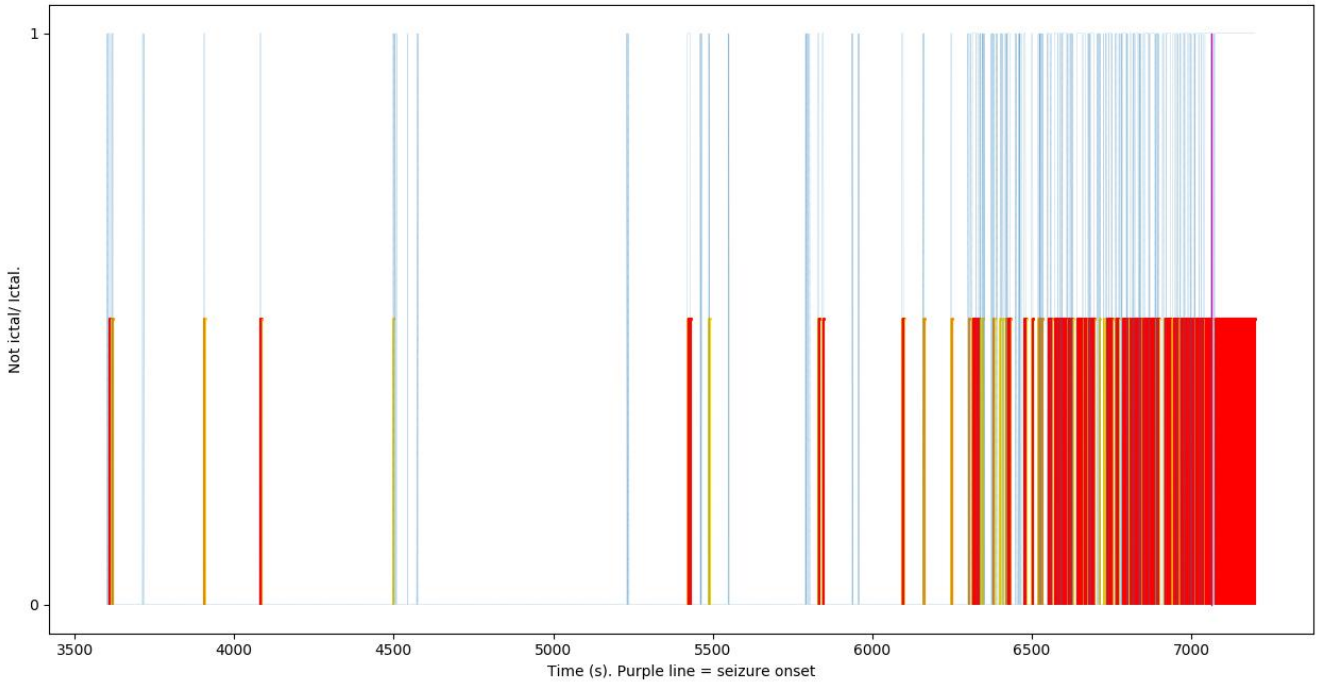

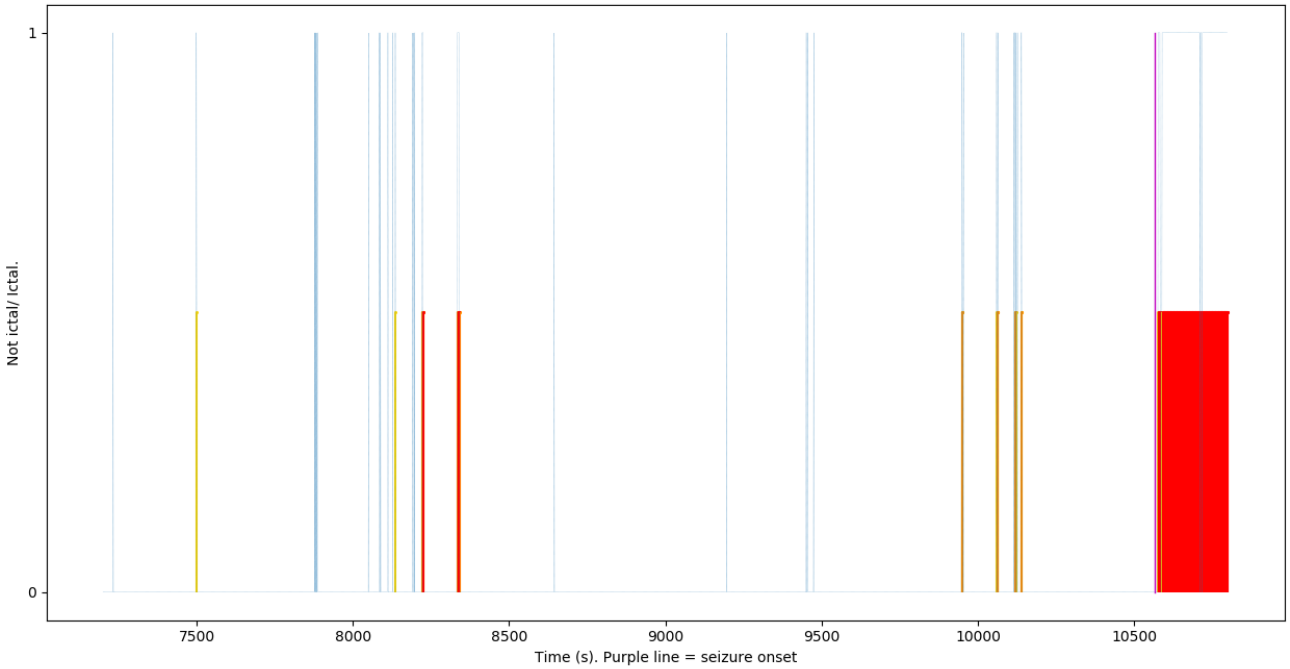
1
0
Not ictal/ Ictal.
7500
8000
8500
9000
9500
10000
10500
Time (s). Purple line = seizure onset

Patient #113902

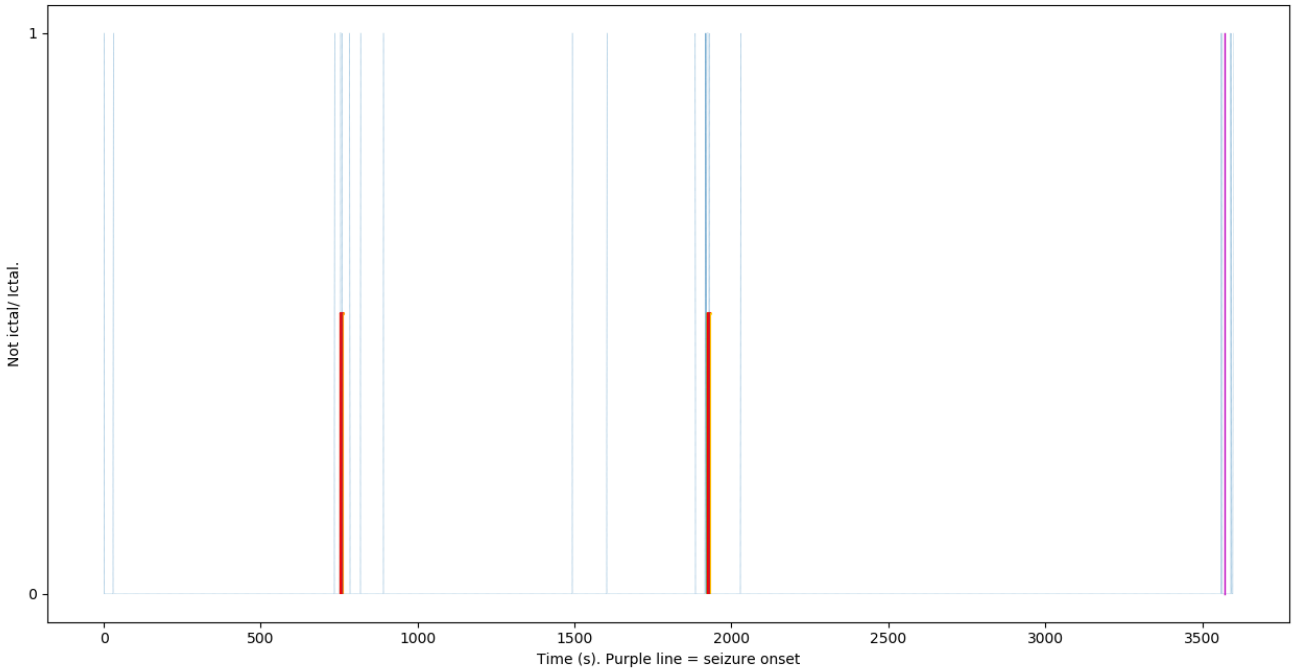

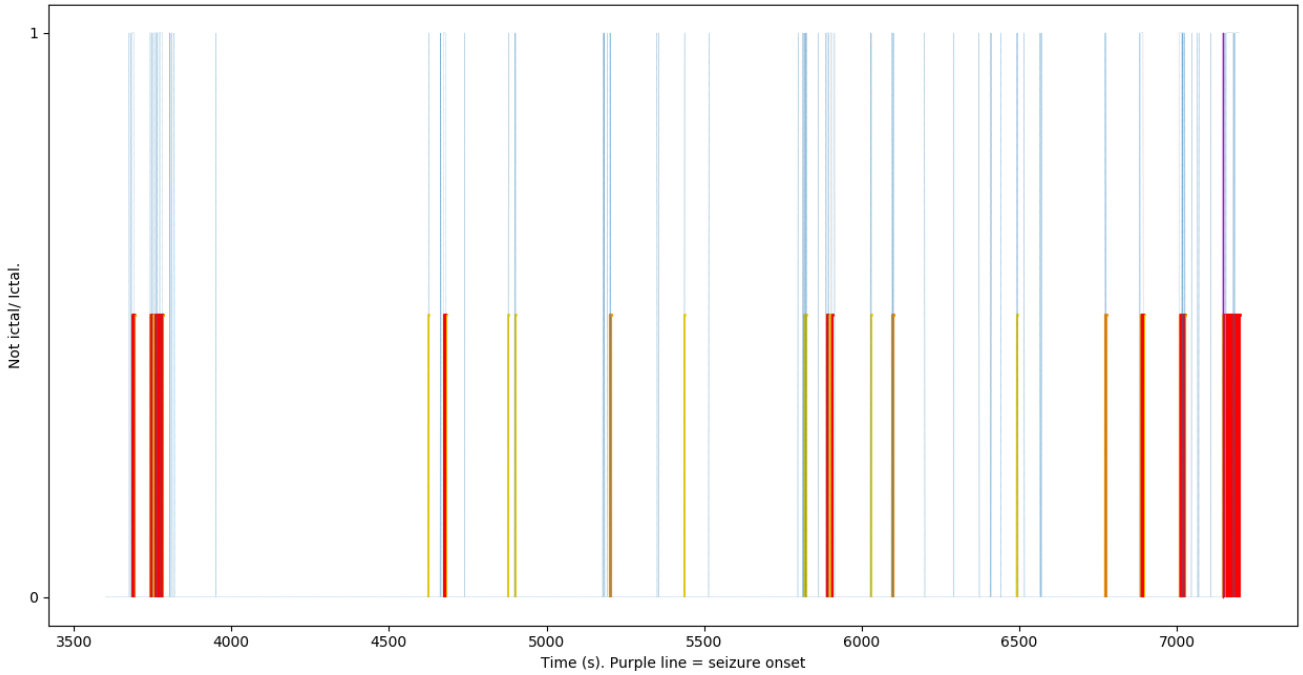

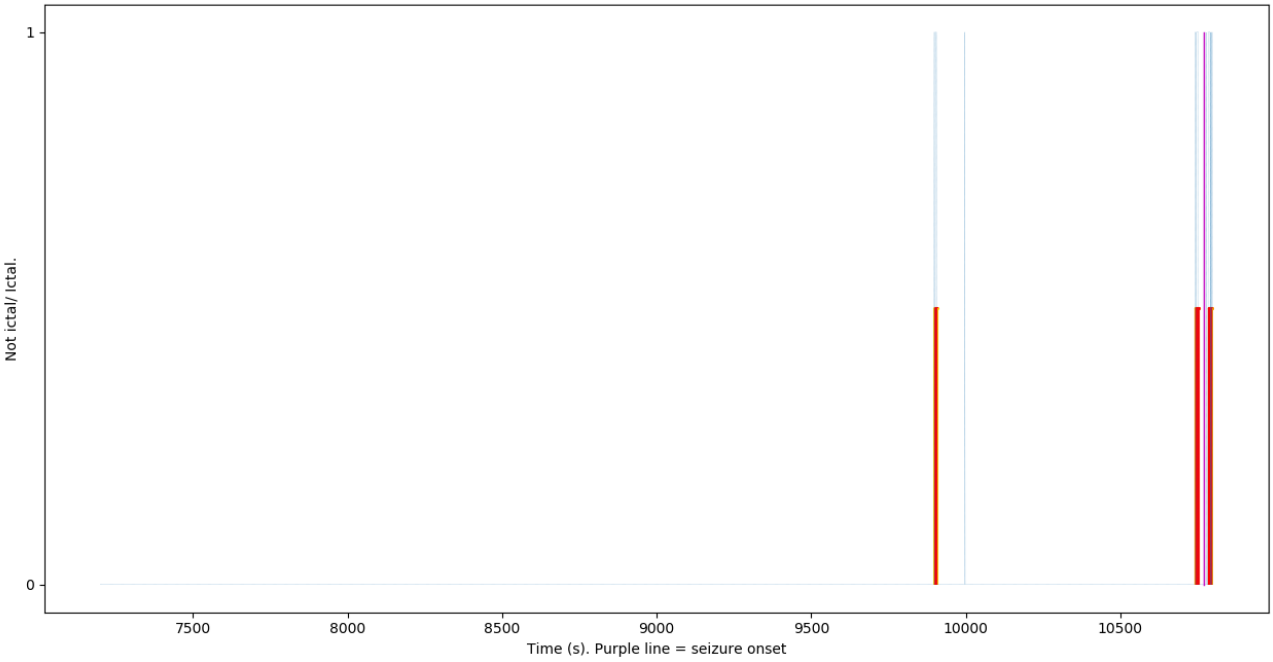
1
0
Not ictal/ ictal.
7500
8000
8500
9000
9500
10000
10500
Time (s). Purple line = seizure onset

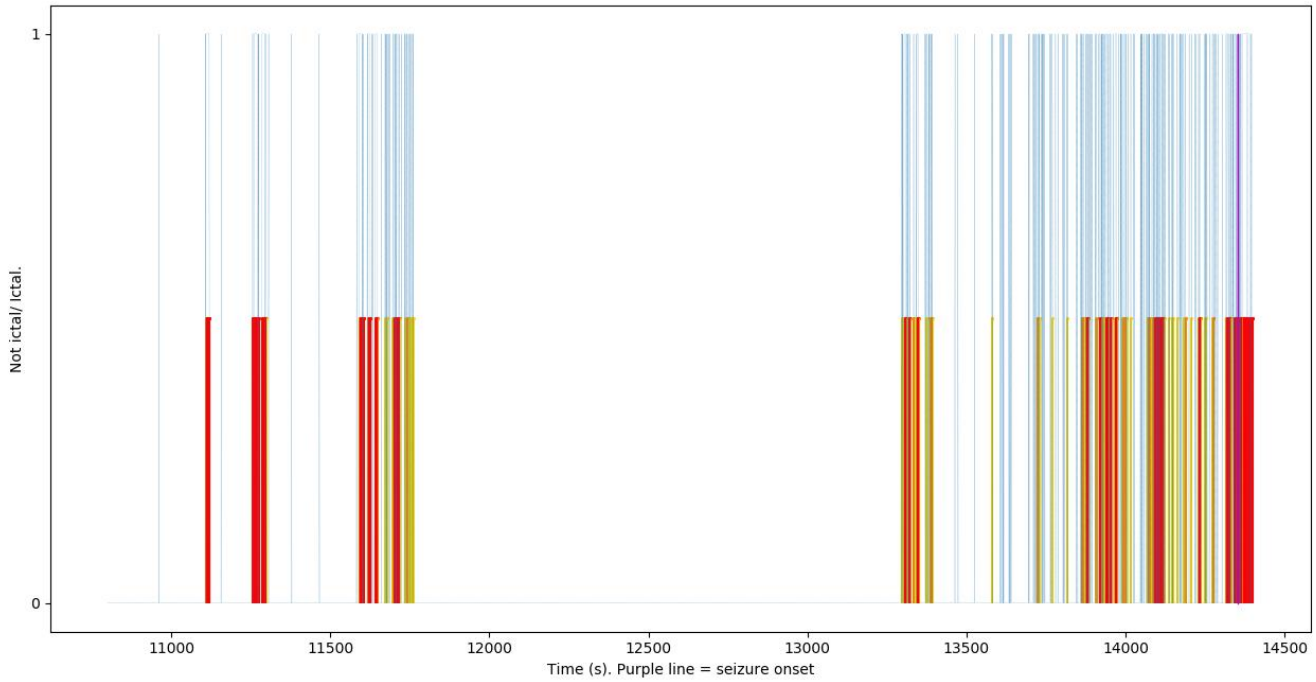
1
0
Not ictal/ ictal.
11000
11500
12000
12500
13000
13500
14000
14500
Time (s). Purple line = seizure onset

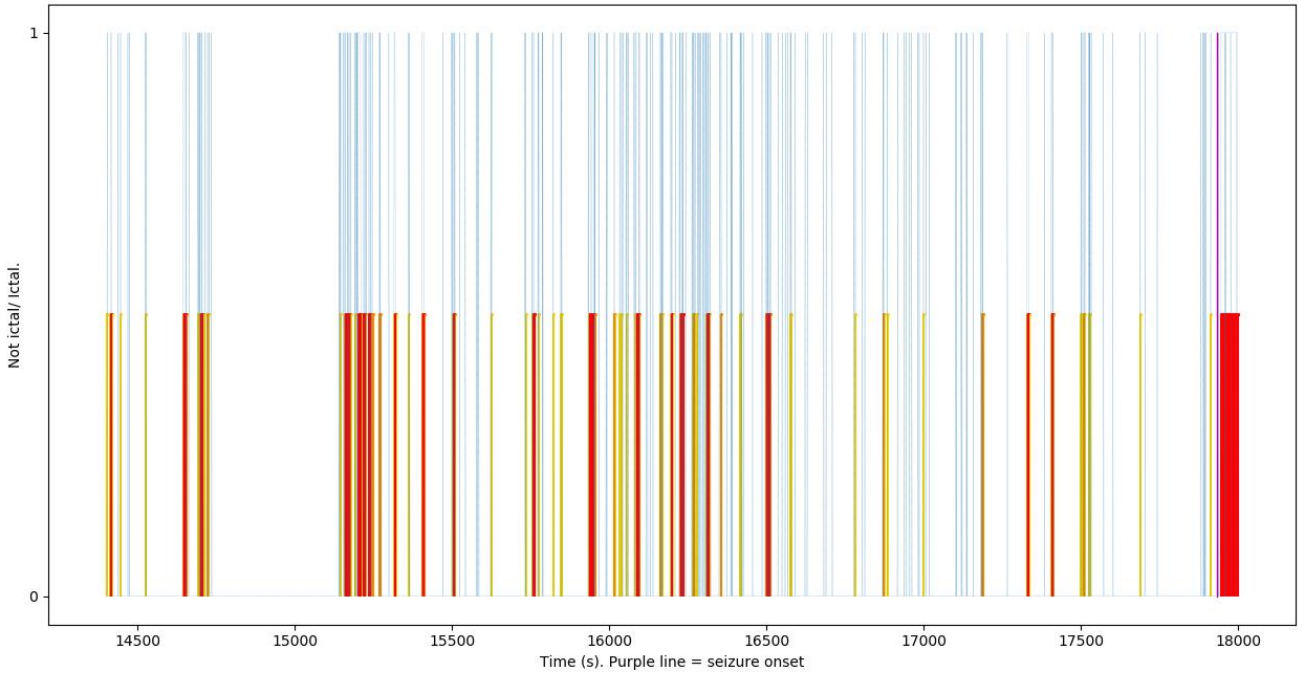
1
0
Not ictal/ ictal.
14500
15000
15500
16000
16500
17000
17500
18000
Time (s). Purple line = seizure onset

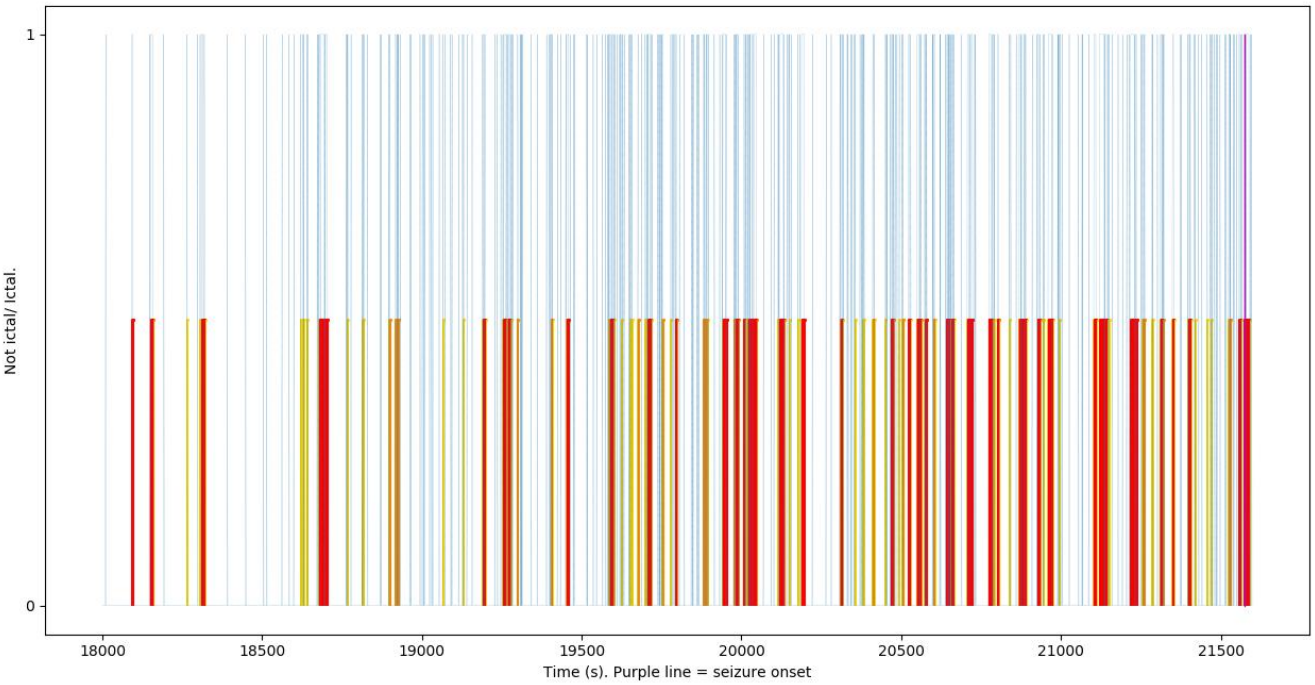
1
0
Not ictal/ ictal.
18000
18500
19000
19500
20000
20500
21000
21500
Time (s). Purple line = seizure onset

Patient #114902

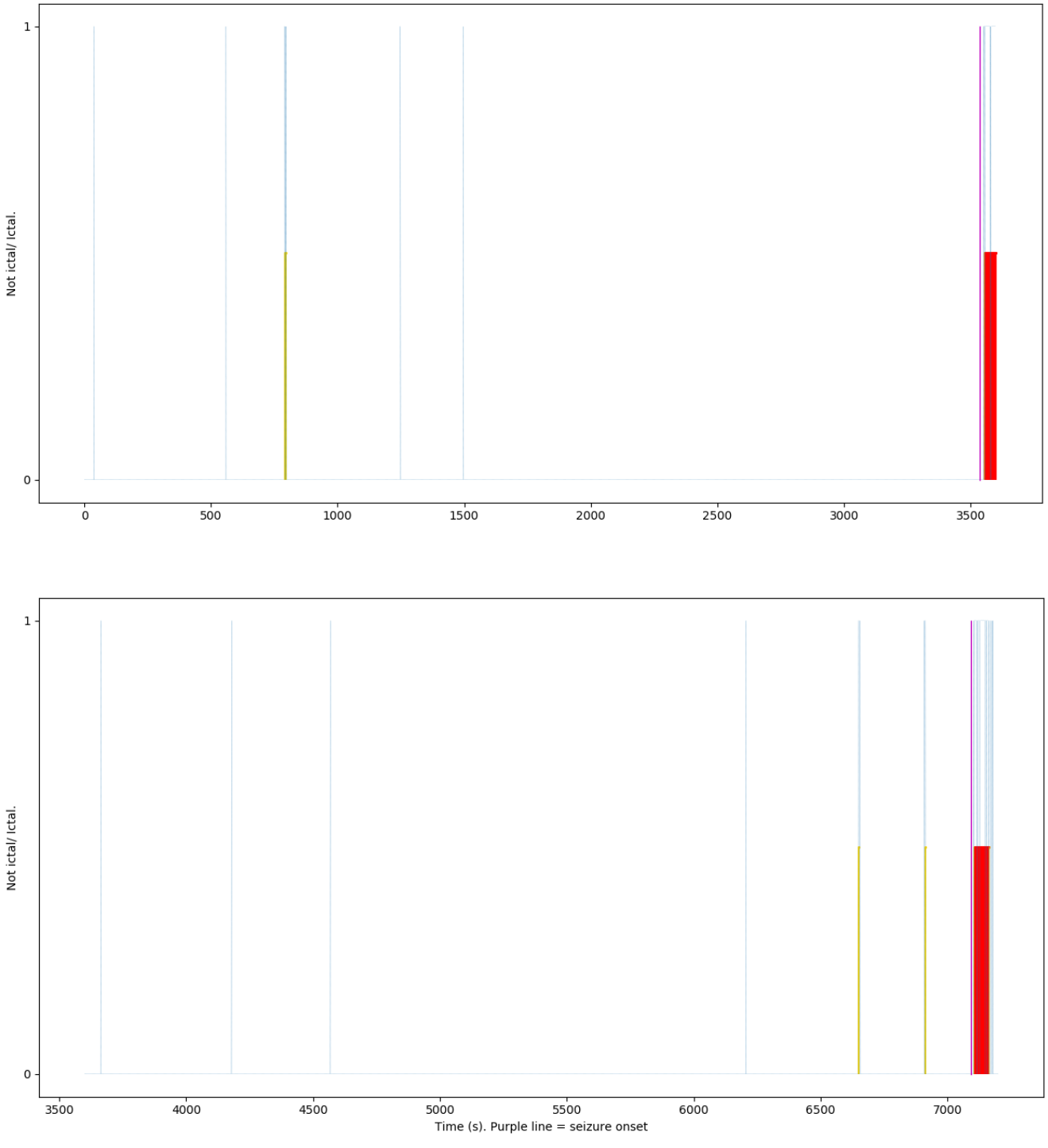

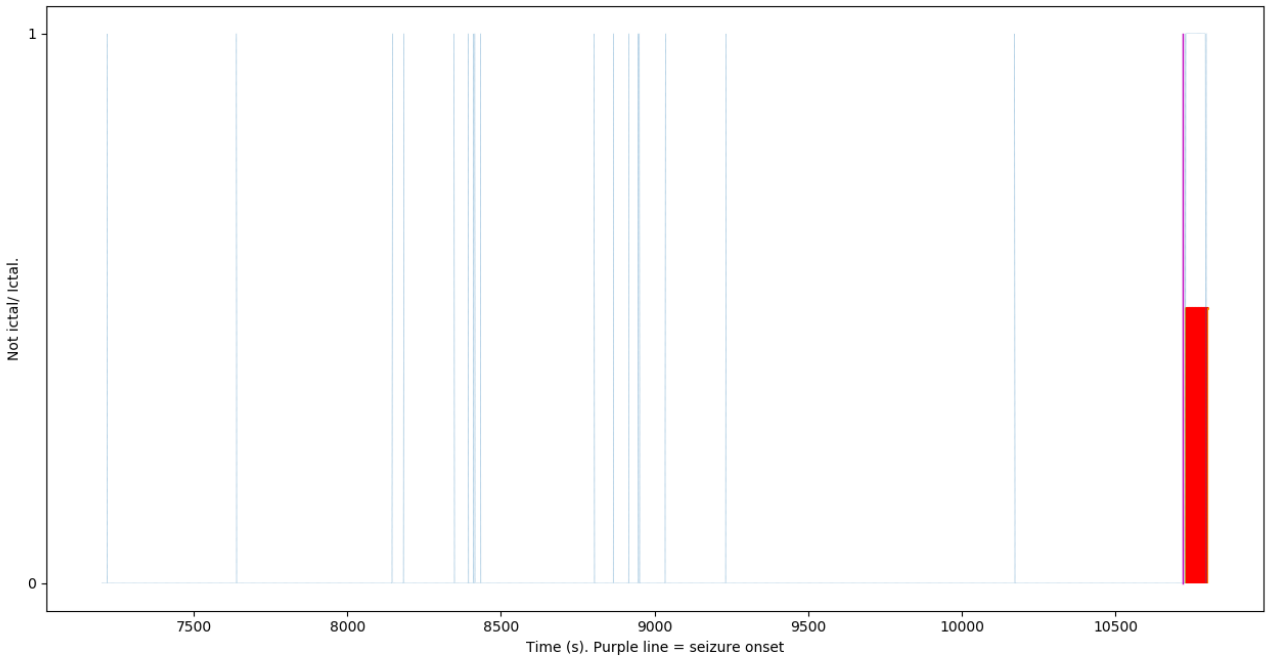
1
0
Not ictal/ Ictal.
7500
8000
8500
9000
9500
10000
10500
Time (s). Purple line = seizure onset

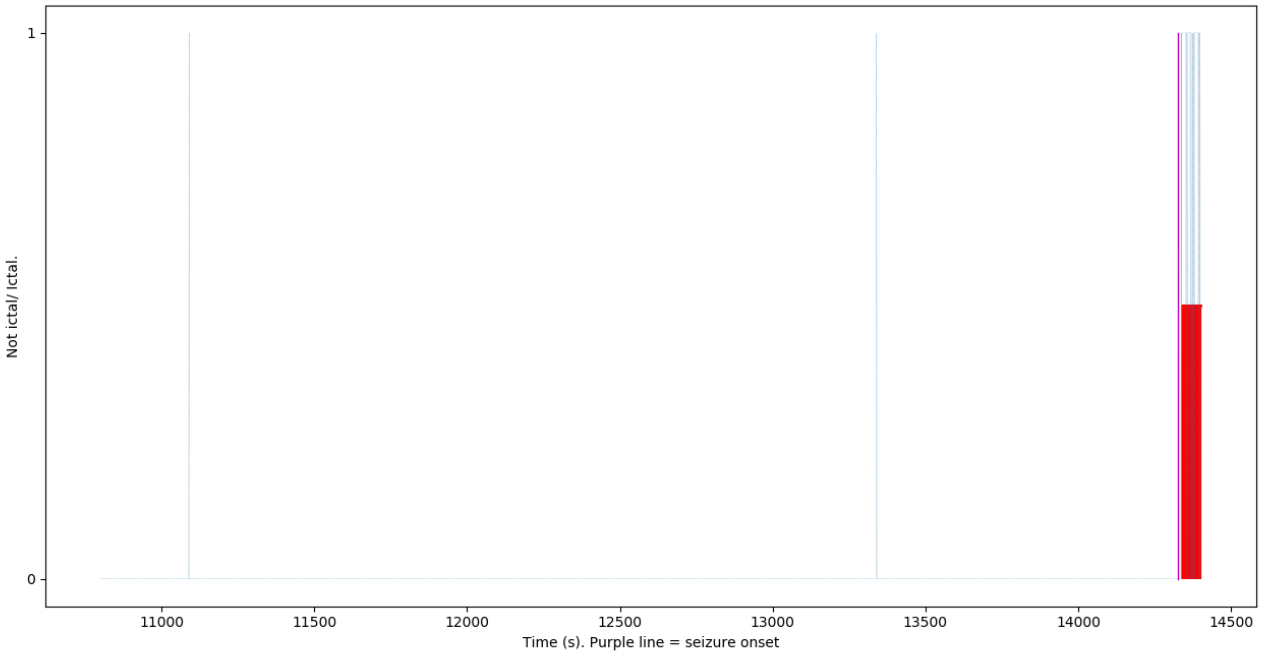
1
0
Not ictal/ Ictal.
11000
11500
12000
12500
13000
13500
14000
14500
Time (s). Purple line = seizure onset

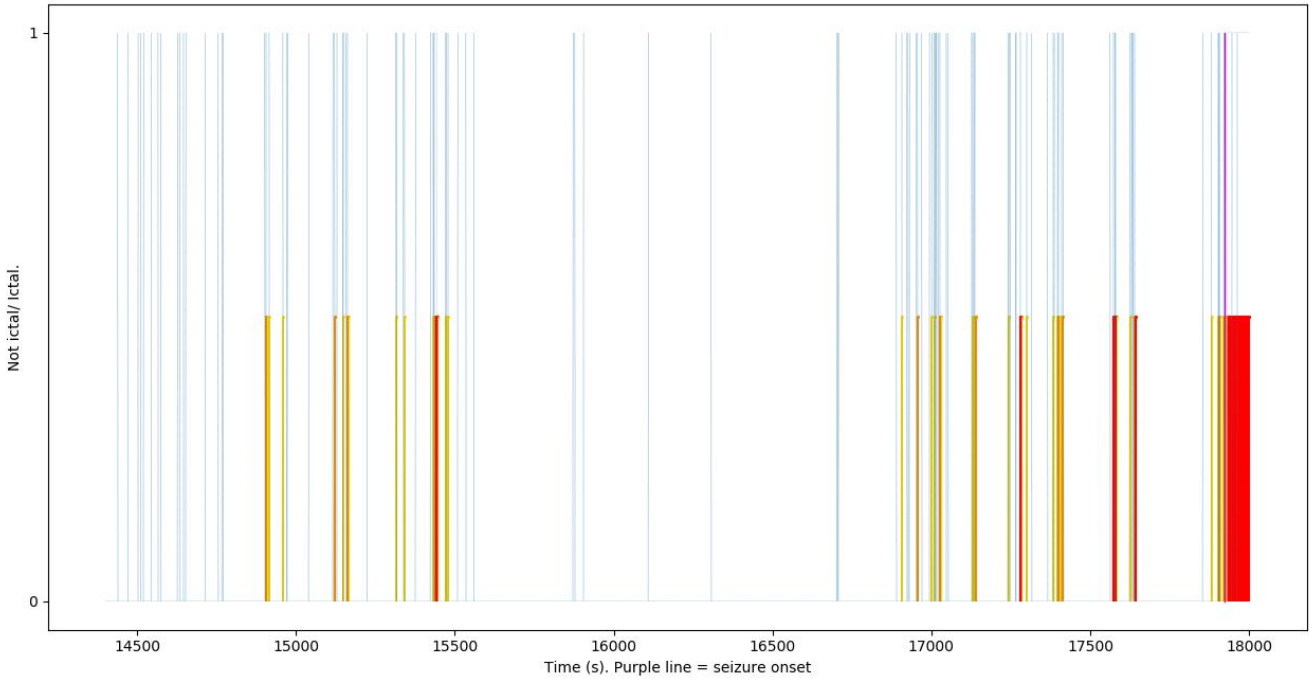
1
0
Not ictal/ ictal.
14500
15000
15500
16000
16500
17000
17500
18000
Time (s). Purple line = seizure onset